Finite Element Modeling Of Contaminant Transport Through Confined Disposal Facilities

by

Timothy N. Tyler

DISSERTATION submitted to the Faculty of the

Virginia Polytechnic Institute and State University

in partial fulfillment of the requirements for the degree of

DOCTOR OF PHILOSOPHY

IN

CIVIL ENGINEERING

APPROVED:

T. Kuppusamy, Chair

Ron Kriz

James R. Martin

George Filz

Thomas Brandon

February 1996

Blacksburg, Virginia

Key Words: Finite Elements, Contaminant, Confined Disposal Facility, Arsenic, Seepage

FINITE ELEMENT MODELING OF CONTAMINANT TRANSPORT THROUGH CONFINED DISPOSAL FACILITIES

by

Timothy N. Tyler

Dr. William Knocke, Chairman

Department of Civil Engineering

ABSTRACT

The US Army Corps of Engineers is responsible for regular dredging of shipping channels which produces about 300 million yd^3 of dredged sediments annually. Many of these sediments have to be contained within confined disposal facilities (CDFs) due to the presence of heavy metals, PCB's and other harmful constituents within the pore water of the dredge soils. However, these contaminants frequently seep back into the water from which the dredge was removed. The primary objective of this research was to modify the existing finite element program POLUT2D to evaluate the rate and quantity of contaminant transport through CDFs. Two actual field problems were evaluated using the modified program. One of these problems was a new CDF to be located along the US coast and the other was the existing Buffalo Harbor Dike facility located on Lake Erie in Buffalo, New York. The analyses of the coastal facility indicated that a cumulative quantity of about 43 kilograms of arsenic will seep back into the bay at the end of 50 years following filling of the CDF with arsenic contaminated dredge. Analyses of the Buffalo

Harbor facility indicated that about 45 kilograms of chlorobenzene seeps annually into Lake Erie from the dredge material contained within this structure.

Sensitivity analyses were also performed to evaluate the effect of soil properties, boundary conditions, etc. on contaminant transport through CDFs. The results indicated that some soil properties such as unit weight, molecular diffusion, and transverse dispersivity have little impact on contaminant transport. Other properties, such as the distribution coefficient and the longitudinal dispersivity, have only a slight to moderate impact on contaminant transport, while the coefficient of hydraulic conductivity can have a significant impact on contaminant transport though CDFs. Analyses also indicated that tidal fluctuations and infiltration from precipitation impact contaminant transport and must be modeled. Additional studies indicated that a slurry trench may provide better containment than a soil liner, and that a combination of a slurry trench and soil cover can reduce contaminant loading by a factor of about 4 depending on the thickness of the soil cover.

ACKNOWLEDGMENTS

This research project was funded by the US Army Corps of Engineers Waterways Experiment Station (WES) under contract number DACW-39-92-K-0037. This support is gratefully acknowledge. The author would also like to thank his committee chairman, Dr. T. Kuppusamy, for the opportunity to work on this project and for his helpful assistance throughout the project. The input of the committee members including Dr. Jimmy Martin, Dr. George Filz, Dr. Ron Kriz and Dr. Tom Brandon is also greatly appreciated. The author would also like to thank his family, especially his wife Lynn, for their support, encouragement and patience. Finally, for the opportunity, ability and endurance needed to complete this project, the author thanks Him who is the giver of every good and perfect gift (James 1:17).

TABLE OF CONTENTS

List of Figures

List of Tables

CHAPTER 1

Introduction

1.1 Background

The US Army Corps of Engineers is responsible for the maintenance of 25,000 miles of the nation's waterways including ports, harbors, lakes and rivers. One of the primary tasks of the Corps is regular dredging of shipping channels which produces about 300 million yd^3 of sediments annually (Palermo, 1992). Prior to the early 1970's, much of this material was dumped at the most convenient and most economical location, often just outside of the shipping lanes or out at sea. However, this practice has been curtailed because many of the sediments have been found to contain high levels of contaminants. This is particularly a problem in urban areas where industrial and agricultural contaminants such as heavy metals, PCBs and oil and grease have been detected in dredged sediments.

In the late 1960's the Corps of Engineers initiated a dike disposal program in the Great Lakes. This program involved the construction of confined disposal facilities (CDFs) for the placement of contaminated dredge materials. These CDFs have been located completely inland, or more commonly, along the water's edge. A plan view and a cross section of a typical CDF are shown in Figure 1-1. The perimeter dike is constructed with soil or crushed stone which is placed hydraulically or in the dry. Once the dike is completed, contaminated dredge sediments are pumped as a slurry within the confines of the perimeter dike. The suspended particles settle down within the CDF, and the supernatant water exits the structure through a weir or an outlet pipe. Studies on the concentration of contaminants entering and leaving a CDF through these outlet structures

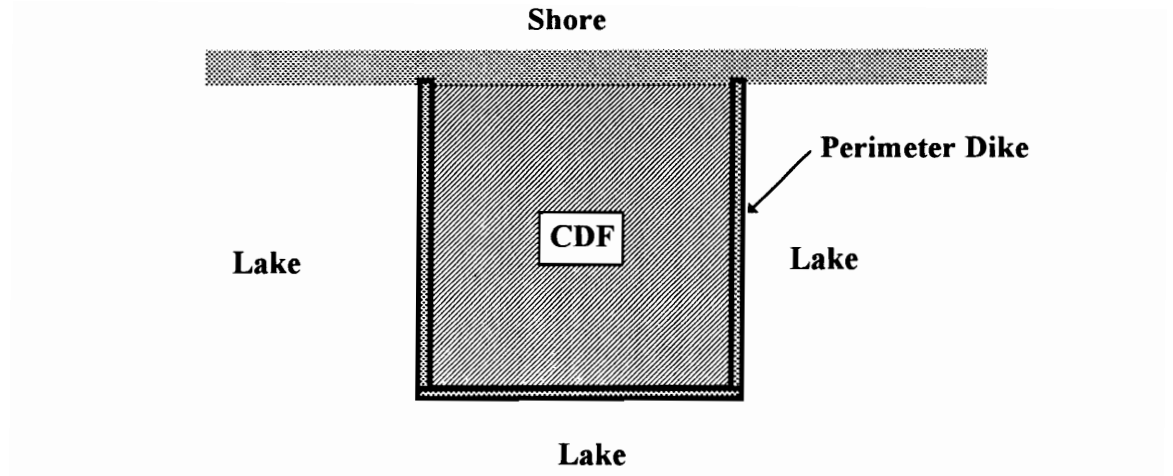

a) Plan View

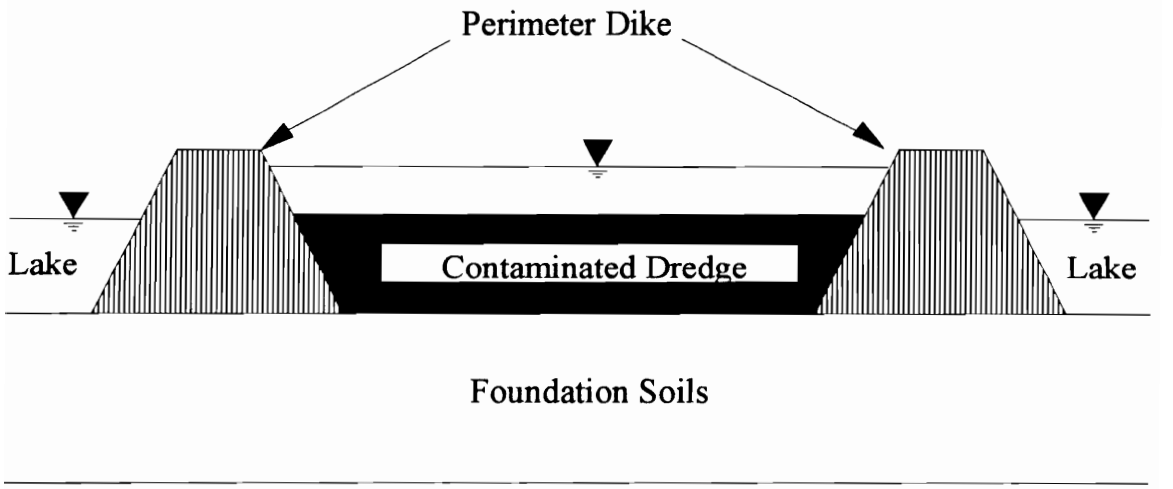

b) Cross-section

FIGURE 1-1: Plan View and Cross-section of a Typical CDF.

have shown that the effluent may have only 5% of the amount of pollutants as the influent (Krizek, et al., 1974). However, this apparently high degree of containment within a CDF may be deceptive if the leachate seeping through the perimeter dike and/or through the foundation soils contains high levels of dissolved contaminants.

The amount of seepage through a CDF depends primarily on the properties of the dike and foundation soils. If crushed stone is used for the perimeter dike, some type of low permeability material, such as grout filled fabric mattresses, must be placed along the inside of the dike to reduce seepage. Often, low permeability silts and clays are used to construct the dike. In any event, it is generally impossible to completely eliminate contaminant migration due to seepage from confined disposal facilities. Therefore, some type of analysis must be employed to evaluate the quantity and the concentration of the contaminant as it seeps through the CDF.

1.2 Objective and Scope

The primary objective of this research is to modify the existing finite element program POLUT2D by Kuppusamy and Ahmad (1991) to meet the specific needs of the Corps of Engineers for the analysis of CDFs. POLUT2D is a user-friendly computer program that evaluates the concentration level of a given contaminant as the plume spreads through a porous media via the mechanisms of advection, mechanical dispersion and molecular diffusion. A description of the program is presented in Chapter 4. Some modifications to this program were required to make it suitable for the analysis of CDFs. One important modification was to include the effect of contaminant attenuation due to sorption. Sorption is a mechanism whereby the contaminant comes out of solution and adheres to the porous media through which flow is taking place. This phenomena is a common process in many geologic materials and can play a significant role in contaminant

transport by decreasing the amount of dissolved pollutant in the groundwater. Thus, an excessive estimate of contaminant transport may be determined if sorption is not considered. Another modification to the existing program is the consideration of fluctuating water levels on the boundaries of a CDF. The water level of all of the Great Lakes varies with time. This fluctuation affects the rate of contaminant transport through CDFs. Also, many confined disposal facilities have been and will be constructed along coastal waters where the effect of the local tide will influence contaminant migration. Accordingly, the existing program was modified to incorporate these fluctuations.

There are several other objectives of this study which are beyond the scope requested by the Corps of Engineers (COE). The simple linear sorption model incorporated for the COE may not always be applicable for a given contaminant. The literature contains considerable research showing the applicability of various sorption models such as the linear Freundlich and non-linear Langmuir equilibrium isotherms models. The effect of these various sorption models on contaminant transport will be evaluated in this research. In addition, the program will be modified to study the effect of construction and boundary condition assumptions using a quasi-construction simulation technique and a quasi-finite contaminant capacity simulation method.

This research is limited to modeling in two dimensions. Three dimensional modeling, while more accurate than 2-D, requires additional soil properties that may be difficult to evaluate and would necessitate the use of additional computational effort. The analyses which will be performed are limited to contaminants that are soluble in water. Non-aqueous phase liquids, which are defined as those liquids that do not readily dissolve in water but are lighter (LNAPL's) or denser (DNAPL'S) than water, are not modeled in the program.

1.3 Outline of the Report

A discussion of several existing confined disposal facilities is presented in Chapter 2 to illustrate the basic design and construction considerations, typical construction materials and geometries that are used for these structures. Chapter 3 presents the theory of saturated and unsaturated fluid flow and contaminant transport through soil. The finite element approximation of the governing equations of the theory is presented in Chapter 4 including the derivation of the element matrix equations and the solution of these equations using the Gauss Quadrature numerical integration technique, general beta time integration scheme and the Picard iteration method for non-linear analysis. A survey of the literature regarding finite element modeling of contaminant transport is also included in Chapter 4. A brief summary of the program POLUTIDAL which is the modified version of program POLUT2D is also presented. An actual field CDF problem is analyzed in Chapter 5 using POLUTIDAL. Chapter 5 also includes a sensitivity analysis on various problem parameters such as soil properties, boundary conditions and containment methods. Chapter 6 presents the results of analyses for another field problem located in Lake Erie. The effect of infiltration due to precipitation on contaminant transport is evaluated for this problem, as well as the effect of different types of remediation containment methods. Finally, a summary and conclusion from this research is presented in Chapter 7.

CHAPTER 2

Dredging: Regulations, Methods and Disposal

2.1 Introduction

Dredging of shipping channels disturbs aquatic habitats and increases the turbidity of the water by suspending the bottom sediments during the dredging process. However, the greatest concern is not with the effects of dredging but what to do with the vast amount of potentially contaminated material that is dredged. A brief overview of the regulations concerning dredging and disposal is presented below and is deemed beneficial for an understanding of the importance of contaminant transport modeling of confined disposal facilities. In addition, dredging methods, sediment quality evaluation and the construction of CDFs are discussed in the following sections of this chapter.

2.2 Regulations

Dredging of the nation's waterways and disposal of the dredged material is regulated by various laws passed by the Congress of the United States. The River and Harbor Act of 1899 gave the Corps of Engineers the authority to protect navigable waters against any activity which would obstruct or harm navigation such as filling or dumping any solid materials into the water, or the construction of piers, bridges or any other structure. Any activity which could affect the navigability of any waterway had to be reviewed and given a permit by the COE. The intent of this law was to protect navigation; environmental considerations due to dredging/disposal were not addressed. Thus, for many years the Corps issued dredging and filling permits based solely on their effect on navigation.

In 1958 the Fish and Wildlife Coordination Act was passed out of concern that dredging and filling may harm the aquatic feeding and nursery habitats. This law required that local and state fish and wildlife agencies be involved in the permitting process for any

activities that may present ecological hazards to the marine life. Hollis (1976) reports that the first real challenge to this (and other) legislation was the Zabel v. Tabb suit brought against the Corps in 1969. The claimants were the owners of the land adjacent to a tidal water in Florida who wanted to fill in 11 acres of the backwater to provide land for a trailer park. After receiving local permits, they applied to the Corps for a Federal permit for the proposed filling. About 700 local residents and several state agencies requested that the Corps reject their permit application due to extensive damage to the local ecosystem that would undoubtedly occur. The Corps rejected the owners application on these grounds even though the filling would not affect navigation in any way. The owners took the Corps to Federal district court who decided in favor of the claimants on the basis of the River and Harbor Act, and the Corps was ordered to issue the permit. However, this order was overturned on appeal, and the Supreme Court refused to review the case.

Several other important pieces of legislation include the National Environmental Policy Act (NEPA) of 1969, the Federal Water Pollution Control Act Amendments (FWPCA) of 1972, and the Marine Protection, Research and Sanctuaries Act (MPRSA) of 1972. The latter two Acts require the Corps to work in conjunction with the Environmental Protection Agency (EPA) during the dredging/disposal permitting process and gives the EPA veto power over any project that is awarded a permit by the Corps of Engineers. Section 404 of the Federal Water Pollution Control Act regulates effluent discharge from confined disposal facilities (Bradley, 1976), and any leachate which seeps back into the receiving waters is also subject to this regulation (Palermo, 1992).

2.3 Methods of Dredging

Dredging of waterways is performed using one of two types of dredges: mechanical or hydraulic. Mechanical dredges physically excavate and remove bottom sediments using some type of bucket. Dragline or clam shell bucket dredges are examples

of mechanical dredges. These dredges excavate the material which is then transported by pipeline, conveyor belt or barge to a disposal site. Hydraulic dredges do not use buckets to excavate and lift the sediment from the channel bottom, rather pumps are used to suck the sediments from the bottom of the channel. Since hydraulic dredges are used more frequently, they will be discussed in greater detail. A discussion of the various types of mechanical dredges can be found in Mohr (1976) and Bray (1979).

The most common hydraulic dredge is the cutterhead pipeline dredge (Figure 2-1). This dredge consists of a rotating cutterhead attached to the ladder which loosens and dislodges the sediment. Cutterheads can excavate material ranging from soft silt to fractured rock (Gren, 1976). Suction applied by the dredge pump pulls the sediment, along with channel water, up the suction tube and into a discharge pipe. The erosive action of the water as it is pulled into the suction tube plays a major role in removing sediments from the channel bed. The sediment slurry is then transported to the final dumping site by way of pipelines connected to the discharge pipe. The use of booster pumps located along the pipeline enables the dredged material to be disposed of at considerable distances from the actual dredging operations. Spuds or mooring anchors are used to control the alignment of the dredge vessel. Other types of hydraulic dredges do not have a cutterhead but rather rely on the erosive action of the water entering the suction tube to loosen and remove the material from the channel bottom.

2.4 Disposal of Dredged Material

A major concern of dredging is what to do with the dredged material. As indicated in Chapter 1, many sediments contain harmful substances such as heavy metals, chlorinated hydrocarbons, etc. Unrestricted dumping of these contaminated materials during or after dredging can create harmful effects to the aquatic life and ultimately to human life. If, however, the dredge material is not contaminated, it may be dumped in the

FIGURE 2-1: Typical Cutterhead Pipeline Dredge (After Bray, 1979).

waterway with much less impact on the environment. The Corps of Engineers and the EPA developed the Elutriate test to evaluate if dredged material can be open dumped or if it must be placed in a confined disposal facility. Details of the test can be found in O'Connor (1976) and Palermo (1992), however, a summary of the test is presented herein. The Elutriate test is performed prior to dredging and attempts to simulate the dredging and disposal process. Samples of the channel bottom material are mixed with water from the proposed disposal site at a ratio of 1 part sediment to 4 parts water (by volume). This slurry is shaken in a flask for 30 minutes and then allowed to settle for one hour. Following settling, the material is centrifuged and filtered, and the supernatant is analyzed for the total dissolved concentration of various constituents. If the concentrations exceed acceptable limits, the dredge material may not be dumped in open water but must be properly confined.

Confined disposal facilities may have just about any capacity. Large facilities have been built in the Great Lakes regions with dredge material volume up to 5 million cubic yards (Krizek and Salem, 1974). Smaller CDFs have been built around the Chesapeake Bay area with capacities of 38,000 cubic yards and smaller (Aggour, et al., 1983). Confined disposal facilities can also have a variety of geometries. They may have the shape of a peninsula, being bounded on one side by the shoreline. They may be completely surrounded by water as an island or they may be constructed in abandoned structures along the shore such as boat slips.

Once a site and geometry have been determined, perimeter dikes are constructed using the most economical material available. Often the dikes consist of uncontaminated dredge material that is hydraulically placed along the dike alignment by pipelines connected directly to cutterhead dredges. The dike material may range in size from silt to coarse sand. Organic soils are usually not recommended due to stability problems, and

hydraulically placed clay sediments, although generally suitable for the dike, require a long time for consolidation to occur and may not be desirable (Hammer and Blackburn, 1977). Coarser materials have also been used for perimeter dikes such as the Monroe Harbor CDF which was constructed of crushed limestone (Moloney and O'Bryan, 1984). In this particular facility, grout-filled mattresses were placed against the inside of the dikes to minimize seepage through the permeable rock material. Dike materials that are placed below the water level are allowed to reach their angle of repose and may be further shaped using draglines.

Once the CDF has been constructed, contaminated dredge material is pumped inside the perimeter dikes from a pipeline attached directly to a cutterhead dredge or from pipes connected to a barge or hopper dredge containing the dredge material slurry. The CDF then acts as a sedimentation basin, allowing the suspended solids to settle out within the confines of the perimeter dikes while allowing the supernatant liquid to return back to the waterway through a weir or other outlet structure. Figure 2-2 shows a plan view of a typical CDF in operation. As indicated above, this effluent must meet the criteria dictated by the Federal Water Pollution Control Act.

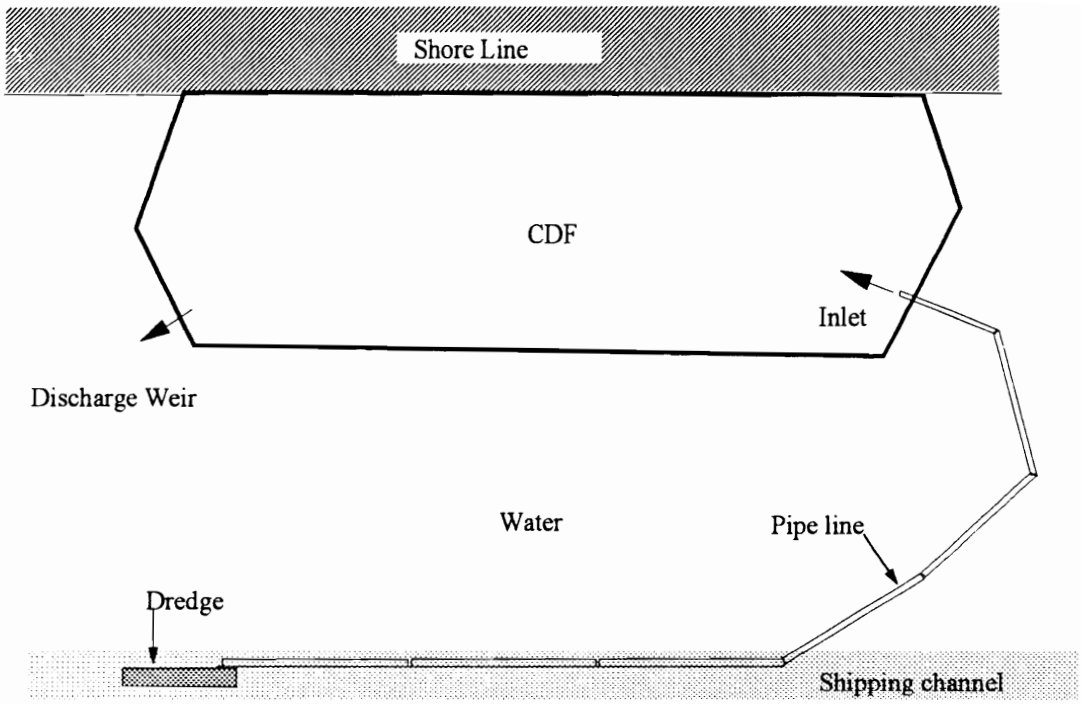

FIGURE 2-2: Plan View of a CDF being Filled by a Dredge.

CHAPTER 3

Movement of Contaminants through Porous Media

3.1 General

The objective of this study is to evaluate the movement of contaminants through confined disposal facilities and into the surrounding waters. Two general processes must be considered in order to accomplish this objective: (1) fluid flow through porous media, and (2) contaminant mass transport through porous media. A description and a derivation of the governing equations for each of these processes will be given in this chapter.

3.2 Fluid Flow through Porous Media

3.2.1 Darcy's Law

The fundamental relationship for evaluating fluid flow through porous media is the following well-known equation developed by Darcy in 1856:

$$v = K\frac{dh}{dL} \tag{3.1}$$

where v is the specific discharge, K is the coefficient of hydraulic conductivity and dh/dL is the hydraulic gradient (change in total head h over the flow length L). The total head can be separated into the elevation head (y) and pressure head (ψ) as:

$$h = y + \psi \tag{3.2}$$

The above equation ignores the velocity head because flow velocities through porous media are usually very small. Although Darcy developed Equation 3.1 from soil laboratory test results, several investigators have derived this equation based on simplifications of the Navier-Stokes equations (Harr, 1962 and Hubbert, 1956).

The governing equations for saturated and unsaturated fluid flow through porous media presume the validity of Darcy's law. However, it is widely acknowledged that Darcy's law is not always valid for flow in coarse grained media when the flow velocity

becomes too large. The dimensionless Reynolds number (R_e) is commonly used as the criterion to evaluate the validity of Darcy's law. It is given as:

$$R_e = \frac{qd}{\mu} \tag{3.3}$$

where q is the discharge, μ is the kinematic viscosity of the pore water and d is the length of a flow path, usually taken as the average grain size diameter. Muskat (1937), Harr (1962) and Bear (1979) indicate that Darcy's law should be valid in coarse soils as long as Reynolds number does not exceed a value of about one. Fishel (1935) ran tests on sand with very low hydraulic gradients (thus the discharge and Reynolds number were also low). He found that Darcy's law was valid for gradients as low as 2 to 3 inches per mile. Consequently, there does not appear to be a lower limit of R_e beyond which Darcy's law is not valid for coarse-grained soils.

Laboratory tests performed on saturated fine grained soils have also shown that Darcy's law is not always valid. Lutz and Kemper (1959) found that the specific discharge through saturated clay samples increased at a greater rate than predicted by Equation 3.1. They suggest that this behavior may be attributed to adsorbed cations in the diffuse double layer. Hansbo (1960) observed similar results for tests performed on undisturbed fat clay (CH) samples. Hansbo found that the relationship became linear at hydraulic gradients above about 9. He proposed that the nonlinear behavior may be caused by clay particle migration during flow which clogs and unclogs the pores of the soil. Miller and Low (1963) did not observe any flow below a certain threshold hydraulic gradient in their laboratory tests on bentonite. The threshold gradient varied between 10 and 75 depending in the amount of clay in the sample. They proposed that the water adsorbed between the clay particles has a "quasi-crystalline" structure which is semi-rigid until the gradient is large enough to break the structure and allow water to flow. This is further explained by

Low (1961). A summary of the above theories can be found in Scheidegger (1974). Mitchell and Younger (1966) suggested that the difficulty of performing laboratory tests on low permeability soils may be responsible for the observed deviations from Darcy's law. These deviations may easily be attributed to experimental error such as minute leakage of the test apparatus, biological growth within the sample during the test, etc. They also pointed out that standard laboratory permeability tests are performed at hydraulic gradients that are almost always considerably greater than the field gradient. Thus, the hydraulic conductivity value determined in the lab may be greater than the actual field value. Since there is no generally accepted theory which describes the above observations, Darcy's law will be assumed to be valid for saturated fine grained soils in this study. In unsaturated media, Darcy's law can also be assumed to be valid as indicated by Irmay (1954) and Freeze and Cherry (1979).

3.2.2 Derivation of the Governing Equation

Contaminants that are released into the subsurface may undergo both unsaturated and saturated flow. For example, a pollutant originating from a source located above the groundwater table will generally travel downward through the vadose zone until it reaches the groundwater table. In most cases the pollutant will then move in the general direction of the groundwater flow within the saturated zone. Thus, the solution of this problem requires the consideration of both the flow through the unsaturated zone and the saturated zone. The line of separation between these two zones is often called the groundwater table. Figure 3-1 shows a cross section for a typical soil profile and a corresponding plot of the variation of the static pore water pressure with depth. As indicated, the pore pressure is negative above and positive below the groundwater table.

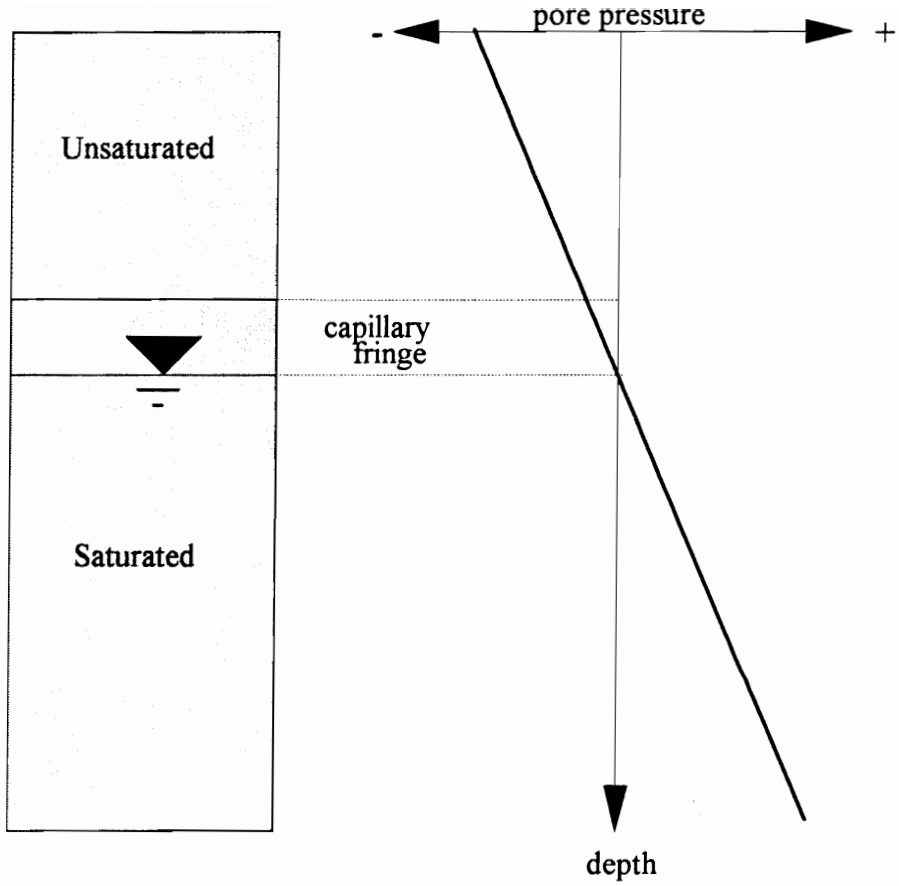

FIGURE 3-1: The Variation of Static Pore Pressure with Depth in a Porous Medium.

Note that a zone of saturated soil exists above the groundwater table. The soil in this zone, called the capillary fringe, is saturated due to the affect of capillary rise which pulls water upward into the pores of the soil due to surface tension forces. Thus, the definition of the groundwater table may be more accurately defined as the locus of points where the pore water pressure is zero.

Consider the control element of a porous media shown in Figure 3-2. The element has a fixed position and boundaries in the medium but the amount of water within the element may change with time. Let ρV_x and ρV_y equal the mass rate of fluid flow into the element in the x and y directions, respectively, where ρ is the fluid density and V_i is the specific discharge in the i-direction. The amount of water contained in the porous medium can be expressed as ρnS where n is the porosity and S is the degree of saturation. For the control element, the law of conservation of mass can be stated as follows: the difference between the rate of water flowing into the element and the rate of water flowing out of the element must equal the rate at which the amount of water stored in the element changes with time. This can be written mathematically as:

$$\rho V_x + \rho V_y - \left[\rho V_x + \frac{\partial}{\partial x}(\rho V_x) + \rho V_y + \frac{\partial}{\partial y}(\rho V_y) \right] = \frac{\partial}{\partial t}(\rho n S) \tag{3.4}$$

The left side of Equation 3.4 can be simplified, and the right side can be expanded according to the chain rule to obtain:

$$-\frac{\partial}{\partial x}(\rho V_x) - \frac{\partial}{\partial y}(\rho V_y) = \rho n \frac{\partial S}{\partial t} + \rho S \frac{\partial n}{\partial t} + n S \frac{\partial \rho}{\partial t} \tag{3.5}$$

The last two terms on the right side of Equation 3.5 can be omitted since the change in porosity and fluid density with time is usually very small. In fluid flow through a porous medium, it is convenient to express the degree of saturation (S) as θ/n, where θ is the

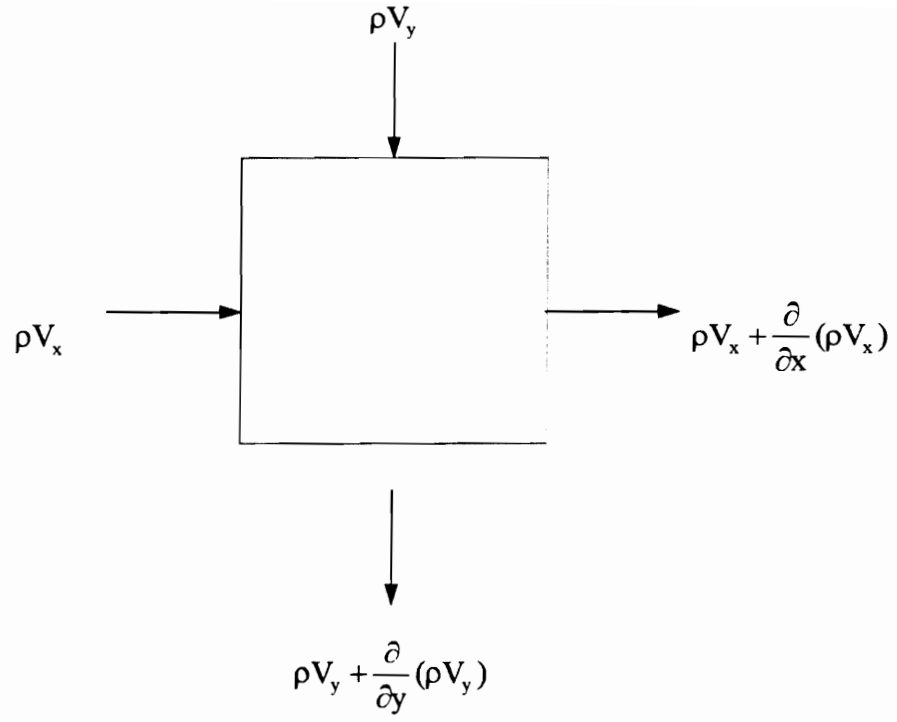

FIGURE 3-2: Control Element for Derivation of the Governing Equation for Fluid Flow.

volumetric water content (the volume of water divided by the total volume of the medium). Making the above changes, Equation 3.5 can be written as:

$$-\frac{\partial}{\partial x}(\rho V_x)-\frac{\partial}{\partial y}(\rho V_y)=\rho n\frac{\partial}{\partial t}\left(\frac{\theta}{n}\right) \tag{3.6}$$

If the density of the permeating fluid is constant, it can be divided from both sides of Equation 3.6. Darcy's law can be substituted for V_x and V_y in the left side of 3.6, and the right side can be simplified to obtain the following:

$$\frac{\partial}{\partial x}\left(K_x\frac{\partial h}{\partial x}\right)+\frac{\partial}{\partial y}\left(K_y\frac{\partial h}{\partial y}\right)=\frac{\partial \theta}{\partial t} \tag{3.7}$$

In the above equation, K_x and K_y are the unsaturated coefficients of hydraulic conductivity which are functions of the pressure head ψ. These coefficients will be discussed in Section 3.2.4. Equation 3.2 can be substituted for h in the right side of the above equation to obtain:

$$\frac{\partial}{\partial x}\left(K_x\frac{\partial h}{\partial x}\right)+\frac{\partial}{\partial y}\left(K_y\frac{\partial h}{\partial y}\right)=C_m\frac{\partial h}{\partial t} \tag{3.8}$$

where C_m equals $\partial\theta/\partial\psi$ and is called the ***coefficient of moisture capacity*** or ***specific moisture capacity***. In order to solve this equation, the coefficient of moisture capacity and the unsaturated coefficients of hydraulic conductivity must be determined. Methods for finding these parameters are described in the sections below.

Equation 3.8 is the governing equation for transient unsaturated flow through porous media. Note that the right side of the equation equals zero during steady state

flow. Also, K_x and K_y are constant in the saturated zone. Thus, Equation 3.8 reduces to the following well known Laplace equation for steady state saturated flow:

$$K_x \frac{\partial^2 h}{\partial x^2} + K_y \frac{\partial^2 h}{\partial y^2} = 0 \qquad (3.9)$$

3.2.3 Coefficient of Moisture Capacity, C_m

As indicated in Figure 3-1, pore water pressures become larger (more negative) with distance above the groundwater table due to capillary forces. It is apparent that the moisture content and degree of saturation will decrease with distance above the groundwater table. Thus, the moisture content decreases with decreasing pore water pressure. The relationship between these two parameters is needed to evaluate C_m and can be determined from laboratory or field tests. A brief description of laboratory methods is presented below. Detailed information regarding sample preparation, fluid properties, equipment, etc. can be found in Klute (1986).

In laboratory suction tests, a soil sample is placed on a saturated porous stone in a pressure chamber. If the sample is not already saturated, back pressure is sometimes applied to bring the specimen to 100 percent saturation. A constant suction pressure is then applied to the sample through the porous stone until pore water stops flowing out of the sample. Klute (1986) states that it may take 1 to 7 days before equilibrium is reached depending on the soil type. The volumetric water content of the soil can then be obtained if the amount of water removed from the sample is recorded. Thus, the water content resulting from a given suction pressure can be determined. This procedure is repeated with higher suction pressures to develop a θ - ψ relationship. The resulting S shaped curve is called a ***soil water retention curve***. A typical soil water retention curve is shown in Figure 3-3. The slope of this curve is the coefficient of moisture capacity. The moisture content at saturation is designated as θ_s. Note that at large negative pressures, the curve

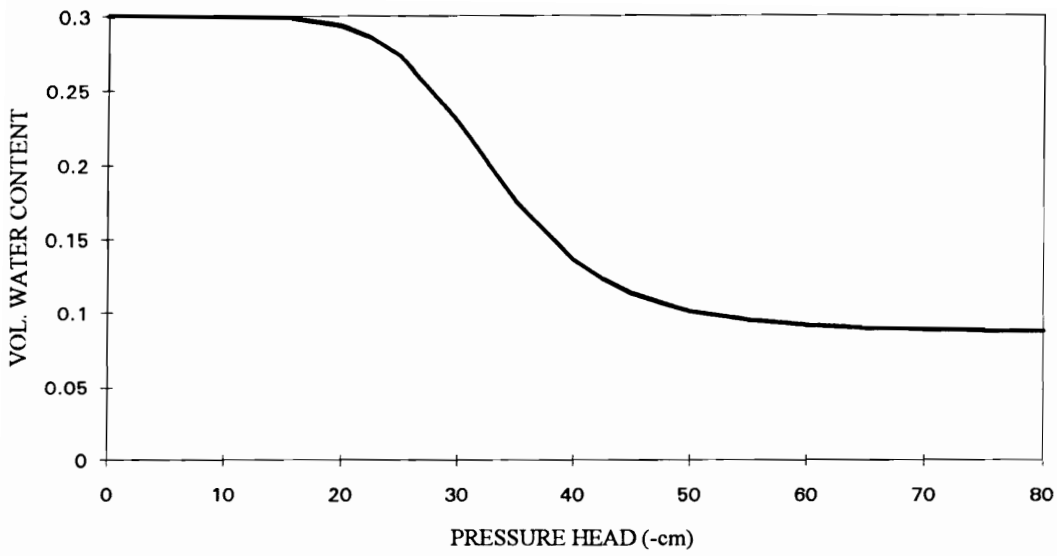

FIGURE 3-3: Typical Soil Water Retention Curve.

in Figure 3-3 becomes approximately asymptotic to a moisture content of 0.1. This value is called the ***residual*** moisture content or ***irreducible*** moisture content (θ_r). The θ - ψ relation can also be determined in a test which forces water into a dry soil sample rather than sucking moisture out of the sample. This test gives a water retention curve with a slightly different S shape. Thus, there is a hysteresis effect which describes the soil behavior. Consequently, different values for C_m, θ_s and θ_r would be obtained for the same soil. Thus, it may be important to conduct the test consistent with the anticipated field conditions.

3.2.4 Unsaturated Hydraulic Conductivity

Evaluation of fluid flow in the vadose zone requires the determination of the unsaturated hydraulic conductivity, K_u. Various laboratory and field methods are available to determine this parameter. These methods are summarized by Klute and Dirksen (1986) and Green et al. (1986). Maulem (1986) lists several drawbacks of direct measurement of K_u through laboratory and field tests. He states that the tests are often expensive and time consuming because numerous measurements are needed due to the variability of the soil. Consequently, many researchers have developed empirical relationships to predict K_u. Others have attempted to derive equations for K_u from analytical and statistical techniques. Good discussions of these methods can be found in Brutsaert (1967) and Maulem (1986). A brief overview of the various methods used to predict the unsaturated hydraulic conductivity is presented below.

Two terms frequently found in the literature are ***relative hydraulic conductivity*** and ***effective saturation***. Relative hydraulic conductivity (K_r) is defined as the ratio of the unsaturated hydraulic conductivity (K_u) to the saturated hydraulic conductivity (K_s), or:

$$K_r = \frac{K_u}{K_s} \tag{3.10}$$

Effective saturation (S_e) is defined as:

$$S_e = \frac{\theta - \theta_r}{\theta_s - \theta_r} \tag{3.11}$$

The θ_i terms are the same as those defined above. It can be seen that S_e equals one when θ equals θ_S.

Poblubarinova-Kochina (1962) reports that Averjanov was one of the earliest investigators of unsaturated hydraulic conductivity. In 1950, he considered water flow in unsaturated porous media to be approximately equivalent to water flow through a cylindrical pipe, of which the center portion of the pipe was filled with air. He assumed that the water velocity on the pipe edges was negligible, but that the velocity was maximum at the air-water interface. Using these boundary conditions and the Navier-Stokes equations for fluid flow, he developed an equation for discharge through the pipe. The water content of the model could be varied depending on the radius of the air space within the pipe. Thus, his model related discharge to the moisture content. Once the discharge was known, Darcy's law was used to find the hydraulic conductivity. Averjanov did this for a pipe with air and water, and for a pipe flowing full of water and obtained the following expression for relative hydraulic conductivity:

$$K_r = S_e^{3.5} \tag{3.12}$$

The exponent 3.5 was selected as the best fit from experimental data.

Many other researchers have used the Hagen-Poiseuille equation for flow through a thin capillary tube to model flow through the pores. This equation, developed experimentally by Hagen in 1839, and independently by Poiseuille in 1840 (Streeter and Wylie, 1979) is given by:

$$v = \frac{r^2 \Delta P}{8 \mu L} \tag{3.13}$$

where:

v = average velocity in the tube
r = tube radius
μ = fluid viscosity
ΔP = pressure drop over distance, L.

This equation, used in conjunction with Darcy's law, enables the derivation of an expression for hydraulic conductivity. The only difficulty is selecting the appropriate value(s) for the radius. Irmay (1954) used this procedure and found that the radius drops out of the expression when evaluating the relative hydraulic conductivity. He found that K_r could be defined as:

$$K_r = S_e^3 \tag{3.14}$$

Note the similarity between Equations 3.12 and 3.14.

Purcell (1949) modeled the porous media as a bundle of parallel capillary tubes with equal lengths but varying radii. He related pore radius to capillary pressure using the capillary law given by:

$$r = \frac{2\sigma \cos\theta_c}{P_c} \tag{3.15}$$

where r = pore radius
σ = surface tension
θ_c = angle between capillary tube and air-water interface
P_c = capillary pressure.

He substituted this expression for radius into the Hagen-Poiseuille equation. He defined the total flow through the porous medium as the sum of the flow through each capillary tube. Purcell also included a tortuosity factor (ξ) to account for the tortuous path a particle of water would follow through the soil pores. Assuming typical values of σ and θ_c, he obtained the following expression for saturated hydraulic conductivity:

$$K_s = 0.66 \cdot \xi \cdot n \cdot \int_{S=0}^{S=1} \frac{dS}{P_c^2} \tag{3.16}$$

where S equals saturation. He performed lab tests to obtain the saturated hydraulic conductivity and the capillary pressure versus saturation curve. He found ξ to be 0.216 by back calculation.

Gates and Lietz (1950) suggested that the unsaturated hydraulic conductivity would have the same form as Purcell's equation except that the integral limits should vary from 0 to S. Thus, the relative hydraulic conductivity reduces to the form of:

$$K_r = \frac{\int_0^S \frac{dS}{P_c^2}}{\int_0^1 \frac{dS}{P_c^2}} \tag{3.17}$$

Laboratory determined values of K_r were lower than values predicted by (3.17). They suggested that the tortuosity factor ξ must be different in unsaturated flow than in saturated flow.

Willie and Spangler (1952) considered a porous medium to consist of parallel "channels" with arbitrary shapes but constant cross sections. They used the Kozeny-Carman equation which was derived from the Hagen-Poiseuille equation by replacing the radius in Equation 3.13 with a hydraulic radius. Details about the Kozeny-Carman equation can be found in Wyllie and Gardner (1958a). The final form of their equation for K_r was:

$$K_r = \left[\frac{F}{F_e \cdot S}\right]^2 \frac{\int_0^S \frac{dS}{P_c^2}}{\int_0^1 \frac{dS}{P_c^2}} \tag{3.18}$$

where F and F_e are electrical resistance factors obtained in the lab which are an indirect measure of the tortuosity of the medium.

Burdine (1953) studied experimental results on petroleum reservoir rocks in an attempt to better define the tortuosity factor. He observed an almost identical relationship between S_e and ξ. Thus, he derived the following equation for K_r:

$$K_r = S_e^{\,2} \frac{\int_0^S \frac{dS}{P_c^2}}{\int_0^1 \frac{dS}{P_c^2}} \tag{3.19}$$

Wyllie and Gardner (1958b) derived an expression for K_r identical to Equation 3.19 by modeling the porous media as a bundle of capillary tubes with varying radii. However, they used a statistical approach to define the distribution of the pore radii within the medium.

Brooks and Corey (1964) found from a number of tests on porous rocks that the integral ratio of Equation 3.19 reduced to S_e^2. Thus, the relative permeability could be written as:

$$K_r = S_e^4 \tag{3.20}$$

Childs and Collis-George (1950) developed a statistical method of calculating K_r. Their model also considered the porous medium to consist of a bundle of capillary tubes with varying radii. However, they took into account the variation of pore sizes perpendicular to and parallel with the direction of water flow. Using the Kozeny-Carman equation, they derived an equation for K_u as:

$$K_u = M \sum_{r=0}^{r=R} \sum_{l=0}^{l=R} r^2 f(r)dr \cdot f(l)dr \tag{3.21}$$

where M is a constant based on geometry and fluid characteristics and R is the radius for a given moisture content. The term inside the summation symbol includes the term for the distribution of the pore radii in the medium. The pore size distribution can be readily obtained from capillary pressure versus moisture content (or saturation) curves since pore radius is related to pressure according to Equation 3.15. A description of this procedure can be found in Brutsaert (1966). A similar approach was performed by Marshall (1958) and Millington and Quirk (1960).

Mualem (1976) developed a modified version of the Childs and Collis-George model by including a tortuosity factor expressed as a power function of the effective saturation. Thus, he obtained:

$$K_r = S_e^{\,n} \cdot \left[\frac{\int_{R_{min}}^{R} r \cdot f(r) dr}{\int_{R_{min}}^{R_{max}} r \cdot f(r) dr} \right]^2 \qquad (3.22)$$

Here R_{max} and R_{min} refer to the maximum and minimum pore radius, respectively. He found that n = 1/2 from a regression analysis. By substituting the relationship between capillary pressure and pore radius, Equation 3.22 becomes:

$$K_r = S_e^{0.5} \left[\frac{\int_{0}^{\theta} \frac{d\theta}{d\psi}}{\int_{0}^{\theta_{sat}} \frac{d\theta}{d\psi}} \right]^2 \qquad (3.23)$$

where ψ equals the capillary pressure, P_c. Maulem compared his model with those of Millington and Quirk (1960) and Wyllie and Gardner (1958) for lab tests of 45 soils and found it to produce results in better agreement with the experimental values.

In order to incorporate Mualem's equation into numerical analyses, van Genuchten (1980) developed an equation for the θ - ψ relationship so that the integrals in Equation 3.23 would reduce to a closed form solution. He found that the S-shaped water retention curve could be defined by:

$$\theta = \frac{1}{[1+(\alpha\psi)^n]^m} \tag{3.24}$$

where α, m, and n are curve fitting parameters that describe the shape of the curve. Van Genuchten recommended that :

$$m = 1 - 1/n \tag{3.25}$$

The coefficient of moisture capacity can be obtained by taking the derivative of Equation 3.24 to obtain:

$$C_m = \frac{\partial\theta}{\partial\psi} = \left[\frac{-\alpha m(\theta_s - \theta_r)}{1-m}\right] S_e^{-m}(1 - S_e^{-m})^m \tag{3.26}$$

Rearranging equation 3.31 to give ψ as a function of θ, substituting this expression into Equation 3.23 and simplifying gives the following equation for relative hydraulic conductivity:

$$K_r(\psi) = \frac{[1-(\alpha\psi)^{n-1}(1+[\alpha\psi]^n)^{-m}]^2}{[1+(\alpha\psi)^n]^{\frac{m}{2}}} \tag{3.27}$$

Thus, the van Genuchten model gives closed form solutions for C_m and K_r if θ_s, θ_r, α and n are known. The author describes a procedure which can be used to determine α and n from soil water retention curves. He also developed a nonlinear least squares program that solves for these parameters. To evaluate the reliability of the above expressions, van Genuchten (1980) determined θ_s, θ_r, α and n from soil water retention curves for four soils and a sandstone. He then used his model to predict K_r for various values of ψ and

compared these values to experimentally determined values. He found very good agreement between the predicted and measured values of K_r.

Other researchers have used van Genuchten's model and have also obtained good agreement between predicted and measured values of relative (and unsaturated) hydraulic conductivity. Stephens and Rehfeldt (1985) obtained good predictions for a fine sand sample. Dane (1980) performed in-situ tests to obtain K_u. He found that van Genuchten's model yielded similar results. Hopmans and Dane (1986) found that reasonably accurate results were obtained for a sandy loam using the van Genuchten model. Milks et al. (1989) evaluated the utility of the van Genuchten model for containers used in horticulture. These containers sometimes consist of clay, bark, peat and/or vermiculite. They found that the van Genuchten model predicted the shape of the θ - ψ curve very well. Wallach et al. (1992a, 1992b) also evaluated the model for horticultural uses. They ran soil water retention and unsaturated hydraulic conductivity tests on materials commonly used in Israel, including grape seeds, volcanic tuff and scoria. They also obtained very good agreement between the predicted and measured K_r values. A list of some of the θ_s, θ_r, α and n values obtained by several authors is included in Table 3-1. Based on the generally good agreement of numerous investigators with various porous materials, the van Genuchten model was incorporated in POLUT2D to define C_m and K_r.

3.2.5 Hydraulic Conductivity of Soils Permeated by Contaminants

The hydraulic conductivity of soil for seepage problems is normally evaluated in the laboratory using distilled or tap water. However, in contaminant transport problems, the permeating fluid in the field will contain either chemicals dissolved in the groundwater or non-aqueous fluids. Thus, an estimate of the hydraulic conductivity of the soil to the actual permeant must be obtained. Research conducted on fine-grained soils has shown

TABLE 3-1: Measured Values of the van Genuchten Model Parameters for Various Soil Types.

Soil Type	α (cm^{-1})	n	θ_s	θ_r	Reference
Silt loam	0.005	7.14	0.47	0.19	van Genuchten (1980)
Clay	0.0015	1.17	0.45	0.0	
Loamy sand	0.0355	2.78	0.35	0.06	Dane (1980)
Fine sand	0.0327	3.57	0.34	0.07	Stephens and Rehfeld (1985)
Sandy loam	0.0153	1.28	0.36	0.07	Parker et al. (1985)
Silt loam	0.0346	1.28	0.39	0.10	
Clay	0.0007	1.43	0.59	0.11	
Clay loam	0.003	1.79	0.62	0.25	Milks et al. (1989)

that some inorganic and organic contaminants can significantly affect the hydraulic conductivity. The influence of various contaminants on the permeability of fine-grained soils is presented below. Additional information can be found in Mitchell and Madsen (1987) and Daniel (1993).

The effect of inorganic salt solutions in the pore water of saturated clay samples was demonstrated by Fireman (1944). His tests showed one to two orders of magnitude increase in the coefficient of hydraulic conductivity for salt solutions (sodium and calcium chloride) compared to distilled water as the permeant. Similar results were obtained by McNeal and Coleman (1966) and Ho and Pufahl (1987). Alther et al. (1985) evaluated the hydraulic conductivity of a bentonite slurry filter cake to 16 salt solutions. They observed an increase in hydraulic conductivity as the concentration of the salt solution increased. In addition, divalent cation solutions had a larger coefficient of hydraulic conductivity than monovalent cation solutions. They proposed that the observed permeability increase can be explained by the Gouy-Chapman diffuse double layer theory which states that the thickness of the double layer is proportional to the pore water electrolyte concentration and cation valence. This can be written as:

$$T \propto \sqrt{\frac{D}{n_o v_c^2}} \tag{3.28}$$

where T equals the double layer thickness, D is the dielectric constant of the fluid in the pores, n_o is the concentration of the pore water electrolyte, and v_c is the cation valence (Daniel, 1993). If the thickness of the diffuse double layer reduces (due to an increase in n_o or v_c), there is a tendency for a flocculated structure to form which allows higher flow through the soil.

Equation 3.28 also indicates that the thickness of the diffuse double layer will decrease if the dielectric constant (D) decreases. Organic permeants such as xylene,

benzene, and acetone have dielectric constants of about 2.5, 2.3 and 21.5, respectively, whereas water has a dielectric constant of about 80. The effect of these low dielectric constants is seen in the work of Fernandez and Quigley (1985), Bowders and Daniel (1987), and Budhu et al. (1991) where higher coefficients of hydraulic conductivity were observed when these and other organic fluids were used to permeate soil specimens as compared to water. Bowders and Daniel (1987) compared the results of permeability tests using dilute (53 mg/L) and pure concentrations of heptane as the permeant. The dielectric constant for the dilute and pure concentrations were 80 and 2, respectively. The laboratory tests showed little to no difference between water and dilute heptane coefficients of hydraulic conductivity, but the pure heptane permeant yielded a hydraulic conductivity 2 orders of magnitude higher than that with water as the permeant.

The effect of acidic and caustic fluids on the permeability of kaolinite and montmorillonite soils was studied by Lentz et al. (1987). They found that the hydraulic conductivities were not significantly affected using permeant solutions with pH values of 1, 3, 5, 9, 11 or 13. Similar results were obtained by Peterson and Gee (1987) who evaluated the effect of acidic main tailings leachate (pH = 2) on natural clay soils. Gipson (1987) performed hydraulic conductivity tests on natural clay soils and on a silty sand-bentonite mixture using an acid liquor with a pH of 2.2. The coefficients of hydraulic conductivity for the natural soils using the acid as a permeant was somewhat lower than the same soils using tap water as the permeant. Gipson believes this may be attributed to the precipitation of minerals in the pore spaces. The silty sand-bentonite mixture, however, showed a permeability increase of more than an order of magnitude when the acidic permeant was used as compared to tap water. It appears that bentonite is dissolved by acidic solutions which causes the hydraulic conductivity to increase. This is also indicated by Daniel (1993) and Mitchell and Madsen (1987).

Many have studied the influence of the type of permeameter on the results of hydraulic conductivity tests. Foreman and Daniel (1986) conducted permeability tests on kaolinite and two natural clays using a flexible wall permeameter, a rigid wall compaction mold and a consolidometer. They obtained similar permeabilities using each apparatus when water was used as the permeant. However, the rigid compaction mold device gave higher hydraulic conductivities than the other permeameters when pure organic liquids (methanol and heptane) were used as the permeants. They suggested that the higher value was due to shrinking of the clay specimen induced by the organic permeant which allowed for leakage between the soil and the side of the mold. Similar results were obtained by Brunelle et al. (1987) using an actual landfill leachate consisting of heavy metals, arsenic and organics such as toluene and ethyl benzene. Anderson (1982) reported the results of permeability tests using a rigid wall permeameter on four clay soils using organic liquids including methanol and xylene as permeants. Coefficients of hydraulic conductivity were one to three orders of magnitude higher than those where water was used as the permeant. Similar increases in permeability were obtained by Anderson et al. (1985) using the same permeants in a double-ring fixed wall permeameter. Uppot and Stephenson (1989) used a flexible wall permeameter to test the permeability of kaolinite and montmorillonite using the same permeants. The permeabilities for the soils showed an increase by factors of only 2 to 3 when compared to the water based permeabilities. They suggest that the large permeability increases reported in the literature are caused by the leakage between the soil and permeameter when rigid wall devices are used rather than any significant effect of the permeant. Additional information regarding the advantages and disadvantages of flexible and fixed wall permeameters and consolidometers is presented in Zimmie (1981), Daniel et al. (1985) and Mitchell and Madsen (1987).

In conclusion, it is recommended that hydraulic conductivity testing of soils be performed using the permeant which the soil is expected to be exposed. Most research seems to indicate that flexible wall permeameters or consolidometers should be used rather than fixed wall permeameters. In should be noted that very little information is available regarding the effect of inorganic or organic contaminants on silt or coarse-grained soils. These soils do not contain a diffuse double layer and would not be affected by the mechanisms described above. However, highly acidic permeants may cause solutioning of the soil matrix which could in turn increase the hydraulic conductivity of the soil.

3.3 Contaminant Transport through Porous Media

3.3.1 Mechanisms of Contaminant Transport

In order to derive the equation which governs the migration of contaminants through porous media, it is helpful to first evaluate the mechanisms which are responsible for transport. These mechanisms include advection, mechanical dispersion, molecular diffusion, sorption, radioactive decay, biodegradation, etc. Depending on the nature of the contaminant and the porous medium, each of these mechanisms may be occurring simultaneously to increase or decrease the rate at which the contaminant is transported. A description of these mechanisms is presented below.

3.3.1.1 Advection

When a contaminant is released into the subsurface, it is spread through the medium by the movement of the groundwater. This simple transport mechanisms is called ***advection***. The rate of contaminant movement due to advection alone is equal to the average linear velocity of the groundwater. Thus, if a contaminant (solute) is released into the groundwater at some point, it should be possible to calculate the arrival time of the contaminant at some location down gradient. However, it has been observed in laboratory

and field tests that a small amount of the solute arrives at the down gradient point before the estimated arrival time. This phenomena is due to ***mechanical dispersion*** and ***molecular diffusion***. These two mechanisms are often collectively termed as ***hydrodynamic dispersion***.

3.3.1.2 Mechanical Dispersion

Figure 3-4 shows how a typical water soluble contaminant might spread through a porous medium with time. In Figure 3-4a, the contaminant is continuously entering the subsurface through a point source, whereas in Figure 3-4b the contaminant is instantaneously released into the medium at a point. Note that in both cases the resulting plume increases in size as it moves in the direction of groundwater flow. Plume spreading in the direction perpendicular to flow is called ***transverse dispersion***; spreading in the direction of flow is called ***longitudinal dispersion***. As readily seen in Figure 3-4, longitudinal dispersion is greater than transverse dispersion. Both of these types of dispersion are caused by microscopic and macroscopic heterogeneities (National Research Council, 1990). Figure 3-5a shows an enlarged cross section of a hypothetical porous medium. The tortuous flow path around soil particles causes dissolved contaminants to spread out as the plume advances. Freeze and Cherry (1979) state that dispersion is also caused by microscopic variation of the velocity within the individual pore channels and between adjacent pore channels. All of these are examples of microscopic heterogeneity. Figure 3.5b shows how dispersion may occur due to soil variability on the macroscopic (regional) scale.

3.3.1.3 Molecular Diffusion

Spreading of a contaminant plume can also be attributed to a mechanism known as molecular diffusion. Molecular diffusion occurs when dissolved pollutant ions in the

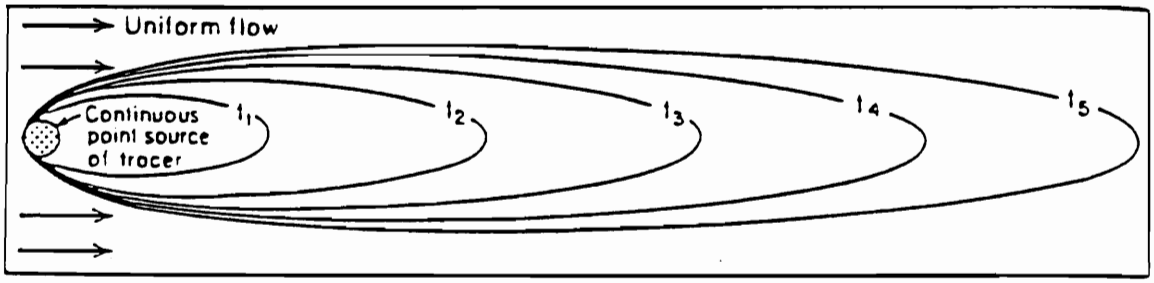

(a)

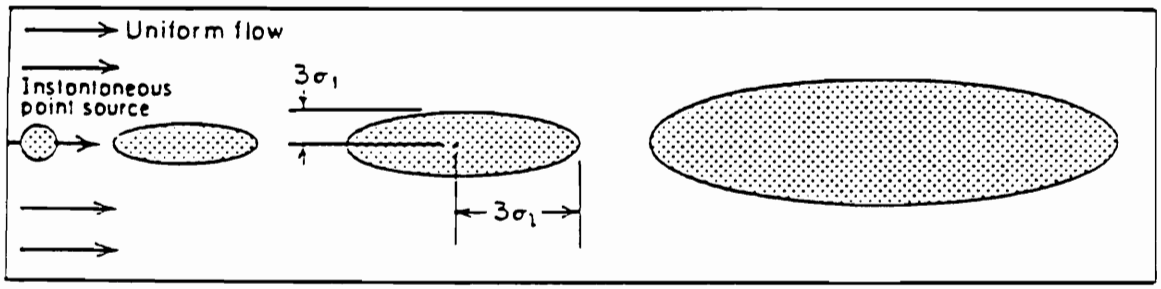

(b)

FIGURE 3-4: Dispersion of a Contaminant Plume from: (a) a Continuous Point Source, and (b) an Instantaneous Point Source (After Freeze and Cherry, 1979).

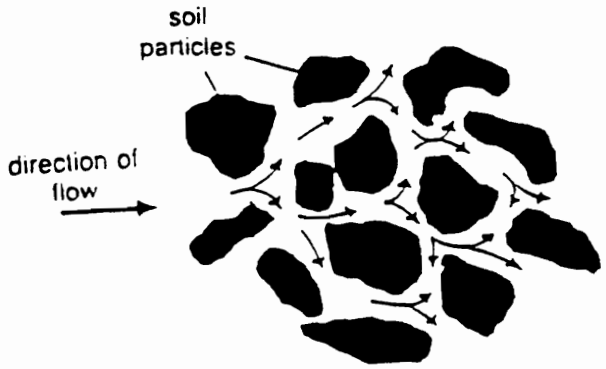

(a)

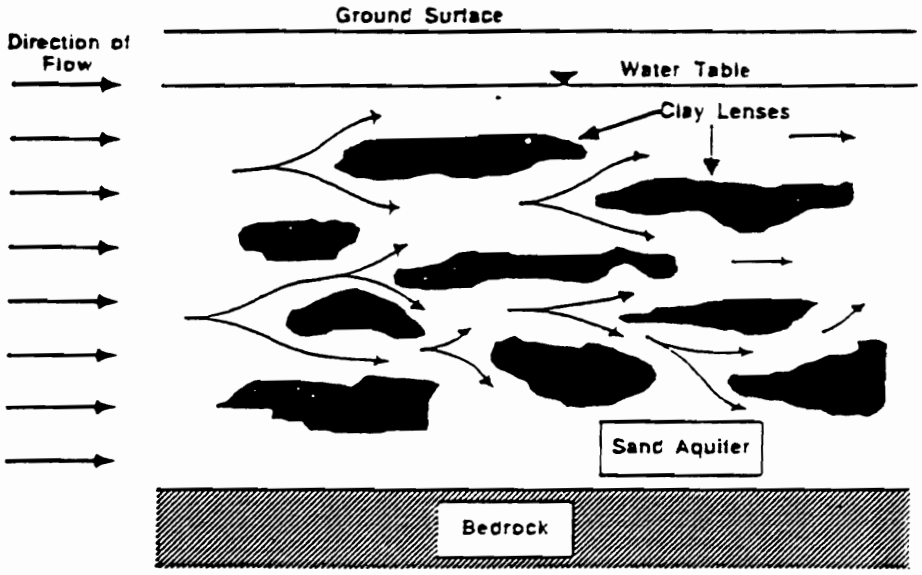

(b)

FIGURE 3-5: Dispersion of a Contaminant at the: (a) Microscopic Scale, and (b) Macroscopic Scale (After Fried, 1975 and Schackelford, 1993).

plume move from areas of high concentration to areas of low concentration. This is a result of the kinetic activity of the ions or molecules of the contaminant. Thus, the ions will tend to spread out away from the center of the plume until equilibrium is reached. Molecular diffusion, unlike advection and mechanical dispersion, does not depend on the velocity of the groundwater. Crooks and Quigley (1984) reported that a leachate spread through a clay landfill liner to distances of about 1.5 meters whereas seepage had only occurred for about 3 to 4 cm. Shackelford and Daniel (1991) state that diffusion, not hydraulic conductivity, governs the rate of contaminant transport through compacted waste disposal barriers. The overall effect of molecular diffusion is to spread out the plume causing dilution of the contaminant.

3.3.1.4 Sorption

Sorption is a general term that is used to describe the process whereby dissolved contaminants come out of solution and become attached to the surface or interior of a solid soil particle. The actual mechanism which causes sorption may be physical, chemical or both, and is often difficult to assess. However, a main cause of sorption may often be attributed to differences in ionic charge between the contaminant and the soil through which it is flowing. Heavy metal contaminants often exist in solution as cations which are attracted to negatively charged clay particles. These cations may adsorb to the clay particle to satisfy an overall negative charge or may exchange places with an existing cation already adsorbed onto the clay surface. Even organic molecules may exhibit an overall positive charge which would tend to adsorb to soil surfaces (Yong, et al., 1992). Anions (negatively charged ions) often adsorb to iron, aluminum and magnesium oxides on a soil surface. Non-charged organic molecules may be adsorbed onto the organic portion of the soil solids due to the hydrophobic (water hating) nature of the organic molecules (National Research Council, 1990).

From the discussion above, it can be seen that sorption is a process which reduces the concentration of dissolved contaminants in the groundwater and the extent to which the contaminants are spread. This is demonstrated by the curves in Figure 3-6. The dashed lines represent the position of an advancing plume if advection alone is considered. Curve a shows the variation of the concentration when hydrodynamic dispersion is also considered, and curves b and c show the combined effect of advection, hydrodynamic dispersion and sorption. As indicated, sorption reduces the extent of contaminant transport. Thus, sorption generally tends to keep a contaminant near the source of the release. It should be noted, however, that sorption is often reversible. As the plume advances beyond a particular location in the subsurface, desorption of the contaminant from the soil particle back into the groundwater may occur to maintain a concentration equilibrium.

3.3.1.5 Other Mechanisms

There are several other processes which can occur in the subsurface which affect contaminant transport. These mechanisms include:

- radioactive decay
- dissolution/precipitation
- hydrolysis
- biodegradation/biotransformation

These processes, like sorption, tend to reduce the rate and extent of contaminant transport through groundwater by removing the harmful compounds or causing them to precipitate out of the water, etc. The effect of these mechanisms is not considered in this study.

3.3.2 Derivation of the Governing Equation

3.3.2.1 Advection and Hydrodynamic Dispersion

The derivation which follows is adopted from Istok (1989) and Freeze and Cherry (1979) and assumes that the contaminant does not significantly effect the density of the

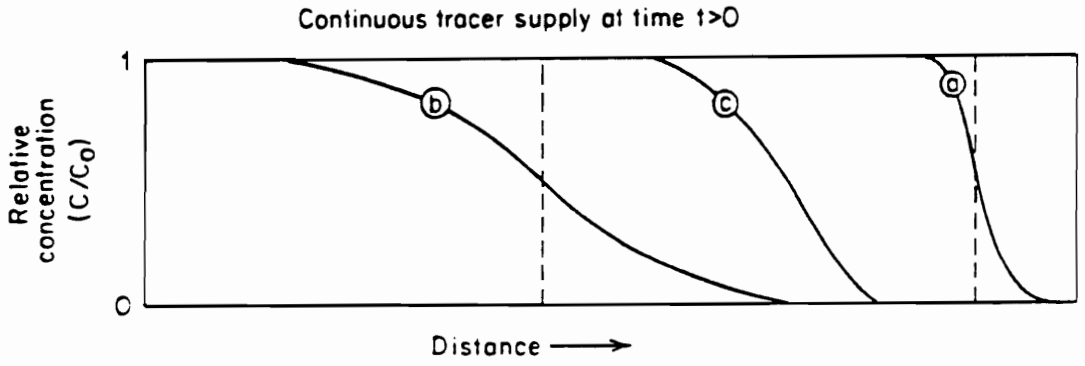

FIGURE 3-6: Effect of Advection, Hydrodynamic Dispersion and Sorption on the Time-Concentration Curve. (After Freeze and Cherry, 1979).

groundwater. Contaminant transport due to advection alone can be modeled as follows. Let C equal the concentration of the contaminant in the aqueous (liquid) phase with units of mass of solute per volume of solution. Contaminant transport flux due to advection in the x and y directions is defined by $V_x C$ and $V_y C$, where V_i are the Darcy velocities.

It is commonly assumed that hydrodynamic dispersion (mechanical dispersion and molecular diffusion) follows Fick's first law which states that the rate of mass dispersion (and diffusion) in a solution is proportional to the concentration gradient, or:

$$F = -D\frac{dC}{dx} \tag{3.29}$$

where D is the coefficient of hydrodynamic dispersion which contains the effect of both mechanical dispersion and molecular diffusion (Freeze and Cherry, 1979 and Bear, 1979). The negative sign is needed in the above equation because mass transport occurs from areas of high solute concentrations to areas of low solute concentration.

Bear (1979) summarizes the approaches that are commonly used to obtain the coefficient of hydrodynamic dispersion. A common approach is to consider the porous medium as a network of interconnected capillary tubes. This method was performed by Bear who derived an equation for D which is a function of pore geometry, tortuosity, and average linear velocity. The final form of the equation is given as:

$$\begin{aligned} D_x &= a_L \frac{V_x^2}{\overline{V}} + a_T \frac{V_y^2}{\overline{V}} + D_d \\ D_y &= a_L \frac{V_y^2}{\overline{V}} + a_T \frac{V_x^2}{\overline{V}} + D_d \end{aligned} \tag{3.30}$$

where a_L and a_T are the coefficients of longitudinal and transverse dispersivity, respectively, D_d is the coefficient of molecular diffusion, and $\overline{V}$ is the average velocity

given by $\sqrt{V_x^2 + V_y^2}$. It can be seen from the equation above that molecular diffusion dominates when the velocity is very low. Using the above expression for hydrodynamic dispersion, the contaminant transport flux due to mechanical dispersion and molecular diffusion can defined as $-D_i \partial\theta C / \partial x_i$, where θ accounts for the porosity of the medium.

Equation 3.30 contains three coefficients that need to be determined. Shackelford and Daniel (1991a and 1991b) and Shackelford (1991) give a very good description of molecular diffusion and the laboratory tests that have been used to determine D_d. Fick's first law, as presented by Equation 3.29, is also assumed to be applicable for molecular diffusion without mechanical dispersion. Fick's second law for transient conditions can be written as:

$$\frac{\partial C}{\partial t} = D_d \frac{\partial^2 C}{\partial x^2} \tag{3.31}$$

A typical laboratory test for determining D_d would consist of exposing one end of a cylindrical saturated soil sample to some type of tracer material in an enclosed container. The concentration of the tracer in the soil specimen with time and position is then obtained during the test. The resulting data is graphed, and the value for D_d is obtained by fitting the data with the numerical solution of Equation 3.31.

A similar method is used to evaluate the coefficients of longitudinal and transverse dispersivity. Klutz and Moser (1974) performed about 2500 lab tests on saturated sand to determine the longitudinal dispersivity. They found that a_L was affected by grain size and grain size distribution. However, the shape and angularity of the sand particles did not significantly influence a_L. Field methods are also performed to obtain data which is used to determine the dispersivity coefficients. Fried (1975) gives an overview of several of the procedures used and the techniques employed to determine dispersivity coefficients from

field data. A comparison between laboratory and field values has shown that lab testing consistently underestimates the values of the longitudinal and transverse dispersivity. Freeze and Cherry (1979) believe the variation is caused by heterogeneities which the small laboratory sample does not represent. Most investigators agree that lab values for dispersivity are not representative of the actual field values and should be treated with that perspective. Dispersivity values obtained from 59 field tests in various soils can be found in Gelhar, et al. (1992).

The derivation of the governing equations for contaminant transport which follows only considers the mechanisms of advection and hydrodynamic dispersion. The effect of sorption on this equation will be shown in subsequent paragraphs. Let the combined mass contaminant flux due to advection and hydrodynamic dispersion in the x and y directions be defined as F_x and F_y, respectively, where:

$$F_x = V_x C - D_x \frac{\partial \theta C}{\partial x}$$
$$F_y = V_y C - D_y \frac{\partial \theta C}{\partial y} \qquad (3.32)$$

Consider the control element of the porous medium shown in Figure 3-7. The element has a fixed position and boundaries in the medium but the amount of contaminant within the element may change with time. The law of conservation of mass states that the difference between the rate at which a contaminant enters the element and the rate at which a contaminant leaves the element must be equal to the rate at which the amount of contaminant contained in the element changes with time. This is written as:

$$F_x + F_y - \left(F_x + \frac{\partial F_x}{\partial x} + F_y + \frac{\partial F_y}{\partial y} \right) = \frac{\partial \theta C}{\partial t} \qquad (3.33)$$

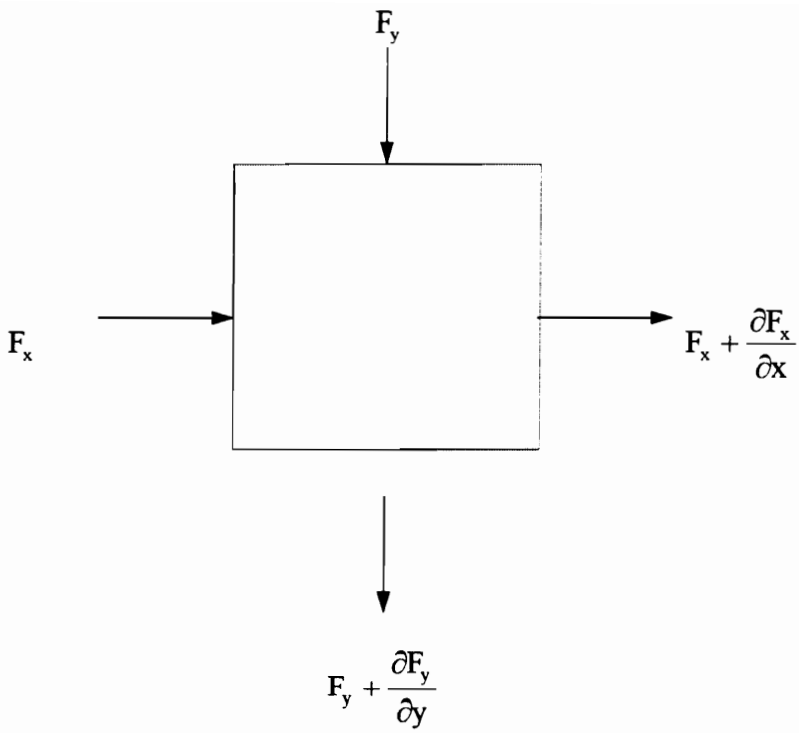

FIGURE 3-7: Control Element for Derivation of the Governing Equation for Contaminant Transport.

Equation 3.33 can be simplified as:

$$-\frac{\partial F_x}{\partial x}-\frac{\partial F_y}{\partial y}=\frac{\partial \theta C}{\partial t} \tag{3.34}$$

Substituting Equation 3.32 into 3.34 yields:

$$-\frac{\partial}{\partial x}\left[V_x C-D_x\frac{\partial \theta C}{\partial x}\right]-\frac{\partial}{\partial y}\left[V_y C-D_y\frac{\partial \theta C}{\partial y}\right]=\frac{\partial \theta C}{\partial t} \tag{3.35}$$

Taking the negative sign into the brackets gives:

$$\frac{\partial}{\partial x}\left[D_x\frac{\partial \theta C}{\partial x}-V_x C\right]+\frac{\partial}{\partial y}\left[D_y\frac{\partial \theta C}{\partial y}-V_y C\right]=\frac{\partial \theta C}{\partial t} \tag{3.36}$$

The most common form of Equation 3.36 is obtained by separating the advection and hydrodynamic dispersion terms to obtain:

$$\frac{\partial}{\partial x}\left[D_x\theta\frac{\partial C}{\partial x}\right]+\frac{\partial}{\partial y}\left[D_y\theta\frac{\partial C}{\partial y}\right]-\frac{\partial (V_x C)}{\partial x}-\frac{\partial (V_y C)}{\partial y}=\frac{\partial \theta C}{\partial t} \tag{3.37}$$

Equation 3.37 gives the solution for C(x,y,t) if the average linear velocities and coefficients of hydrodynamic dispersion are known. This equation is valid for both saturated and unsaturated contaminant transport. The velocities can be obtained by solving Equation 3.8. Thus, the mathematical solution of pollutant transport in porous media problems requires coupling of the fluid flow and contaminant transport equations.

Two techniques are commonly used to couple the fluid flow and contaminant transport equations. In the weakly-coupled technique, the head is determined at each node, and the velocity though the element is then obtained. These velocities are then used to evaluate the contaminant transport portion of the problem. Thus, there is one time step lag between the solution of fluid flow and contaminant transport portions of the problem. In the fully-coupled technique, the advection portion of the mass transport equation is

directly coupled with the fluid flow equation, and a solution is obtained for both simultaneously. Generally, there are no significant differences between the results obtained from either method. The weakly-coupled formulation will be used in this project. Details regarding the finite element formulation for this method is presented in Chapter 4. Equation 3.37 will be modified in the following section to include the effect of sorption.

3.3.2.2 Sorption

Considerable research has been conducted to evaluate the adsorption of many types of solutes flowing through various types of porous media. A good review of some of this work can be found in Travis and Etnier (1981). In general, modeling of sorption can be separated into two groups: equilibrium based models and kinetic based models. These groups are differentiated by the rate at which sorption is considered to occur. Equilibrium based models assume that the change in aqueous phase concentration due to sorption occurs at a faster rate than the change in concentration due to advection, hydrodynamic dispersion, or by any other means. Thus, these models assume that sorption occurs immediately within the porous medium relative to any other transport mechanism. This assumption has not always been found to be accurate, thus, kinetic based models were developed. The discussion which follows is limited to equilibrium based models.

Laboratory tests are usually performed to evaluate the sorption of a given contaminant to the soil in question. The soil is exposed to the contaminant in a glass container of water. The amount of mass adsorbed onto the soil medium (S) is plotted against the concentration of the contaminant in solution (C). The test is usually performed over a period of time until equilibrium is reached when adsorption stops and the solution concentration is constant. The data is plotted, and a curve fitting procedure is used to obtain an expression for the S-C relationship. These curves are called ***isotherms*** because

the tests are usually performed at a constant temperature. If a linear relationship is obtained, i.e.

$$S = K_d C \tag{3.38}$$

the sorption model is called a linear adsorption isotherm. This is one of the most common sorption models used in practice due to its ease to incorporate into computer modeling. The coefficient K_d is called the distribution coefficient and is simply the slope of the S-C line. This simple relationship has been used to describe the sorption of strontium (Patterson and Spoel, 1981), cesium (Elprince, 1978), benzene (Karickhoff, et al., 1979), herbicides (Mallawatantri and Mulla, 1992), and sodium (Lai and Jurinak, 1972). Thus, this linear model is applicable to a variety of solutes.

Another very common equilibrium model is based on the Freundlich isotherm. This isotherm is defined by:

$$S = KC^n \tag{3.39}$$

where K and n are curve fitting parameters. When n equals one, the Freundlich equation gives the same sorption relation as the linear model above. The value for n is rarely ever greater than one. It is usually suggested that precipitation and sorption are occurring simultaneously when $n > 1$ (Fetter, 1993). The non-linear form of the Freundlich equation has been used to describe the adsorption of atrazine (Swanson and Dutt, 1973), zinc (Saeed and Fox, 1979), arsenic (Elkhatib, et al., 1984), picloram (van Genuchten, et al., 1974), phosphate (Kuo and Lotse, 1973), alachor (Locke, 1992) and boron (Elrashidi and O'connor, 1982).

An obvious limitation of both the linear model and the non-linear Freundlich isotherm equations is that both predict an unlimited amount of contaminant that can be adsorbed by the soil. An equilibrium based model which includes a limiting amount of

adsorption is the Langmuir isotherm developed in 1918 by Langmuir (1918) to describe the adsorption of gases on solid surfaces. The Langmuir isotherm is frequently given as:

$$S = \frac{k'bC}{1 + k'C} \tag{3.40}$$

where k′is a constant related to the strength of the bond between the sorbed contaminant and the soil surface, and b is the maximum amount of contaminant that can be adsorbed.

Plots of Equations 3.38 through 3.40 are shown in Figure 3-8. Note that the plot of the Langmuir model clearly indicates a maximum capacity for contaminant adsorption. The Langmuir equilibrium model has been successfully applied to the adsorption of zinc (Bar-Yosef, 1979), copper (Harter, 1979), lead (Griffin and Au, 1977), phosphate (Kuo, 1988), arsenic (Pierce and Moore, 1980), and boron (Shani, et al., 1992).

Figure 3-9 shows a plot of laboratory data for the adsorption of zinc on soil from the work of Harter and Baker (1977). As indicated, there is a curvilinear relationship for the adsorption data rather than the linear form indicated in Figure 3-8. This nonlinear behavior has been attributed to a number of possible factors including the effect of competition between different ions in solution (Bar-Yosef, 1979, and Griffin and Au, 1977), several different sorption sites on the soil and/or the effect of precipitation (Shukla and Mittal, 1979), a decrease in sorption energy with increasing sorption (Kuo, 1988), etc. All of these possible mechanisms require some modification to the original Langmuir equation. There is some debate as to the validity of these various models in describing the actual sorption mechanism that is occurring. Most believe, however, that the original Langmuir equation and the above referenced models do provide a good empirical fit to

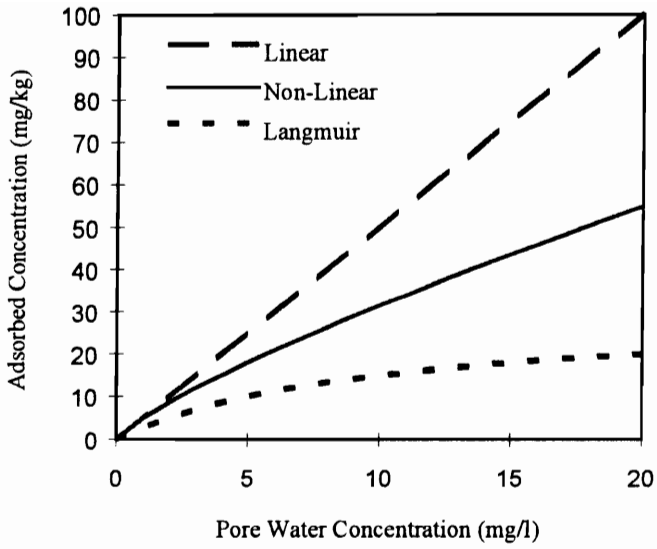

FIGURE 3-8: Plot of Linear and Non-linear Freundlich, and Langmuir Adsorption Isotherms.

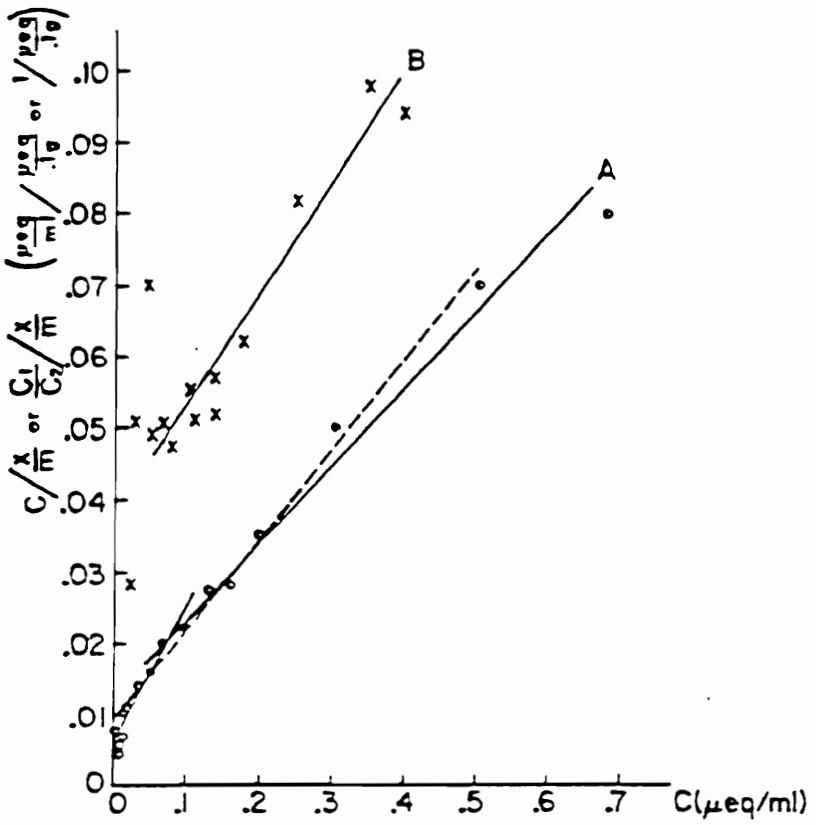

FIGURE 3-9: Laboratory Data for the Adsorption of Zinc. (After Harter and Baker, 1977).

laboratory data and may give a relative indication of the maximum sorption capacity of a given soil for a specific contaminant. The assumptions and limitations of the Langmuir equilibrium model are discussed in Harter and Baker (1977), Posner and Bowden (1980), Harter and Smith (1981), and Harter (1984).

Continuing with the derivation of the mass transport equation, let $\rho_b \partial S/\partial t$ equal the change in the total mass of the contaminant due to the mass adsorbed onto the soil surface per unit time, where ρ_b is the bulk density and S is the concentration in the aqueous phase. Since adsorption causes a reduction in the amount of contaminant in the aqueous, this partial derivative is subtracted from Equation 3.37 to obtain:

$$\frac{\partial}{\partial x}\left[D_x\theta\frac{\partial C}{\partial x}\right]+\frac{\partial}{\partial y}\left[D_y\theta\frac{\partial C}{\partial y}\right]-\frac{\partial(V_xC)}{\partial x}-\frac{\partial(V_yC)}{\partial y}-\rho_b\frac{\partial S}{\partial t}=\frac{\partial\theta C}{\partial t} \qquad (3.41)$$

Using the chain rule, we obtain:

$$\frac{\partial}{\partial x}\left[D_x\theta\frac{\partial C}{\partial x}\right]+\frac{\partial}{\partial y}\left[D_y\theta\frac{\partial C}{\partial y}\right]-\frac{\partial(V_xC)}{\partial x}-\frac{\partial(V_yC)}{\partial y}-\rho_b\frac{\partial S}{\partial C}\frac{\partial C}{\partial t}=\frac{\partial\theta C}{\partial t} \qquad (3.42)$$

where $\partial S/\partial C$ equals the change of mass sorbed onto the soil per change of contaminant concentration in the groundwater. This term represents the partitioning of the contaminant between the solid and aqueous phases. The sorption term can be moved to the right of the equals sign and the equation rearranged to obtain:

$$\frac{\partial}{\partial x}\left[D_x\theta\frac{\partial C}{\partial x}\right]+\frac{\partial}{\partial y}\left[D_y\theta\frac{\partial C}{\partial y}\right]-\frac{\partial(V_xC)}{\partial x}-\frac{\partial(V_yC)}{\partial y}=\frac{\partial}{\partial t}\left\{C\left(\theta+\rho_b\frac{\partial S}{\partial C}\right)\right\} \qquad (3.43)$$

The expressions for the adsorption models used in this study are given below:

Linear Freundlich :
$$\frac{\partial S}{\partial C} = K_d \tag{3.44}$$

Langmuir :
$$\frac{\partial S}{\partial C} = \frac{k'b}{(1+bC)^2} \tag{3.45}$$

In the following chapter, the above equations will be used in the finite element method.

CHAPTER 4

Finite Element Formulation

4.1 General

In this chapter, the finite element formulation is presented for both the fluid flow and mass transport portions of the problem. The derivation of the element matrix equations is given, and an overview of numerical integration and methods of solving nonlinear problems is presented. A review of the literature concerning finite element modeling of contaminant transport through porous media is also presented. Finally, a description of the computer program POLUTIDAL is given as well as several examples to evaluate the validity of the program code.

4.2 Derivation of Element Matrix Equations

4.2.1 Galerkin's Method of Weighted Residuals

Many workers have derived the matrix equations using Galerkin's method of weighted residuals (Pinder, 1973; Pickens and Lennox, 1976; Sykes and Farquhar, 1980; Istok, 1989). This method is particularly useful for the mass transport equation due to its simplicity over other variational methods. In Galerkin's method (or any other method of weighted residuals) an approximate solution to the governing differential equation is defined. Since this is an approximate solution, some error, or ***residual***, is obtained at each node in the finite element mesh. The approximate solution is improved by forcing the weighted average of the residual to be zero over the entire problem domain. As an illustration, consider the following governing differential equation for the field variable ϕ:

$$\alpha \frac{\partial^2 \phi}{\partial x^2} + \beta \frac{\partial^2 \phi}{\partial y^2} - \gamma \frac{\partial \phi}{\partial t} - f(x,y,t) = 0 \qquad (4.1)$$

Let the approximate solution be defined as

$$\phi' = \sum_{i=1}^{m} N_i \phi_i \tag{4.2}$$

where ϕ' is the approximated field variable and N_i is an interpolation function. Thus the residual due to the approximate solution can be written as:

$$\alpha \frac{\partial^2 \phi'}{\partial x^2} + \beta \frac{\partial^2 \phi'}{\partial y^2} - \gamma \frac{\partial \phi'}{\partial t} - f(x,y,t) = R(x,y,t) \neq 0 \tag{4.3}$$

The accuracy of the approximate solution is improved if:

$$\int_{\Omega} W(x,y) \cdot R(x,y,t) d\Omega = 0 \tag{4.4}$$

where W(x,y) is a weighting function and Ω is the domain of the problem. In Galerkin's method, the weighting function is the same as the interpolation function N_i. Thus, the evaluation of Equation 4.4 will give an approximate solution for the field variable ϕ. This technique will be used below to derive the element matrix equations for both fluid flow and mass transport.

4.2.2 Fluid Flow

The governing differential equation for fluid flow through porous media as given by Equation 3.8 is repeated below as:

$$\frac{\partial}{\partial x}\left(K_x \frac{\partial h}{\partial x}\right) + \frac{\partial}{\partial y}\left(K_y \frac{\partial h}{\partial y}\right) = C_m \frac{\partial h}{\partial t} \tag{4.5}$$

Recall that this general equation is valid for saturated and unsaturated porous media as well as steady-state and transient conditions. Let an approximate solution of Equation 4.5 be defined as:

$$h = N_j h_j \tag{4.6}$$

where h is the total head within the element, N_j is the interpolation function to be defined later, and h_j is the total head at the nodes of the element. The partial derivatives of the approximate solution with respect to x, y and t are:

$$\frac{\partial h}{\partial x} = \frac{\partial N_j}{\partial x} h_j \; ; \; \frac{\partial h}{\partial y} = \frac{\partial N_j}{\partial y} h_j \; ; \; \frac{\partial h}{\partial t} = N_j \frac{\partial h_j}{\partial t} \tag{4.7}$$

If these derivatives are substituted into Equation 4.5 and the equation is multiplied by N_j, then the Galerkin formulation of the flow equation has the form of:

$$\int_A N_i \left[\frac{\partial}{\partial x}\left(K_x \frac{\partial N_j}{\partial x} h_j \right) + \frac{\partial}{\partial y}\left(K_y \frac{\partial N_j}{\partial y} h_j \right) - C_m N_j \frac{\partial h_j}{\partial t} \right] dxdy = 0 \tag{4.8}$$

Integration by parts on the first term in the above equation gives:

$$\int_A N_i \left[\frac{\partial}{\partial x}\left(K_x \frac{\partial N_j}{\partial x} h_j \right) \right] dxdy = \oint_S N_i K_x \frac{\partial N_j}{\partial x} h_j l dS - \int_A \frac{\partial N_i}{\partial x} K_x \frac{\partial N_j}{\partial x} h_j dxdy \tag{4.9}$$

where the surface integral is a Neumann boundary condition. Performing integration by parts on the second and third terms of Equation 4.8 and moving the boundary terms to the right side of the equals sign gives:

$$\int_A \left\{ \left[\frac{\partial N_i}{\partial x} K_x \frac{\partial N_j}{\partial x} + \frac{\partial N_i}{\partial y} K_y \frac{\partial N_j}{\partial y} \right] h_j + N_i N_j C_m \frac{\partial h_j}{\partial t} \right\} dxdy = \oint_S N_i \bar{q} dS \qquad (4.10)$$

where $\bar{q}$ is the seepage flux into the element. Rewriting the above equation in matrix forms gives:

$$\int_A \left(\left[\frac{\partial N_i}{\partial x} \quad \frac{\partial N_j}{\partial y} \right] [K_x \; K_y] \begin{bmatrix} \frac{\partial N_i}{\partial x} \\ \frac{\partial N_j}{\partial y} \end{bmatrix} \{h_j\} + N_i N_j C_m \left\{ \frac{\partial h_j}{\partial t} \right\} \right) dxdy = \oint_S N_i \bar{q} dS \qquad (4.11)$$

Complex integration may be needed to evaluate Equation 4.11. Alternatively, a numerical technique called ***Gauss Quadrature*** can be used to solve this equation. This method is one of the most common types of numerical integration methods currently in use. In this technique, the integral is approximated by taking the weighted sum of the integral evaluated at several points within the element. This is represented mathematically by:

$$\int_{-1}^{1}\int_{-1}^{1} f(r,s)drds = \sum_{i=1}^{n}\sum_{j=1}^{n} f(r_i s_j) w_i(r_i) \cdot w_j(s_j) \qquad (4.12)$$

where f(r,s) is some function, n is the number of Gauss points at which the integral is to be evaluated and w_i and w_j are weighting functions (not the same as the weighted residual functions described above). In POLUTIDAL, n equals 4 points, w_i and w_j are both equal to one, and the value of the points where integration is to be performed is (± .5774, ± .5774). Note that the limits of the integral are -1 and +1. This facilitates the evaluation of the integral.

To perform the numerical integration for our problem, the x,y coordinate system must be converted to a r,s coordinate system so that the integral limits can be changed. Figure 4-1a shows a r,s coordinate system which is referred to as the ***local*** coordinate

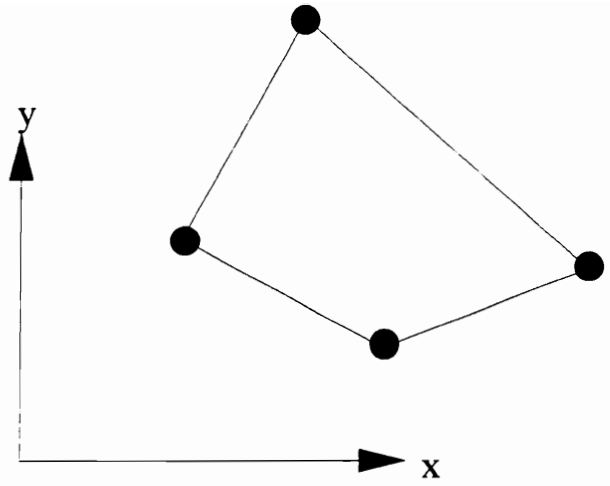

a) global coordinate system

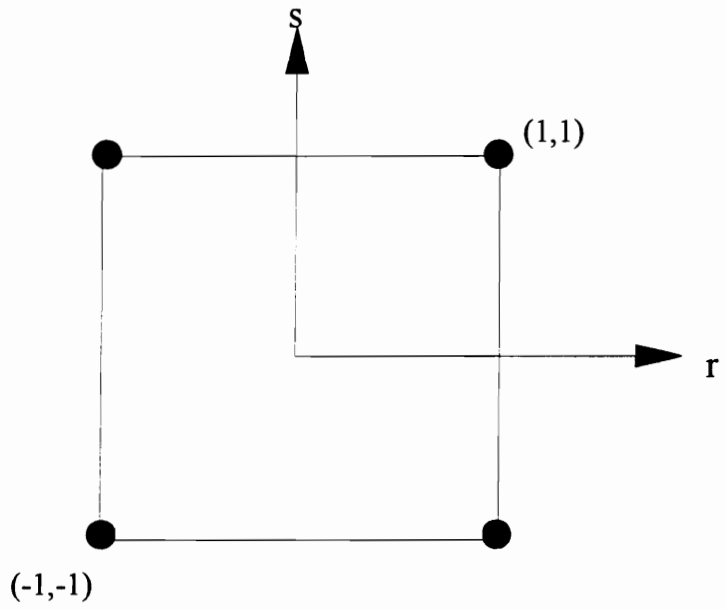

b) local coordinate system

FIGURE 4-1: Global and Local Coordinate Systems for a Typical Element.

system. Let the relationship between the global (x,y) and local (r,s) coordinate systems be defined by:

$$\begin{aligned} x &= N_1x_1 + N_2x_2 + N_3x_3 + N_4x_4 \\ y &= N_1y_1 + N_2y_2 + N_3y_3 + N_4y_4 \end{aligned} \tag{4.13a}$$

where N_i is the interpolation function defined as:

$$\begin{aligned} N_1 &= \frac{1}{4}(1-r)(1-s) \\ N_2 &= \frac{1}{4}(1+r)(1-s) \\ N_3 &= \frac{1}{4}(1+r)(1+s) \\ N_4 &= \frac{1}{4}(1-r)(1+s) \end{aligned} \tag{4.13b}$$

It is common to use the same interpolation function for both the coordinate transformation and the approximate solution (Equation 4.6). The derivatives of N_i must be obtained in order to evaluate Equation 4.11. This is accomplished in the following manner. In matrix form, the derivative of N_i with respect to r and s is given by

$$\begin{Bmatrix} \frac{\partial N_i}{\partial r} \\ \frac{\partial N_i}{\partial s} \end{Bmatrix} = \begin{bmatrix} \frac{\partial x}{\partial r} & \frac{\partial y}{\partial r} \\ \frac{\partial x}{\partial s} & \frac{\partial y}{\partial s} \end{bmatrix} \begin{Bmatrix} \frac{\partial N_i}{\partial x} \\ \frac{\partial N_i}{\partial y} \end{Bmatrix} \tag{4.14a}$$

or

$$\begin{Bmatrix} \frac{\partial N_i}{\partial r} \\ \frac{\partial N_i}{\partial s} \end{Bmatrix} = [J] \begin{Bmatrix} \frac{\partial N_i}{\partial x} \\ \frac{\partial N_i}{\partial y} \end{Bmatrix} \tag{4.14b}$$

where $[J]$ is the Jacobian matrix. Rearranging Equation 4.14b gives:

$$\begin{Bmatrix} \frac{\partial N_i}{\partial x} \\ \frac{\partial N_i}{\partial y} \end{Bmatrix} = [J]^{-1} \begin{Bmatrix} \frac{\partial N_i}{\partial r} \\ \frac{\partial N_i}{\partial s} \end{Bmatrix} = [B] \tag{4.15}$$

Thus the $[B]$ matrix is the derivative of the interpolation function with respect to the global coordinates. If Equation 4.15 is substituted into Equation 4.11 and the limits of integration are changed to -1 and +1, the following equation is obtained:

$$\int_{-1}^{1}\int_{-1}^{1} [B]^T[C][B]\{h_j\}|J|drds + \int_{-1}^{1}\int_{-1}^{1} [N]^T[N][C_m]\left\{\frac{\partial h_j}{\partial t}\right\}|J|drds = \{Q\} \tag{4.16}$$

or

$$[K]\{h\} + [K_T]\{\dot{h}\} = \{Q\} \tag{4.17}$$

where

$$[C] = \begin{bmatrix} K_{xx} & K_{xy} \\ K_{yx} & K_{yy} \end{bmatrix}$$

$$\{\dot{h}\} = \left\{\frac{\partial h_j}{\partial t}\right\} \tag{4.18a,b}$$

$$\{Q\} = \{\bar{q}_j\} \tag{4.18c}$$

The determinant of the Jacobian, $|J|$, in Equation 4.16 is due to the transformation from global to local coordinates. The solution of Equation 4.17 requires the uses of a time

integration scheme. The scheme used in POLUTIDAL is presented in Section 4.3 below. The next section shows the derivation of the element matrix equations for mass transport.

4.2.3 Mass Transport

The governing equation for mass transport using the linear Freundlich sorption model was previously given in Chapter 3 as:

$$\frac{\partial}{\partial x}\left[D_{xx}\theta\frac{\partial C}{\partial x}+D_{xy}\theta\frac{\partial C}{\partial y}\right]+\frac{\partial}{\partial y}\left[D_{yy}\theta\frac{\partial C}{\partial y}+D_{yx}\theta\frac{\partial C}{\partial x}\right]-\frac{\partial(V_x C)}{\partial x}-\frac{\partial(V_y C)}{\partial y}=\frac{\partial\theta C}{\partial t}+\frac{\partial(\rho_b k_d C)}{\partial t} \tag{4.19}$$

This equation assumes no source or sink terms. Derivation of the element matrix equations for this equation is usually done using weighted residual methods due to the difficulty of formulating the problem with other variational methods. Following the procedure used above for the fluid flow equation, an approximate solution for the concentration (C) has the following form:

$$C = N_j C_j \tag{4.20}$$

The partial derivatives of the approximate solution with respect to x, y and t are:

$$\frac{\partial C}{\partial x}=\frac{\partial N_j}{\partial x}C_j\ ;\ \frac{\partial C}{\partial y}=\frac{\partial N_j}{\partial y}C_j\ ;\ \frac{\partial C}{\partial t}=N_j\frac{\partial C_j}{\partial t} \tag{4.21}$$

Substituting these equations into Equation 4.19 and multiplying through by the weighting function N_i gives the residual for the approximate solution. The residual is then set equal to zero and each term in the equation is integrated by parts. This results in the following integrals for the first term in Equation 4.19:

$$\int_A N_i\left[\frac{\partial}{\partial x}\left(D_{xx}\theta\frac{\partial C}{\partial x}+D_{xy}\theta\frac{\partial C}{\partial y}\right)\right]dxdy =$$

$$\oint_S N_i\left(D_{xx}\theta\frac{\partial N_j}{\partial x}C_j l+D_{xy}\theta\frac{\partial N_j}{\partial y}C_j m\right)dS-\int_A\left(D_{xx}\theta\frac{\partial N_j}{\partial x}\frac{\partial N_i}{\partial x}C_j+D_{xy}\theta\frac{\partial N_j}{\partial y}\frac{\partial N_i}{\partial y}C_j\right)dxdy \tag{4.22}$$

where the surface integral represents Neumann boundary conditions. A similar expression is obtained when integration by parts is performed on the second (dispersion) term of Equation 4.19. Integration by parts on the third and fourth (advection) terms yields:

$$\int_A N_i\left(\frac{\partial(V_x C)}{\partial x}-\frac{\partial(V_y C)}{\partial y}\right)dxdy =$$

$$\oint_S N_i(V_x N_j C_j l+V_y N_j C_j m)dS-\int_A\left(V_x N_j C_j\frac{\partial N_i}{\partial x}+V_y N_j C_j\frac{\partial N_i}{\partial y}\right)dxdy \tag{4.23}$$

In this equation, the surface integral represents Neumann boundary conditions for solute flux into the element. Since the time derivatives are first order, integration by parts is not necessary for these terms in Equation 4.19.

Combining all the terms and moving the boundary condition terms to the right side of the equals sign gives:

$$\int_A\left[\left(D_{xx}\theta\frac{\partial N_j}{\partial x}\frac{\partial N_i}{\partial x}+D_{xy}\theta\frac{\partial N_j}{\partial y}\frac{\partial N_i}{\partial y}+D_{yy}\theta\frac{\partial N_j}{\partial y}\frac{\partial N_i}{\partial y}+D_{yx}\theta\frac{\partial N_j}{\partial x}\frac{\partial N_i}{\partial x}-V_x N_j\frac{\partial N_i}{\partial x}-V_y N_j\frac{\partial N_i}{\partial x}\right)C_j\right]dxdy$$
$$+\int_A\left(N_i N_j\frac{\partial C_j}{\partial t}[\theta+\rho_b k_d]\right)dxdy=\{Q\} \tag{4.24}$$

For our analyses, $\{Q\}$ will be assumed to be zero, i.e. no solute flux (Neumann type) boundary conditions will be considered. Rather, only fixed concentration values (Dirichlet type) boundary conditions will be employed. Equation 4.24 can be written in matrix notation as:

$$\int_A \left(\begin{bmatrix} \frac{\partial N_i}{\partial x} & \frac{\partial N_j}{\partial y} \end{bmatrix}^T \begin{bmatrix} D_{xx}\theta & D_{xy}\theta \\ D_{yx}\theta & D_{yy}\theta \end{bmatrix} \begin{bmatrix} \frac{\partial N_i}{\partial x} \\ \frac{\partial N_j}{\partial y} \end{bmatrix} + [N_i \;\; N_j]^T \begin{bmatrix} V_x & 0 \\ 0 & V_y \end{bmatrix} \begin{bmatrix} \frac{\partial N_i}{\partial x} \\ \frac{\partial N_j}{\partial y} \end{bmatrix} \right) \{C_j\} dxdy$$

$$+ \int_A ([N_i]^T(\theta + \rho_b k_d)[N_j])\{\dot{C}\} dxdy = 0 \tag{4.25}$$

Recalling that $\begin{bmatrix} \frac{\partial N_j}{\partial x_i} \end{bmatrix}$ is the $[B]$ matrix and converting to the local coordinate system, the above equation can be written as:

$$\int_{-1}^{1}\int_{-1}^{1} ([B]^T[D][B] + [N]^T[V][B])\{C_j\}|J| drds + \int_{-1}^{1}\int_{-1}^{1} [N]^T(\theta + \rho_b k_d)[N]\left\{\frac{\partial C_j}{\partial t}\right\}|J| drds = \{0\} \tag{4.26}$$

or

$$[K]\{C\} + [K_T]\{\dot{C}\} = \{0\} \tag{4.27}$$

where

$$\{\dot{C}\} = \left\{\frac{\partial C_j}{\partial t}\right\} \tag{4.28}$$

4.3 Time Integration Scheme

Several methods exist for solving time dependent problems. One of the most common techniques for groundwater flow and mass transport problems is to solve the

matrix equations using the finite difference method. The following discussion is adapted from Huyakorn and Pinder (1983). The element matrix equations derived above for fluid flow and mass transport can be written as:

$$[K]\{r\}+[K_T]\{\dot{r}\}=\{R\} \tag{4.29}$$

where $\{\dot{r}\}$ is the time derivative of the variable. Equation 4.29 can be rewritten so that it is evaluated at a time of $t+\beta\Delta t$ as:

$$[K]\{r\}_{t+\beta\Delta t}+[K_T]\{\dot{r}\}_{t+\beta\Delta t}=\{R\} \tag{4.30}$$

From the Mean Value Theorem of calculus, the time derivative vector can be written as:

$$\{\dot{r}\}_{t+\beta\Delta t}=\frac{\{r\}_{t+\Delta t}-\{r\}_t}{\Delta t} \tag{4.31}$$

Referring to Figure 4-2, Equation 4.31 can be rearranged to obtain:

$$\begin{aligned}\{r\}_{t+\beta\Delta t}&=\{r\}_t+\beta\Delta t\left(\frac{\{r\}_{t+\Delta t}-\{r\}_t}{\Delta t}\right)\\&=(1-\beta)\{r\}_t+\beta\{r\}_{t+\Delta t}\end{aligned} \tag{4.32}$$

Substituting Equations 4.31 and 4.32 into 4.30 gives:

$$[K][(1-\beta)\{r\}_t+\beta\{r\}_{t+\Delta t}]+[K_T]\frac{1}{\Delta t}[\{r\}_{t+\Delta t}-\{r\}_t]=\{R\} \tag{4.33}$$

Rearranging yields:

$$\left\{\beta[K]+\frac{1}{\Delta t}[K_T]\right\}\{r\}_{t+\Delta t}=\{R\}+\left\{\frac{1}{\Delta t}[K_T]+(1-\beta)[K]\right\}\{r\}_t \tag{4.34}$$

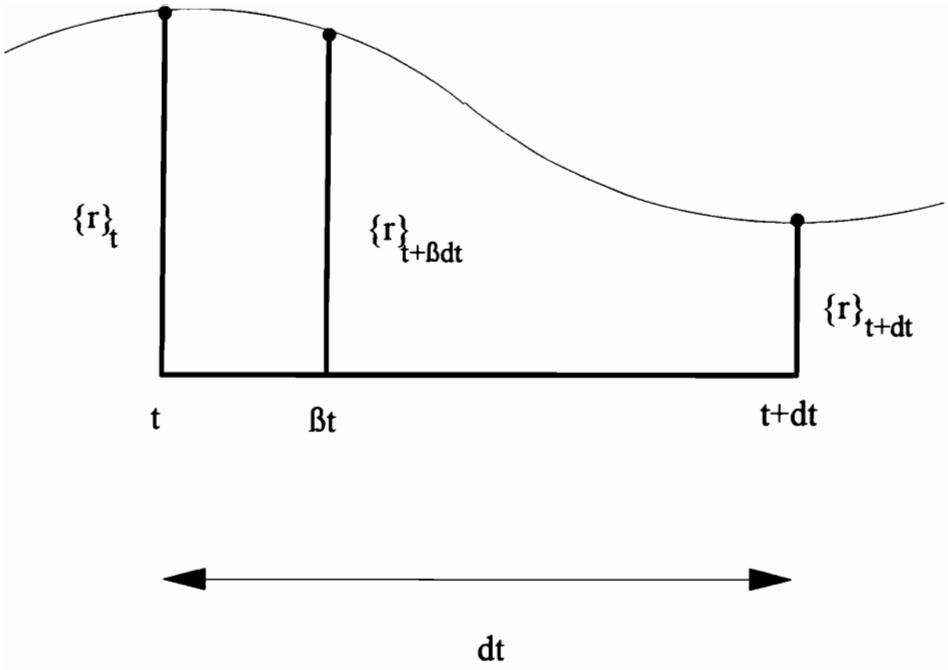

FIGURE 4-2: Plot of the Function {r} at times t and t+dt.

At time equal to zero, the right hand side of Equation 4.34 is known, and the coefficients on the left side of the equation are also known. Thus, this equation can be written as a system of linear equations as:

$$[A]\{s\} = \{V\} \tag{4.35}$$

where

$$[A] = \left\{\beta[K] + \frac{1}{\Delta t}[K_T]\right\}$$

$$\{V\} = \{R\} + \left\{\frac{1}{\Delta t}[K_T] + (1-\beta)[K]\right\}\{r\}_{t=0} \text{ , and} \tag{4.36a,b,c}$$

$$\{s\} = \{r\}_{\Delta t}$$

Once the solution of $\{s\}$ is obtained at time Δt, it then becomes the known value for the next time step. The program POLUTIDAL uses a standard Gaussian elimination subroutine to solve the set of equations represented by Equations 4.36. The value of β can be specified by the user. Stable solutions can be obtained for β values between 0.5 and 1.0.

4.4 Iteration Scheme for Non-linear Problems

As indicated in Chapter 3, the solution of the flow equation gives the total head at each node in the flow domain. However, in order to solve this equation, the hydraulic conductivity, which is a function of the pressure head, must first be determined. In the mass transport portion of the problem, the concentration is calculated at each node within the domain. However, the calculated concentration depends on the amount of retardation due to sorption which in turn depends on the concentration level (for non-linear sorption models). Thus, for both cases an initial estimate of the unknown variable (head and concentration) must be made in order to obtain the [K] and [K_T] matrices. This type of

non-linearity, called a 'material non-linearity', can be solved by a number of techniques. A discussion of the commonly used iteration methods can be found in Reddy (1984), Dhatt and Touzet (1984) and Ahmad (1991).

A popular iteration technique is the Picard method which is also called the substitution method. Following the description of Istok (1989), consider a system of non-linear equations written in matrix form as:

$$[M(x)]\{x\} = \{B\} \tag{4.37}$$

where $[M(x)]$ is a coefficient matrix which is a function of the unknown variable x. $\{B\}$ is assumed to be a known vector which is not a function of x. This equation has the exact form as Equation 4.35 above. In the Picard method, an initial estimate is made for x so that $[M(x)]$ can be determined. Equation 4.37 is then solved to obtain $\{x\}$. A comparison is then made to see how closely the estimated value is to the calculated value. This comparison is called the convergence test and is governed by the degree of accuracy, or tolerable percentage of error, that is required. If $\{x^0\}$ are the estimated values of the unknown value of x at each node, and $\{x^1\}$ are the calculated values of the unknown value of x at each node, then the difference between the two values is the error. If the error is less than a specified amount, say ε, then the solution obtained is acceptable and the analysis continues to the next time step where the procedure is repeated. However, if the error is greater than the tolerable limit, i.e. $(\{r^1\} - \{r^0\}) > \varepsilon\{r^0\}$, then the calculated variable $\{x^1\}$ is substituted into $[M(x)]$ as the new estimated value and the equation is solved for $\{x^2\}$. This method of substitution is performed until the convergence criteria is satisfied.

Depending on the type of problem being solved, the rate at which an acceptable solution converges can be large due to many iterations being required. A modified form of

the Picard method has been found to be very effective for the fluid flow problem. In this method, rather than direct substitution of the preceding solution into the $[M(x)]$ matrix, the average of the values of the initial estimate and the resulting solution are substituted into $[M(x)]$, i.e.

$$\{x^1\} = \frac{\{x^1\} + \{x^0\}}{2} \tag{4.38}$$

This technique has been very successful and was incorporated into POLUTIDAL. Another technique which is often employed when the Picard method takes a long time to converge is the Newton-Raphson method. This method can improve the iteration efficiency but requires additional computational effort Ahmad (1991).

4.5 Literature Survey on Finite Element Modeling of Contaminant Transport

Pinder (1973) developed a 2-D Galerkin method finite element program to model the spread of non-reactive chromium in the groundwater at a site in Long Island New York. He back calculated values for longitudinal and transverse dispersivity by fitting the concentration distribution predicted by the finite element model with the concentration data obtained from monitoring wells. Pickens and Lennox (1976) performed sensitivity analyses using a model they developed to evaluate the effect of dispersivity coefficients and distribution coefficient K_d. They found that a contaminant plume spreads faster as the dispersivity coefficients increase, and that larger K_d values can significantly reduce the spread of contaminants. They also showed that an aquifer can eventually "clean" itself if the contaminant source is removed. Huyakorn (1977) and Huyakorn and Nilkuha (1979) used a finite element program to study the spread of contaminants in porous media due to an injection well. Pickens et al. (1979) and Pickens and Gillham (1980) developed a 2-D Galerkin based finite element program to model fertilizer transport through a saturated and unsaturated sandy soil which contained tile drains. They indicated that two

dimensional closed form solutions were not available to validate the results of their model so they used the program to study a simple 1-D problem for which closed form solutions exist. Their 1-D finite element calculations were in very close agreement with the analytical solution. A similar problem was solved by Kandil et al. (1992) using a Petrov-Galerkin finite element program which also included the effect of infiltration due to rainfall. Burnett and Frind (1987) developed a three dimensional contaminant transport program using the finite element method. They studied the dimensionality effects by comparing their 3-D results for a generic problem involving a leachate plume caused by a surface contaminant source, such as a landfill or waste disposal pond, with the results obtained using 2-D (vertical and horizontal plane) models. The 2-D vertical plane model predicted higher contaminant concentrations and a longer plume length then the 3-D model. These results were attributed to the neglect of dispersion in the horizontal plane. Thus, conservative estimates were obtained.

An abandoned landfill at the Canadian Forces Base, Borden Ontario has been used as a field case to study contaminant transport. The landfill was used as a refuse dump from 1942 to 1973 and was closed in 1976. Extensive groundwater monitoring performed at the site has given considerable detail regarding the flow regime and the leachate plume caused by the refuse. Sykes and Farquhar (1980) developed a finite element program to evaluate contaminant transport which included the effects of biodegredation and adsorption. They calculated the concentration of the potassium plume and obtained results that were similar to the measured field values. Frind and Hokkanen (1987) used an alternating direction Galerkin technique to study the chloride plume at the Borden landfill.

All of the above examples have shown the adaptability and accuracy of the finite element method for contaminant transport problems. However, there is extensive evidence that numerical oscillations can occur if the advective portion of the mass transport

equation dominates, i.e. the flow velocity through the porous medium is considerably greater than the dispersion. These oscillations give erroneous results which include negative concentrations, concentrations that are larger than the input (source) concentration, concentration values which oscillate with time or distance, etc. The cause of these errors is usually attributed to the combined effect of the elliptical dispersion term and the parabolic advection term (Heinrich et al., 1977). Fortunately, these numerical errors can be eliminated or reduced if the grid spacing and time increment meet the following criteria:

$$P_e = \frac{V\Delta x}{D} \leq 2$$

and (4.39)

$$C_r = \frac{V\Delta t}{\Delta x} \leq 1$$

where P_e and C_r are the Peclet and Courant numbers, respectively, V is the seepage velocity, D is hydrodynamic dispersion, Δx is the grid spacing and Δt is the time increment (Daus et al., 1985). However, computer capabilities and costs can become a problem if many nodes and/or small time steps are needed to meet these criteria. Moltyaner (1988) used a Galerkin finite element program to study the transport of non-reacting radio-iodine through a fine sand aquifer. A mesh consisting of 452 nodes and 819 elements gave negative concentration values. These numerical errors were not observed when the mesh was refined using 7,128 nodes and 13,920 elements. Yeh (1988) corrected for numerical errors by developing a program that could automatically refine a mesh by subdividing elements into smaller elements.

Many workers have developed *upwind* or *upstream* techniques to minimize numerical errors. These techniques were first applied to finite difference models and have been expanded to the finite element method. To illustrate the basic principle behind upwinding, let the mass transport equation be rewritten in general terms as:

$$D\frac{\partial^2\phi}{\partial x_i^{\,2}} - V\frac{\partial\phi}{\partial x_i} = 0 \tag{4.40}$$

where the first term represents dispersion (or diffusion) and the second term represent advection. This equation is for steady state conditions and is applicable for convective heat transport problems as well as mass transport problems. Leonard (1979) demonstrates the finite difference approximation of this equation by writing the derivatives as central difference Taylor series expansions. Thus, the first derivative can be approximated as:

$$\frac{\phi_{i+1} - 2\phi_i + \phi_{i-1}}{\Delta x^2} = \left(\frac{\partial^2\phi}{\partial x^2}\right)_i + \frac{1}{12}\left(\frac{\partial^4\phi}{\partial x^4}\right)_i \Delta x^2 + HOT \tag{4.41a}$$

or

$$\left(\frac{\partial^2\phi}{\partial x^2}\right)_i \approx \frac{\phi_{i+1} - 2\phi_i + \phi_{i-1}}{\Delta x^2} \tag{4.41b}$$

where HOT are higher order terms. The Taylor series central difference expansion of the second term yields:

$$\frac{\phi_{i+1} - \phi_{i-1}}{2\Delta x} = \left(\frac{\partial\phi}{\partial x}\right)_i + \frac{1}{6}\left(\frac{\partial^3\phi}{\partial x^3}\right)_i \Delta x^2 + HOT \tag{4.42a}$$

or

$$\left(\frac{\partial\phi}{\partial x}\right)_i \approx \frac{\phi_{i+1} - \phi_{i-1}}{2\Delta x} \tag{4.42b}$$

Note that Equation 4.41a is third order accurate while Equation 4.42a is only second order accurate. Leonard (1979) states that numerical errors are counteracted if a backward difference approach is used to approximate the advection term, giving:

$$\frac{\phi_i - \phi_{i-1}}{\Delta x} = \left(\frac{\partial\phi}{\partial x}\right)_i + \left(\frac{\partial^2\phi}{\partial x^2}\right)_i \Delta x + HOT \tag{4.43a}$$

or

$$\left(\frac{\partial \phi}{\partial x}\right)_i \approx \frac{\phi_i - \phi_{i-1}}{\Delta x} \tag{4.43b}$$

Note that the first truncation term, $(\partial^2\phi/\partial x^2)_i$, in this backward difference approximation is a dispersion (or diffusion) term. This truncation error produces additional "numerical dispersion" which minimizes or eliminates numerical errors when advection dominates. However, the accuracy of the solution is diminished due to this additional numerical dispersion which occurs in addition to physical dispersion.

A standard Galerkin type finite element formulation of the advection-dispersion equation gives a set of equations which are very similar to the central difference approximations above (Huyakorn, 1977, Kelly et al., 1980 and Brooks and Hughes, 1982) and can result in numerical errors. Christie et al. (1976) were the first to apply upwinding to the finite element method. They used test functions that were different than the basis functions to solve the 1-D steady state transport equation. The effect of the test function is to weight an element upstream of a node more heavily than one downstream. Full upwinding basically reduces the advection term to a backward difference approximation. The degree of upwinding can be varied to suit the needs of the problem. Heinrich et al. (1977) and Huyakorn (1977) extended the work of Christie et al. (1976) to two dimensions. Transient conditions were solved by Huyakorn and Nilkuha (1979) using asymmetric weighting functions and an upstream weighting factor (α) which dictated the amount of upwinding of the advection term. The value of α is apparently dependent on the specific problem being studied.

Hughes and Brooks (1979) and Kelly et al. (1980) noted that the effect of upwinding is essentially the same as adding an additional "numerical" dispersion term to the physical dispersion term. Thus, they used a standard Galerkin formulation but added

an artificial dispersion term which was dependent on the element size, velocity and Peclet number. Brooks and Hughes (1982) developed a Petrov-Galerkin finite element model that consistently applied the same weight function to all the terms in the governing differential equation. They used weight functions which were combinations of the test functions and discontinuous upwinding functions. These weight functions were developed to add artificial dispersion only in the direction of flow to avoid over diffusion in the direction perpendicular to flow. They obtained much better (less oscillation) results as compared to standard Galerkin methods. Yu and Heinrich (1986 and 1987) developed Petrov-Galerkin based finite element algorithms to solve 1-D and 2-D transient transport problems. They used weight functions which were functions of both time and space. Westerink and Shea (1989) and Cantekin and Westerink (1990) showed that weight functions that are two polynomial degrees higher than the basis functions give better results than weight functions which are only one degree higher than the basis functions.

In summary, many methods have been proposed to account for numerical oscillation. However, none of these methods have been widely accepted or used. In addition, some of the upwinding parameters are not general enough to apply to many types of problems. Perhaps the biggest drawback to the methods summarized above is the potential for overly dispersive results to be obtained. Leonard (1979) and Greshno and Lee (1979) present strong arguments against using any type of upwinding technique. They suggest that some oscillation may be acceptable for most problems if the overall result looks reasonable. In addition, they point out that the excessive oscillations in a mesh indicate where the numerical approximation to the problem is not adequate and further discretization should be performed. Based on the above discussion, upwinding was not considered as an option in program POLUTIDAL.

4.6 Program POLUTIDAL

4.6.1 General

The description which follows is for the program POLUTIDAL which is a modification of the original program POLUT2D by Kuppusamy and Ahmad (1991). A general description of the original program is given as well as the modifications done by the author. These modifications provided the ability to consider:

- a general beta time integration scheme,
- linear and non-linear contaminant adsorption,
- fluctuating boundary water levels,
- time varying input concentration levels,
- a quasi-finite contaminant capacity, and
- surface water infiltration effects.

The program incorporates a pre-processor for creating and editing input data files and a post-processor for displaying the results on the screen or sending the results to a printer or plotter. Both the pre- and post- processors are written in the C computer language. The main analysis program is accessed by the pre-processor and is written in FORTRAN. A brief description of the main program is presented below. Additional information can be found in Kuppusamy and Tyler (1993).

In order to solve the mass transport equation, the seepage velocity must first be obtained by solving the fluid flow equation. At the first time step, the initial head given in the data file is used to calculate the hydraulic conductivity and coefficient of moisture capacity. Then, the [K] and $[K_T]$ matrices are evaluated using the numerical integration technique described in Section 4.2.2. Using the given initial head data, the time integration scheme described in Section 4.3 is employed to solve Equation 4.17 and obtain the head at every node. The calculated head is then compared with the head values used to evaluate the [K] and $[K_T]$ matrices. The modified Picard method described above is employed until the solution converges to the degree of accuracy specified by the user. The velocity within

each element is then calculated based on the head and hydraulic conductivity. Before advancing to the next time step, the procedure described in the paragraph above is repeated for the mass transport equation. The same basic steps are taken except that iteration is not needed if the linear sorption model is assumed for the problem. Solution of Equation 4.27 gives the value of the contaminant concentration (in the pore water) at each node in the domain. The solution marches through time following the same basic steps. The head and concentration calculated at previous time steps are used to calculate the [K] and $[K_T]$ matrices for the current time step and are also used to calculate the new head and concentration by the time integration scheme.

4.6.2 Tidal Fluctuating Water Levels

Many confined disposal facilities are constructed in coastal waters. Thus, these structures are influenced by water level variations due to changing tides. A typical tidal water level variation as provided by the Corps of Engineers is shown in Figure 4-3. To simulate this variation, the following equation was adapted from Yim and Moshen (1992) to fit this particular problem:

$$h(t) = h_a + h_o \sin\left(\frac{2\pi t}{t_o}\right) \tag{4.44}$$

where: $h(t)$ = tidal head at time t
h_a = average tidal head
h_o = amplitude of the tidal head
t_o = period of the tidal head

A plot of this equation, along with the original data is shown in Figure 4-4. In this example, h_a equals 7 feet, h_o equals 5 feet and t_o equals 690 minutes. The agreement between the measured and simulated data is very good. This equation was incorporated into POLUTIDAL for CDF's located in coastal waters.

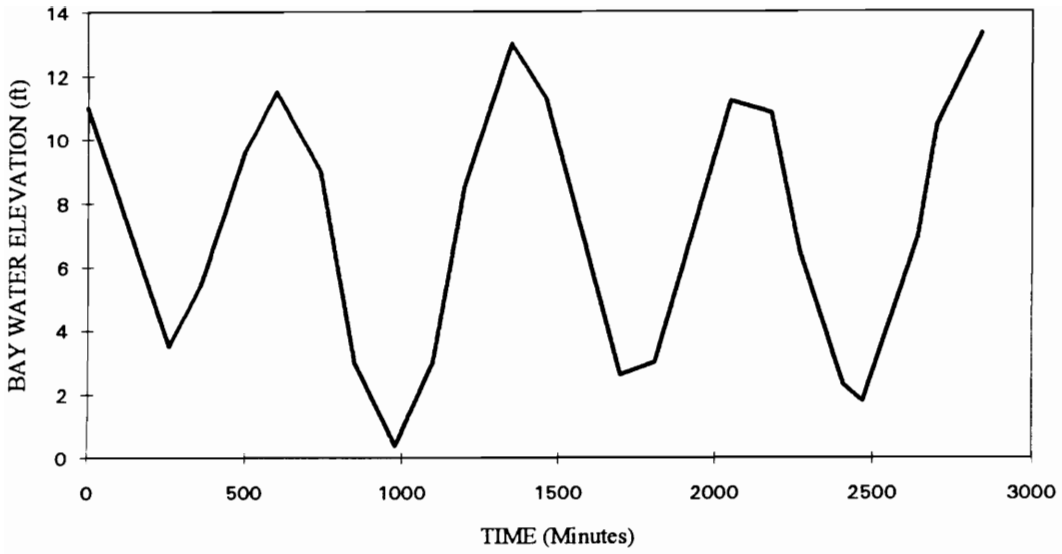

FIGURE 4-3: Measured Data showing the Fluctuation of the Tide with Time.

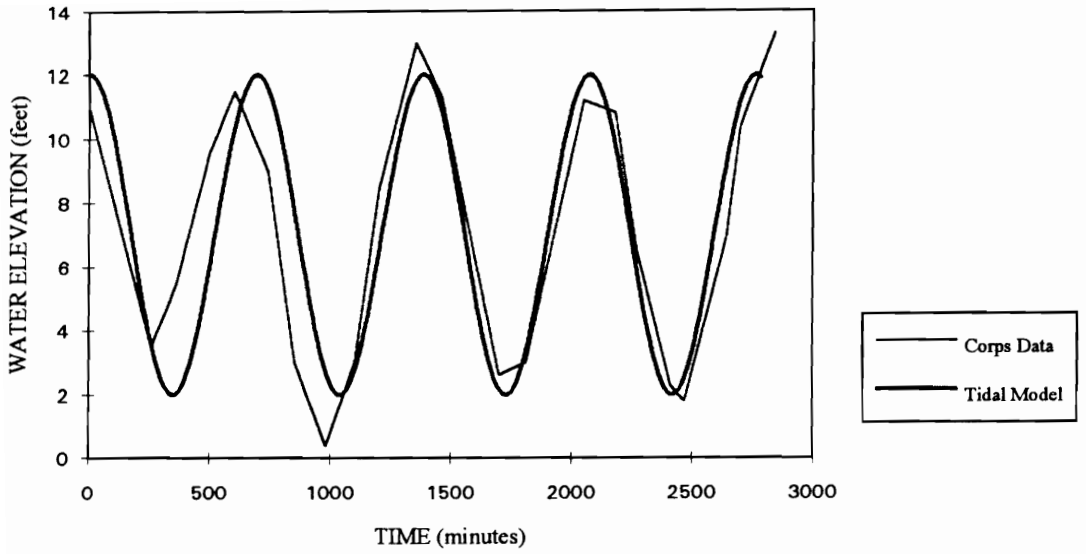

FIGURE 4-4: Comparison of Measured and Simulated Tidal Heads.

4.7 Program Validation

Validation of the program is difficult due to the heterogeneous, anisotropic and transient nature of contaminant transport problems for which no closed form solutions are available. However, there are exact solutions for simple types of transport problems (1-D, homogeneous, steady state flow). Thus, the results generated by the program can be compared to an exact solution for these simple types of problems. In addition, the accuracy of the program can be evaluated by comparing the results obtained by POLUTIDAL with the results obtained by other workers for the same problem. These two methods of model verification were performed as discussed below.

The original program POLUT2D was used by Ahmad (1991) to evaluate the transport of a non-reactive contaminant in a 2-D saturated flow regime problem. This same problem had been previously evaluated by Pickens and Lennox (1976) using the finite element method. The POLUT2D results were very similar to those of Pickens and Lennox (1976).

After the original program was modified by the present author to include the effect of linear adsorption, a simple 1-D saturated contaminant transport problem was solved for which a closed form solution was available. This problem involved a constant flow of a reactive contaminant through a homogeneous medium as shown in Figure 4-5.

The solution for this problem as given by Shackelford (1993) is:

$$\frac{C(x,t)}{C_o} = \frac{1}{2}\left\{ \operatorname{erfc}\left(\frac{R_d x - V_s t}{2\sqrt{R_d D_h t}}\right) + \exp\left(\frac{V_s x}{D_h}\right)\operatorname{erfc}\left(\frac{R_d x + V_s t}{2\sqrt{R_d D_h t}}\right)\right\} \qquad (4.45)$$

where: C(x,t) = contaminant concentration at a distance of x from the source at time t

C_o = constant input concentration

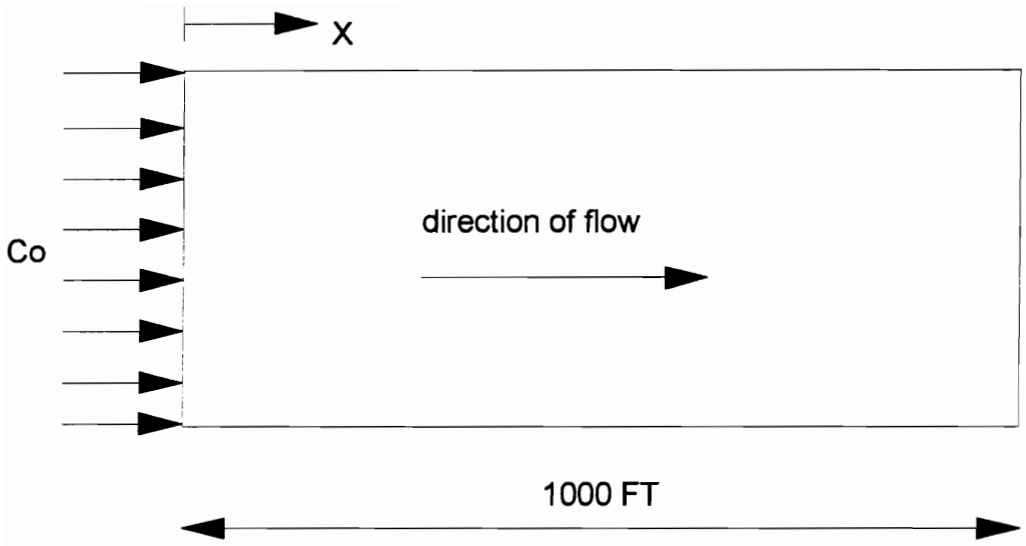

Parameters used in the analysis:

K = 0.1 cm/sec	α_L = 50 ft
n = 0.4	K_d = 1 kg/l
γ = 120 pcf	D* = 0
C_o = 1 mg/l	Δt = 10 sec

FIGURE 4-5: Problem Parameters used to Compare the POLUTIDAL Solution to a Closed Form Solution.

R_d = Retardation factor = $1+\frac{\rho_b}{n}K_d$
ρ_b = bulk density
n = porosity
K_d = distribution coefficient
V_s = seepage velocity
$D_h = \alpha_L V_s + D^*$
α_L = longitudinal dispersivity
D^* = coefficient of molecular diffusion
erfc = complimentary error function

The following boundary conditions are given for the solution of Equation 4.45:

$$C = 0 \text{ for } x \geq 0, \quad t = 0$$

$$C = C_0 \text{ for } x = 0, \; t > 0 \qquad (4.46)$$

The material properties used to solve this problem are given in Figure 4-5. The finite element mesh consisted of 250 elements and 306 nodes as shown in Figure 4-6, and a time increment of 10 seconds was used. The results obtained by POLUTIDAL and the closed form solution are shown in Figure 4-7 for times of 1000, 3000 and 5000 seconds. The program results are identical to the exact solution for this simplified problem.

The program was also used to predict the movement of a non-reactive contaminant through an unsaturated and saturated sandy soil toward a drain tile. This problem was solved by Pickens et al. (1979) using a finite element program that they developed. Figure 4-8 shows the problem configuration and properties. The entire medium was assumed to be saturated at time = 0. Flow was then allowed to occur toward the drain by setting the pressure head at the drain to 0, while the remainder of the boundaries were assumed to have no flow for the entire simulation. The upper 10 cm of the medium was assumed to have an initial relative concentration of 1.0 while the remainder of the medium had an initial relative concentration of 0.0. The material

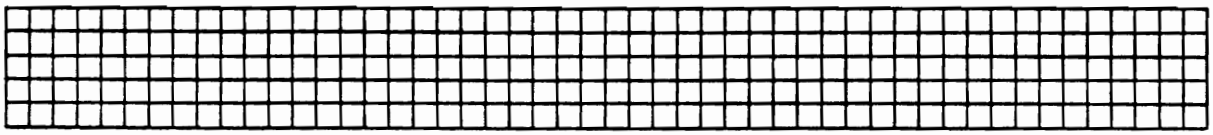

FIGURE 4-6: Finite Element Mesh used to Compare Results with a Closed Form Solution.

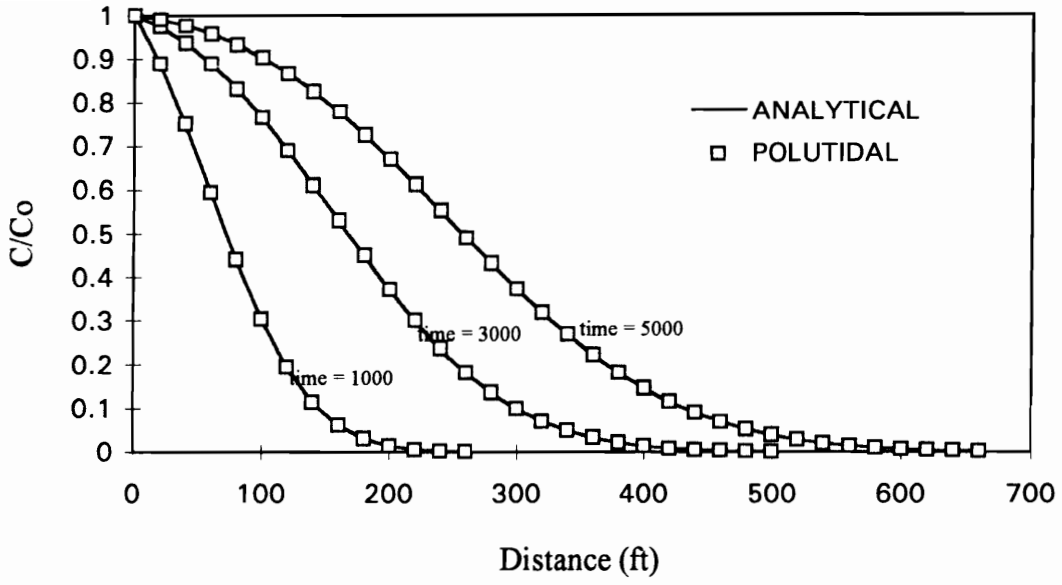

FIGURE 4-7: Comparison of Results between the POLUTIDAL Solution and a Closed Form Solution.

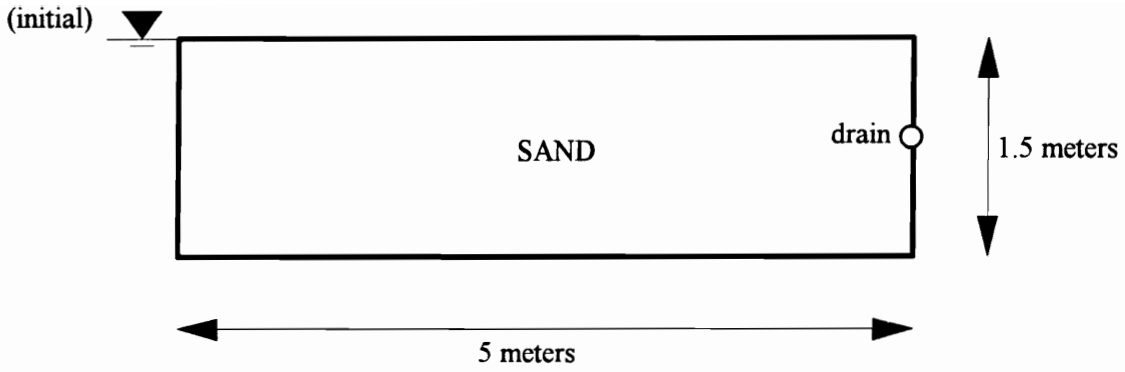

Parameters used in the analysis:

K_{sat} = 0.35 cm/min	Van Genuchten parameters:
α_L = 2 cm	α = 0.031 cm^{-1}
α_T = 0.4 cm	m = 0.8571
D_d = 7.23E-6 cm^2/min	θ_s = 0.3
K_d = 0	θ_r = 0.0864

FIGURE 4-8: Problem Parameters used to Compare the POLUTIDAL Solution to the Solution of Pickens et al. (1979).

properties used in the analysis are shown in Figure 4-8. The van Genuchten parameters were estimated from the soil water retention curve given by Pickens et al. (1979).

A finite element mesh consisting of 800 elements and 867 nodes was used to solve this problem as shown if Figure 4-9. A time increment of 0.5 minutes was used, and a solution was obtained at times of 60 minutes and 720 minutes (12 hours). The solution obtained by Pickens et al. (1979) and by POLUTIDAL are shown in Figure 4-10. The two solutions give similar results for both simulation times. The minor deviations between the two solutions is probably attributed to the estimation of the van Genuchten parameters. In addition, the mesh used by POLUTIDAL was somewhat coarser than that of Pickens et al. (1979) and gave Peclet numbers of up to 6.0 which exceeds the criteria given in Equation 4.39.

From the above discussion, the algorithms and coding of POLUT2D and POLUTIDAL give accurate results for the problems that were studied. It should be noted that additional verification has been proposed to the Corps of Engineers using laboratory and field studies.

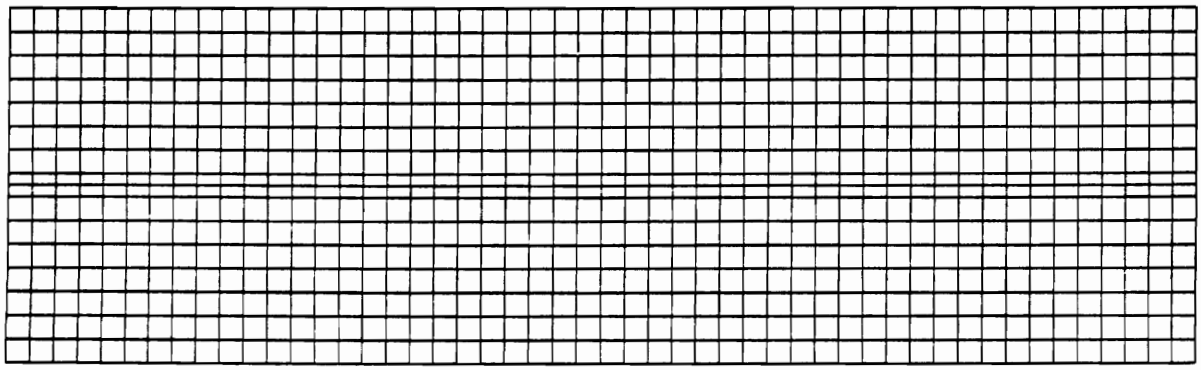

FIGURE 4-9: Finite Element Mesh used to Compare POLUTIDAL Results with those of Pickens, et. al. (1979).

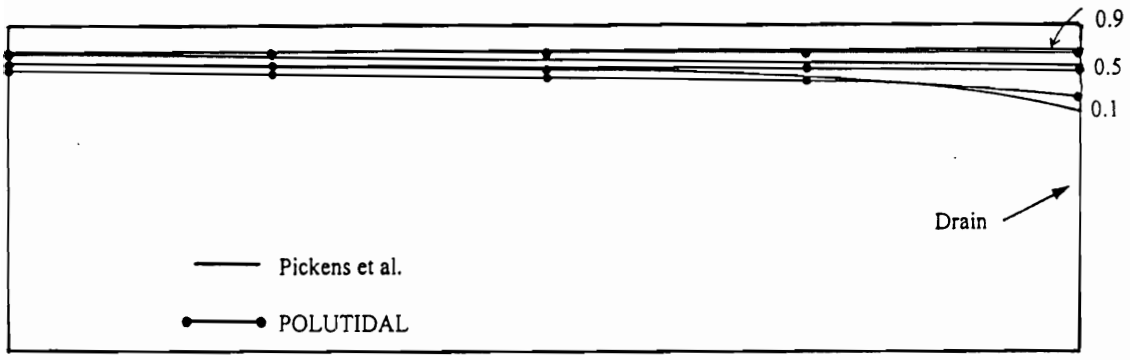

a) time = 60 minutes

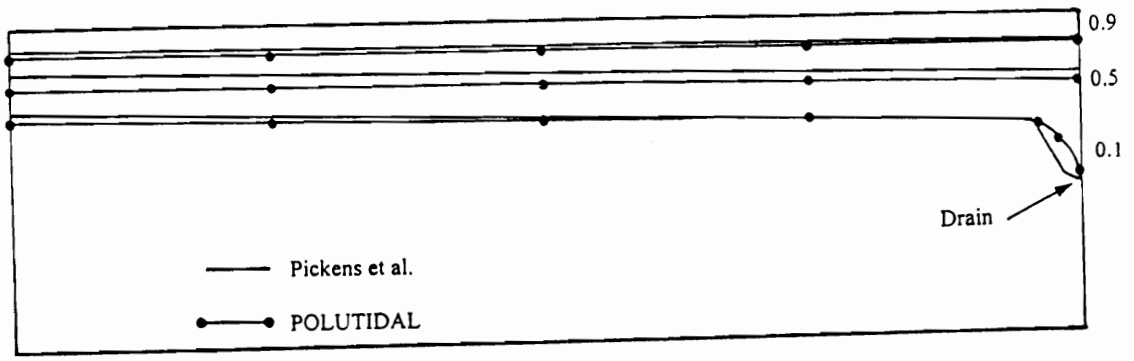

b) time = 720 minutes

FIGURE 4-10: POLUTIDAL and Pickens et al. (1979) Solution for Simulation times of a) 60 minutes and b) 720 minutes.

CHAPTER 5

Problem 1 - Coastal Confined Disposal Facility

5.1 Chapter Overview

In this chapter, POLUTIDAL will be used to analyze an actual confined disposal facility that is proposed for construction in the coastal waters of the U.S. The specific details of the problem were not provided by the Corps of Engineers due to potential litigation. However, most of the geometry and soil parameters were provided and are applicable to several sites that the Corps is involved with. The tidal head model described in Chapter 4 will be used to simulate the local tide at the site. A description of the geometry, subsurface conditions, boundary conditions and finite element approximation is presented below. Sensitivity analyses will also be performed to evaluate which soil properties have a greater impact on the spread of contaminants. The effect of various boundary conditions and sorption models will also be evaluated. The effect of a clay liner and a slurry trench cutoff wall on reducing contaminant transport will also be discussed.

5.2 Problem Description

5.2.1 Geometry

A confined disposal facility is to be constructed in an existing shipping slip. The slip is 2400 feet long and 360 feet wide. A 58 feet high dike consisting of non-contaminated dredge materials and compacted structural fill will be built to close off the slip, and contaminated dredge materials will be placed behind the embankment within the slip. A seven ft thick soil layer and one ft thick layer of asphalt will be placed as a cap over the contaminated dredge material once filling of the CDF is complete. The foundation soils beneath the proposed CDF consist of a 90 ft thick silty sand layer. Underlying this material is low permeability silt. The plan and profile views of the CDF are shown in Figures 5-1 and 5-2, respectively.

5.2.2 Water Level Boundary Conditions

Monitoring wells located 2500 feet upland from the slip indicate a constant water elevation of 10 feet above mean sea level (Figure 5-2). Thus, this is the boundary condition for the upland end of the slip. The water level of the bay fluctuates with the tide as shown in Figure 5-3. This fluctuating boundary conditions was simulated using the approximation given by Equation 4.44. From the measured tide data, h_a is 7 feet, h_o is 5 feet, and t_o is 690 minutes. The measured water level data and the approximation made using Equation 4.44 are shown in Figure 5-4. Note that the approximation fits the measured data very well.

5.2.3 Contaminant Information

The dredge soil contains varying concentrations of arsenic, cadmium, copper, lead, nickel, silver and zinc. These heavy metals are often found in dredge materials because of the industries and large populations associated with the locations of shipping channels and ports. The analyses performed in this study are for arsenic. A brief discussion of this contaminant and its properties for this problem are given below. It should be noted that arsenic has many different compounds, both organic and inorganic, which have different properties related to mass transport. Therefore, the discussion which follows is generalized to be typical of most of the arsenic species.

Arsenic was known to be poisonous as early as 2000 b.c. (Pershagen, 1983). Pershagen reports that 1/3 of the cases of intentional criminal poisoning in France in the 19th century involved arsenic, and that three women conspired together to poison nine people in Hungary in the late 1800's using arsenic laced marmelade, cookies, soup and coffee. The primary reason for the popularity of arsenic as a homicidal poison is because

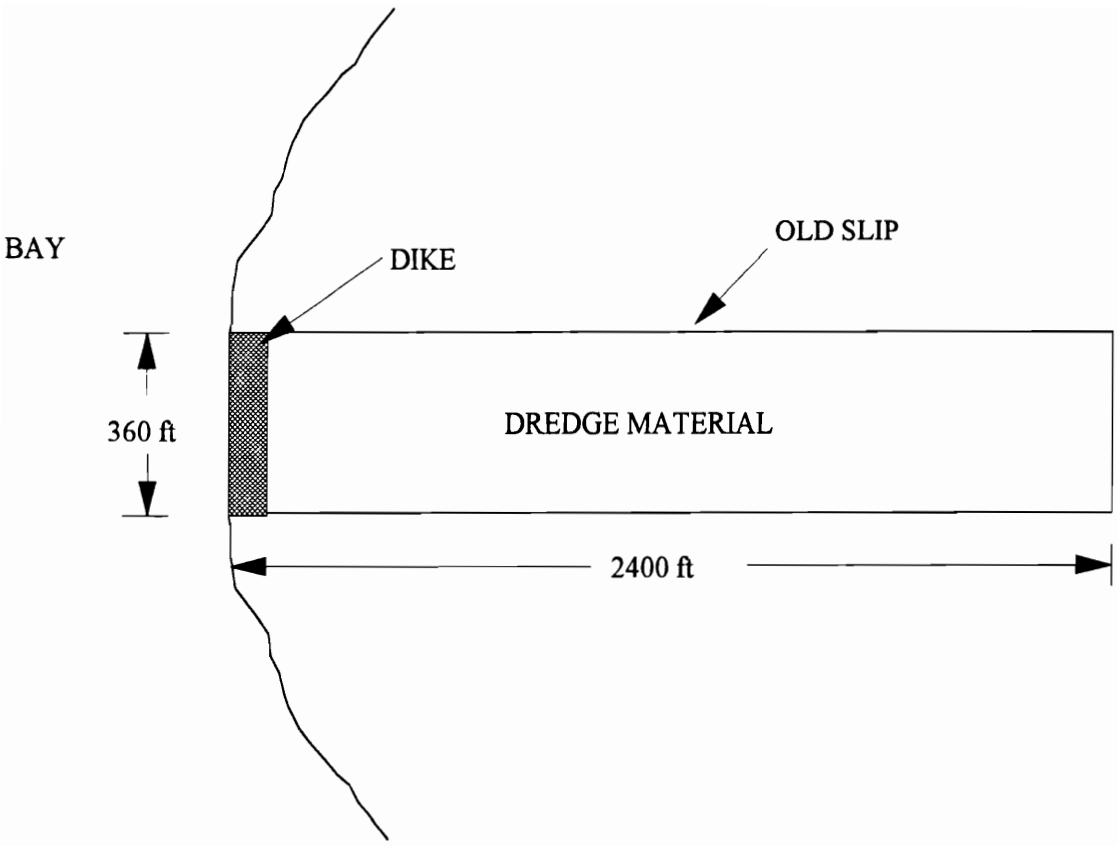

FIGURE 5-1: Plan View of CDF for Problem Number 1.

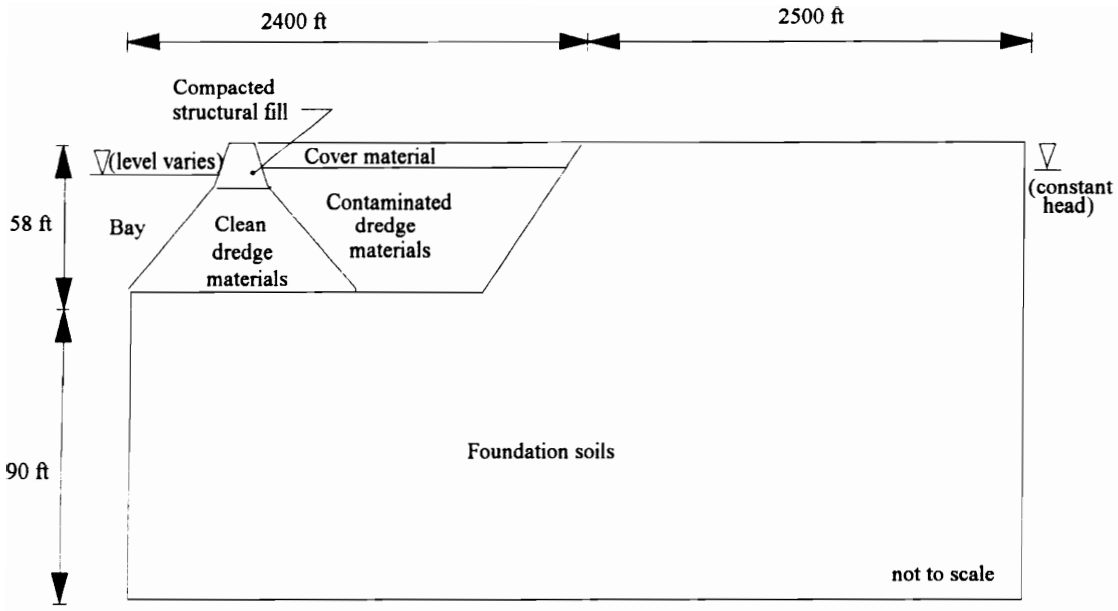

FIGURE 5-2: Profile of CDF for Problem Number 1.

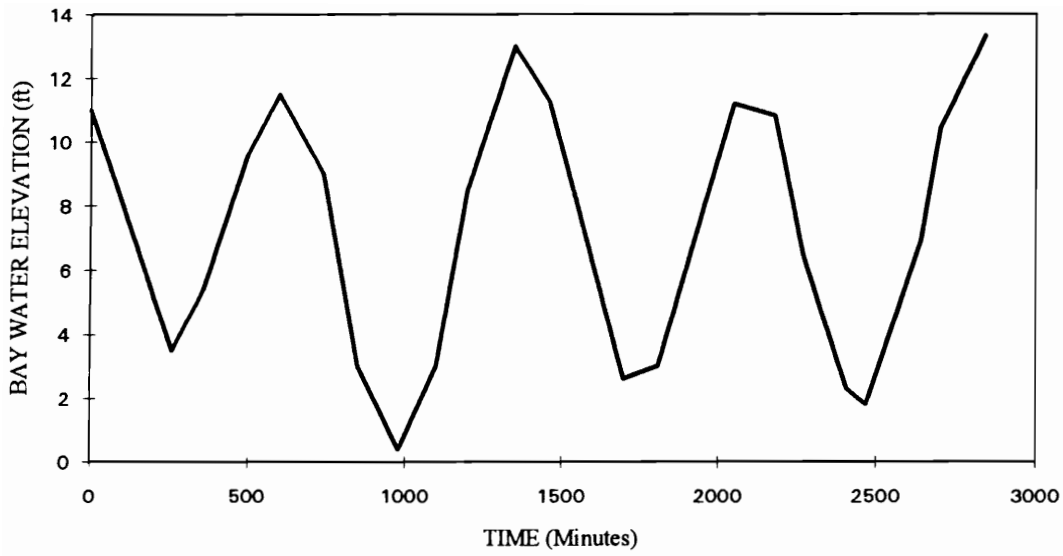

FIGURE 5-3: Fluctuation of the Tide with Time.

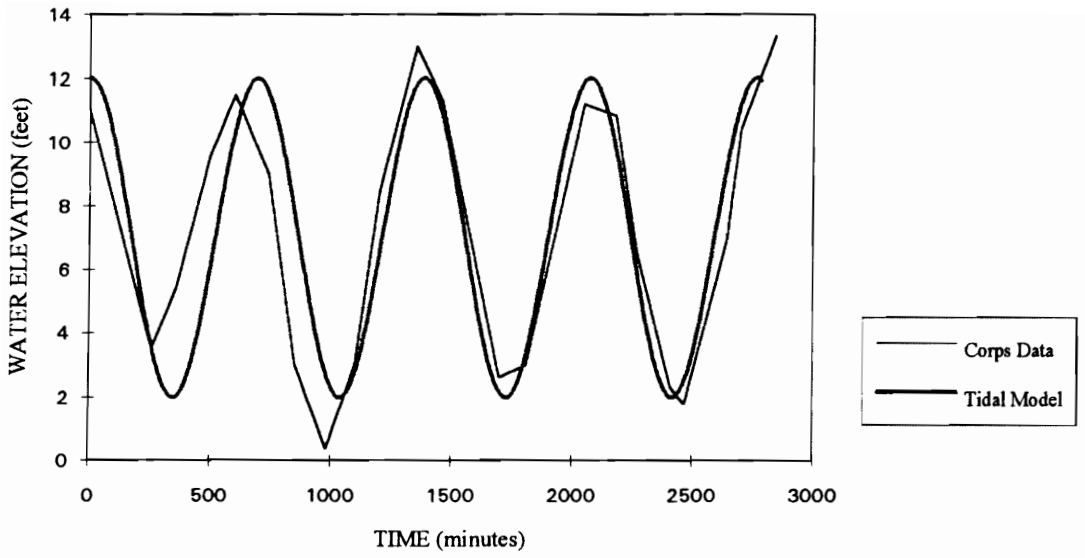

FIGURE 5-4: Comparison of Actual Tide Data and Approximated Tidal Head.

it is odorless and tasteless. Accidental arsenic poisoning has also occurred. In 1900, several thousand people in Manchester were poisoned by drinking arsenic contaminated beer, and 400 Japanese were affected by arsenic contaminated soy sauce (Pershagen, 1983). Hutton (1987) reports that hundreds of people suffered "severe effects" while being treated with Fowler's solution, a medicinal solution consisting of sodium arsenite, which was intended to treat psoriasis and leukaemia. Some of the effects of the above acute exposures include skin lesions, a swelling liver, cardiac arrest, vomitting, diarrhea and other gastrointestinal symptoms.

Chronic exposure to arsenic occurs most commonly through contaminated drinking water and often causes skin ailments such as skin cancer and gangrene. Other sources of exposure include seafood containing arsenic, and wine which was produced from grapes sprayed with arsenic based pesticides.

Natural sources of arsenic release into the environment include volcanic ash and steam, forest fires and runoff from soils with naturally ocurring arsenic. Man-made sources of arsenic release into the environment come primarily from the process of copper smelting. Woolsen (1983) states that even the best scrubbers do not remove all of the arsenic released through furnace stacks and arsenic eventually returns to the earth's surface as dust or through precipitation. The combustion of coal also contributes to the release of arsenic with an estimated annual rate of 840 tons annually (Woolson, 1983). Runoff from fields treated with arsenic based pesticides and herbicides, leaching from mining slag heaps and the discharge of phosphate detergents in waste water effluent are also man-made sources of arsenic release into the environment.

Studies of surface waters containing arsenic have revealled that sediments act as sinks for arsenic. Woolson (1983) indicates that many surface waters are "self-purifying" with respect to arsenic. Arsenic adsorbs on the sediments, lowering the arsenic

concentration in the water. Fowler (1983) states that some studies have shown little to no arsenic concentration in the aquatic biota even though the sediments contained arsenic. Thus, once arsenic is adsorbed on sediments, its effect to the environment may be negligable. However, once the sediments are distrubed by dredging, arsenic may be desorbed and released back into the water. Consequently, placing the dredged material in confined disposal facilities should minimize the potential of re-contaminating a body of water with arsenic. For this problem, the Corps provided an initial arsenic concentration of 0.027 mg/L in the pore water of the dredge material.

5.2.4 Material Properties

The material properties needed to perform the analyses are:

1) Horizontal saturated hydraulic conductivity
2) Vertical saturated hydraulic conductivity
3) Angle of anisotropy
4) Longitudinal dispersivity
5) Transverse dispersivity
6) Molecular diffusion coefficient
7) Saturated volumetric water content (porosity)
8) Residual volumetric water content
9) van Genuchten parmeter m
10) van Genuchten parameter α
11) Back pressure
12) Unit weight
13) Distribution coefficient.

A list of the values used for these properties is given in Table 5-1. The coefficient of permeability, porosity, unit weight and distribution coefficient values are essentially the same as those provided by the Corps of Engineers. The angle of anisotropy and back pressure were assumed to be zero. The van Genuchten parameters were estimated based on material type. Values of 50 feet for the longitudinal dispersivity and 10 feet for the transverse dispersivity were also estimated based on material type. The molecular diffusion coefficients were assumed to be zero for all of the material types since

TABLE 5-1: Material Properties Used in the Analysis.

Soil #	Location	K_x (cm/sec)	Longitudinal Dispersivity (ft)	Transverse Dispersivity (ft)	Dry Unit Weight (pcf)	K_d (l/kg)	Sat. Water Content	Res. Water Content	van Genuchten α (ft^{-1})	van Genuchten m
1	Foundation	1E-2	50	10	83	0.5	0.5	0.1	0.8	0.6
2	Foundation	2E-2	50	10	83	0.5	0.5	0.1	0.8	0.6
3	Foundation	3E-2	50	10	83	0.5	0.5	0.1	0.8	0.6
4	Dike (Dredge)	1E-3	50	10	74	0.5	0.55	0.1	0.8	0.6
5	Dike (Imported Fill)	1E-3	50	10	115	0.5	0.33	0.1	0.8	0.6
6	Cover	1E-6	50	10	100	0.5	0.4	0.1	0.052	0.3
7	Dredge	1E-3	50	10	74	0.5	0.55	0.1	0.8	0.6

NOTE: K_y equals $1/4$ K_x

mechanical dispersion is expected to dominate. However, the effect of molecular diffusion will be evaluated in the Sensitivity Analyses (Section 5.6) of this chapter.

5.3 Finite Element Approximation

5.3.1 Geometry

The initial finite element mesh that was used to subdivide the domain of the problem is shown in Figure 5-5. This mesh consists of 410 nodes and 345 elements. The horizontal and vertical dimensions of the mesh are 5300 ft and 148 ft, respectively. The mesh was designed to eventually include a clay layer beneath the contaminated dredge material as well as a slurry trench through the center line of the embankment. In order to reduce computer run time, the results of several analyses were evaluated to determine if some of the upland portion of the mesh could be removed without affecting the results. It was found that the head at many of the upland nodes were not influenced by the fluctuating head at the bay end. Consequently, there was little to no contaminant transport in these regions. Thus, about 1925 feet of the upland portion of the mesh was removed. The final mesh consisted of 344 nodes and 298 elements. This mesh is shown in Figure 5-6.

5.3.2 Boundary Conditions

A constant head of 10 feet was used as the boundary condition in the upland end of the domain as shown in Figure 5-7. At the bay side of the dike, the tidal head approximation model was utilized at the nodes indicated in Figure 5-7. No flow boundary conditions were assumed along the top and bottom boundaries of the mesh. The boundary condtions for the mass transport portion of the problem are also shown in Figure 5-7. As indicated, a fixed concentration of 0.027 mg/l was assumed throughout the dredge soil.

FIGURE 5-5: Original Finite Element Mesh for Problem Numer 1.

FIGURE 5-6: Final Mesh used for Problem Number 1.

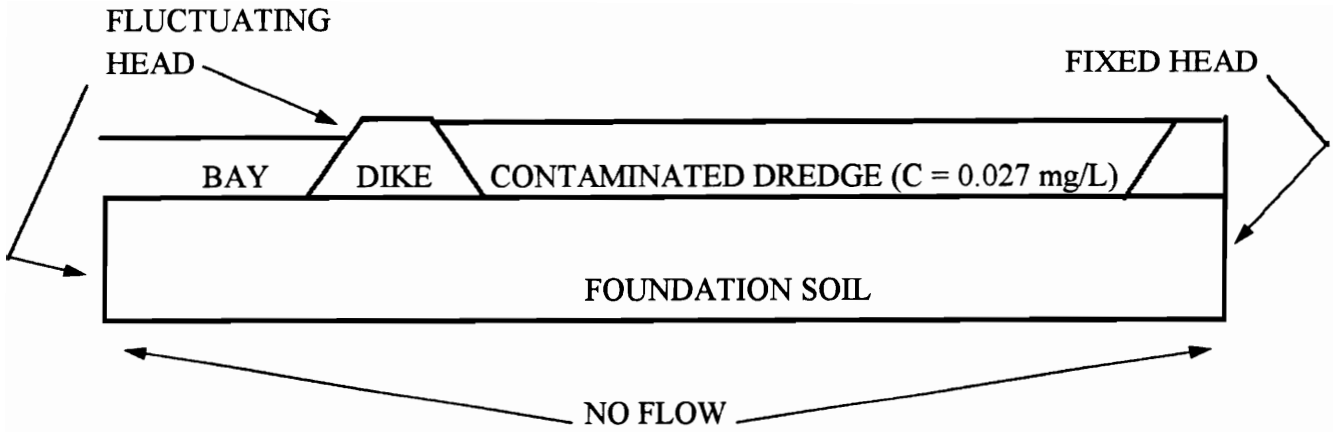

FIGURE 5-7: Boundary Conditions for Problem Number 1.

5.3.3 Initial Conditions

Since this is a time dependent problem, initial conditions must be given for both the total head and the concentration. For the fluid flow portion of the problem, the initial head at all of the nodes was obtained by first performing a steady state analysis assuming a constant average tidal head of 5 feet above mean sea level for the bay portion of the problem. The nodal head values at various output times were observed until they were constant. These values were then used as the initial head for all of the transient analyses. For the mass transport analysis, the initial concentration was assumed to be zero everywhere except in the contaminated dredge material.

5.3.4 General Parameters

There are several other parameters which must be specified to use POLUTIDAL to solve mass transport problems. These parameters are:

1) maximum number of iterations,
2) degree of accuracy,
3) time integration factor, and
4) time increment.

The first two parameters are required to perform the flow analysis portion of the problem where iteration is needed to obtain the hydraulic conductivity in the unsaturated zone as described in Section 4.4. Values of 20 and 5% were used for the maximum number of iterations and the degree of accuracy, respectively, throughout the analyses. The Crank-Nickolson method was used, thus the time integration factor was 0.5. The time increment used for most of the analyses was 10.18 days. Using this time increment, the following tidal heads are obtained for the first few time steps:

time step	tidal head (ft)
1st	12
2nd	7
3rd	2
4th	7
5th	12

This cycle of heads is repeated throughout the simulation time.

5.4 Criteria Used to Evaluate the Results

In the sections below, the results of the analyses for this CDF are presented. To evaluate and compare the results of all the analyses, two curves will be developed from the output generated by POLUTIDAL. These curves will be:

1) the break through curve, and
2) the mass loading curve.

The break through curve is similar to a standard laboratory break through curve for contaminant transport. This plot indicates the concentration history of a contaminant as it is transported away from the source of contamination. In this context, the arsenic concentration at a single node along the embankment adjacent to the bay will be plotted with time. The node evaluated in the results below is the one which has the highest concentration. A typical break through curve is shown in Figure 5-8a. Note that the concentration is normalized with respect to the original arsenic concentration (C_0 = 0.027 mg/l) in the contaminated dredge. The mass loading curve is simply a plot of the cummulative amount (mass) of arsenic that seeps into the bay from the CDF plotted as a function of time (See Figure 5-8b).

5.5 Results of the Analyses for the Original Problem

Using the CDF geometry, soil properties and boundary and initial conditions given above, POLUTIDAL was used to analyze the problem. Figure 5-8a shows the break through curve up to a time of 50 years. This plot indicates that after about 7.5 years, the maximum arsenic concentration that will have seeped through the embankment and foundation soils and into the bay is about 50% of the original concentration. At 50 years, the maximum arsenic concentration reaching the bay will be about 99 % of the original

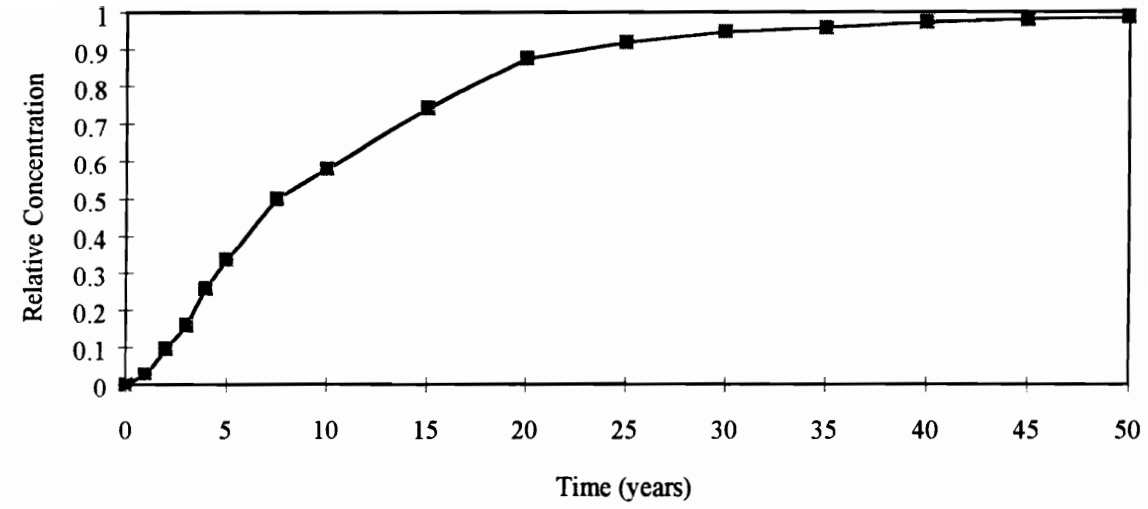

a) Break Through Curve

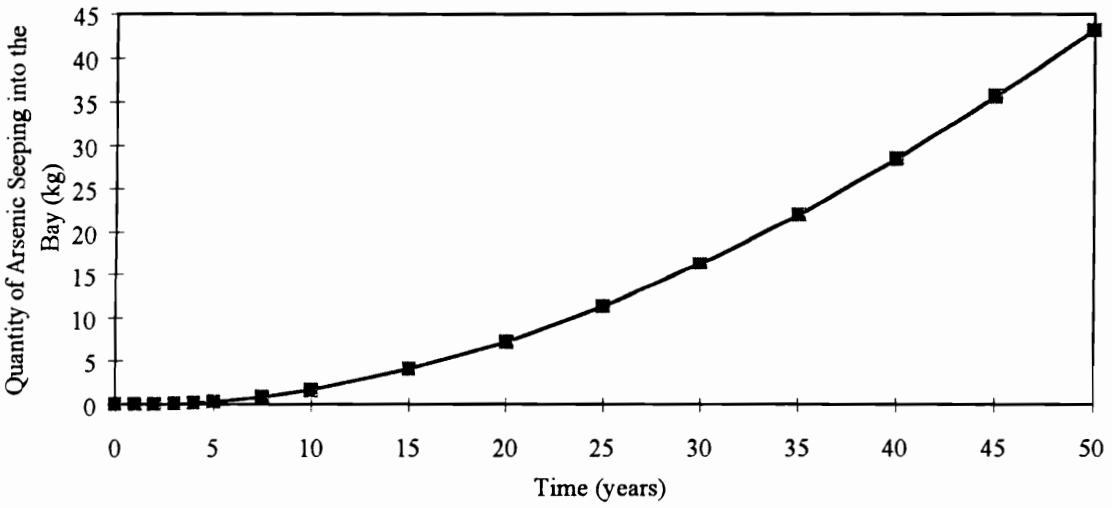

b) Mass Loading Curve

FIGURE 5-8: Break Through and Mass Loading Curves for the Original Problem.

concentration. Figure 5-8b shows the total cummulative amount of arsenic leaching through the embankment and the foundation materials into the bay as a function of time. As might be expected, the amount of arsenic reaching the bay is only a small amount initially, but increases with time as the arsenic plume spreads through the dike and foundation soils. The results indicate that a total of 43 kg of arsenic will leach into the bay after 50 years.

5.6 Sensitivity Analyses

Sensititvity analyses were performed on some of the general problem parameters such as water level boundary conditions, time step, etc. as well as some of the soil properties to evaluate their effect on the overall solution. The results of these sensitivity analyses are summarized below.

5.6.1 Water Level Boundary Condition for The Bay

Analyses were performed to evaluate how the fluctuating tide effects arsenic transport. Rather than considering the tide to vary with time, analyses using constant heads of 2 and 7 feet above mean sea level were performed. These values represent the low and average tide levels respectively. Figure 5-9a shows the break through curves for both of these conditions as well as for the fluctuating tidal model used in the previous analysis. The results using the average tide level (7 feet) predicted a flatter break through curve then the fluctuating tidal model because the seepage velocities were smaller. Note that the low tide analysis (2 feet) predicted a lower relative concentration than the fluctuating tidal model at earlier time levels, but predicts a higher concentration than the fluctuating model after about 23 years. This occurs because a larger portion of the dike is unsaturated when a low tide water level is used. Consequently, it takes a longer time for the contaminant to reach the outer face of the dike. However, once the contaminant plume

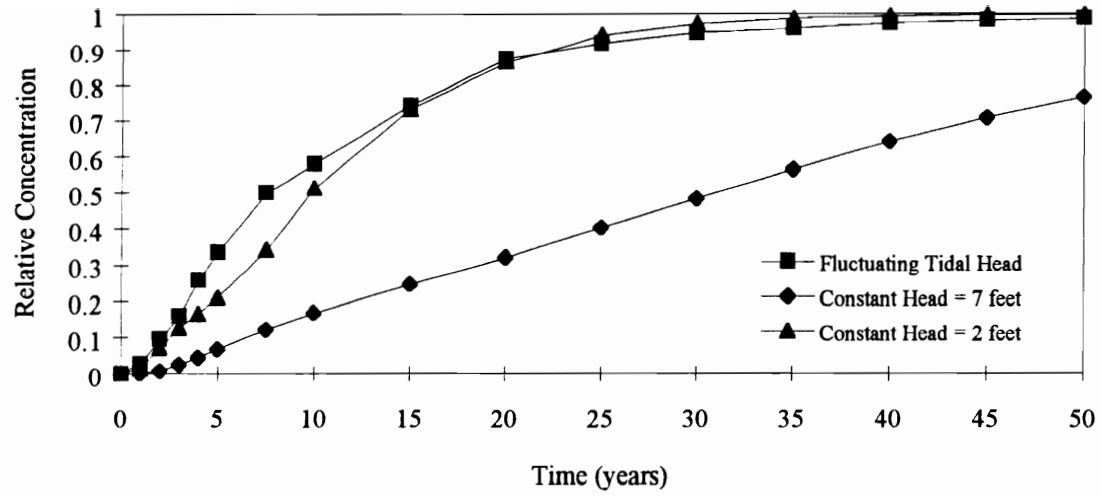

a) Break Through Curves

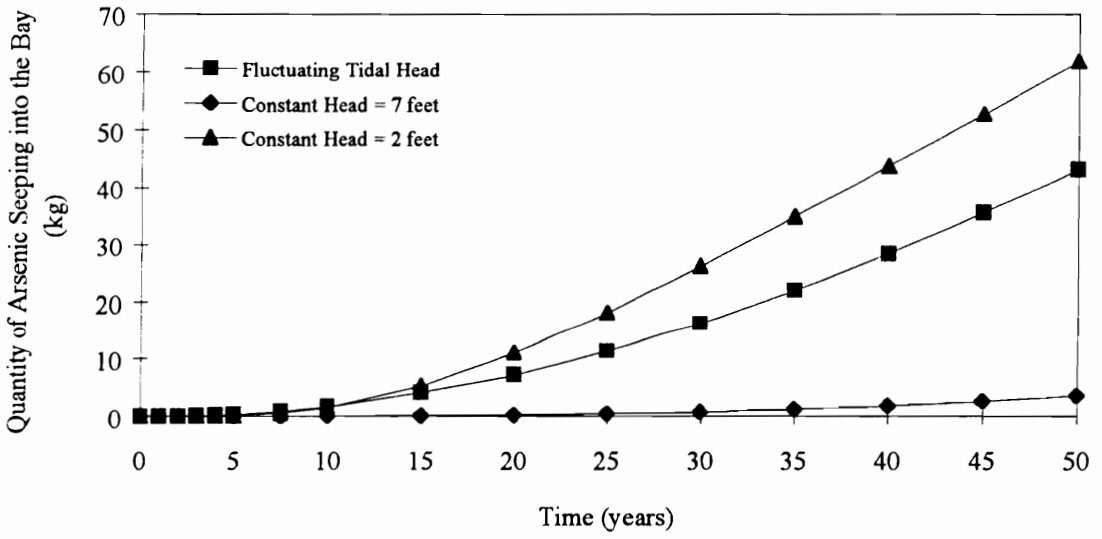

b) Mass Loading Curves

FIGURE 5-9: Effect of Tidal Water Boundary Condition on the Break Through and Mass Loading Curves.

reaches the face of the dike, the higher velocity causes the plume to spread faster than the fluctuating model.

The mass loading curves for all of these bay water level conditions are shown in Figure 5-9b. The average tide model predicts a significantly lower quantity of arsenic transport than the fluctuating model due to lower seepage velocities. For example, the average tide model predicts that 3.5 kilograms of arsenic leachate will seep into the bay by the end of 50 years whereas the fluctuating model predicts that about 43 kg of arsenic will have reached the bay by this time. The low tide model predicts about 43% more arsenic loading into the bay than the fluctuating model. This is also attributed to higher seepage velocities which increases the rate and amount of arsenic transport into the bay. These different models demonstrate the importance of using the correct boundary conditions for the analysis. Incorrect water levels effect the seepage velocity which can in turn decrease or increase the rate of contaminant transport.

5.6.2 Time Increment

The influence of the time increment on the solution of the problem was evaluated by performing additional analyses using time increments of 1, 10 and 100 days. Each of these analyses were performed using a constant head of 7 feet (the average tide level). The results shown in Figure 5-10 indicate that arsenic transport is not effected by the time increment used in the analysis.

5.6.3 Beta Time Factor

The beta time factor (β) used in the above analyses was 0.5 which corresponds to the Crank-Nichalson central difference method. Two analyses were performed using beta

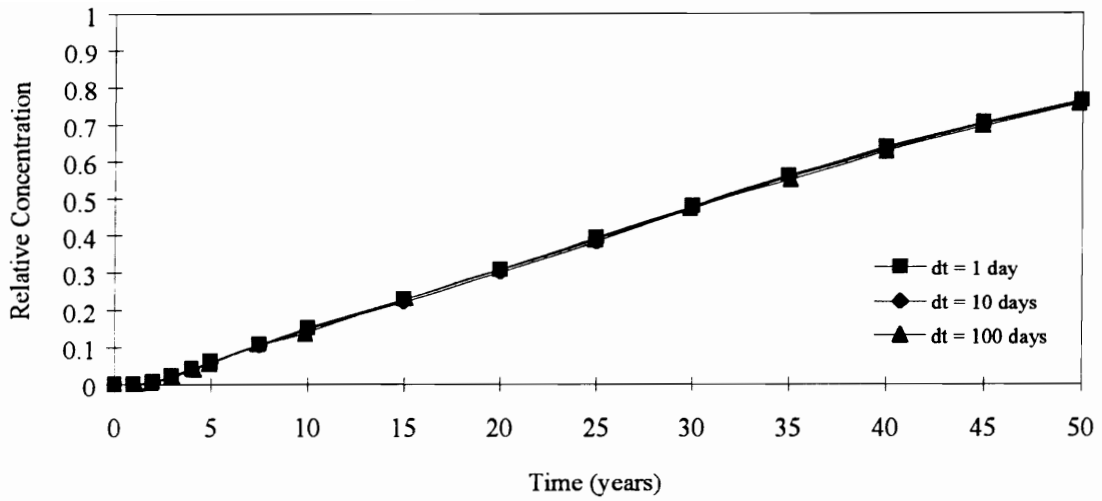

a) Break Through Curves

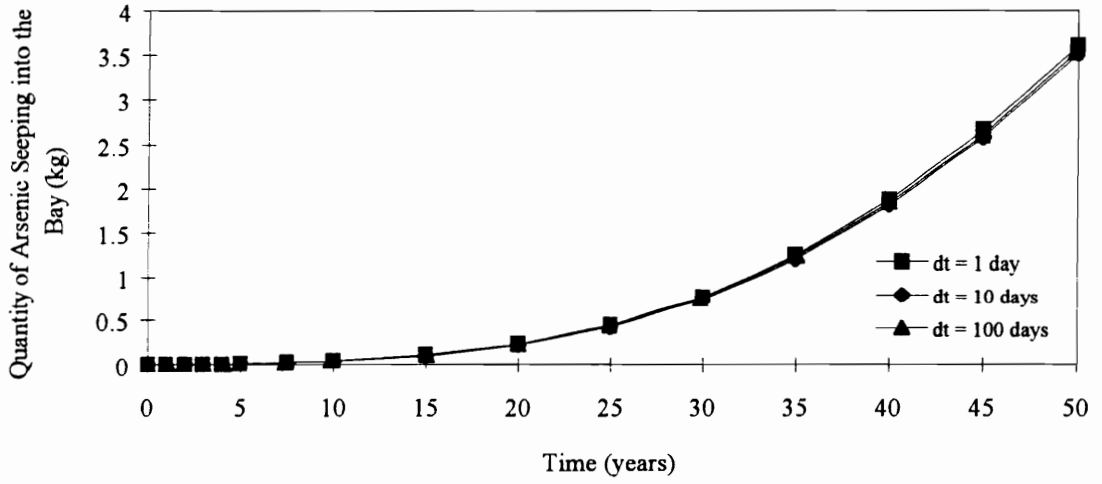

b) Mass Loading Curve

FIGURE 5-10: Effect of the Time Increment on the Break Through and Mass Loading Curves.

values of 2/3 (Galerkin method) and 1 (Backward difference method) to evaluate their effect on arsenic transport. All of the analyses were performed using a constant head of 7 feet (average tide level) on the bay side of the dike and a time increment of 5 days.The results shown in Figure 5-11 indicate that all three of the time factors give about the same result.

5.6.4 Mesh Size

The effect of the spacing of the finite element nodes and the size of the elements on the rate of arsenic transport was evaluated using three different meshes. Each of these meshes is shown in Figure 5-12. The meshes are labelled as being "coarse", "medium" or "fine". The total number of elements and nodes for each mesh are summarized below:

Mesh	Elements	Nodes
Coarse	77	106
Medium	259	314
Fine	409	493

Figure 5-13 shows a comparison of the break through and mass loading curves obtained from the analyses using each of these meshes. The trend shown in the figure indicates that finer meshes predict lower contaminant concentrations than coarser meshes. Note that the difference between the results is not too significant.

5.6.5 Hydraulic Conductivity

The coefficient of hydraulic conductivity is a soil property that can be difficult to quantify with a high degree of confidence. Thus, analyses were performed using hydraulic conductivity values that were one order of magnitude higher and one order of magnitude lower than the original values given in Table 5-1. The results of the analyses for the different soil types for this problem are given below.

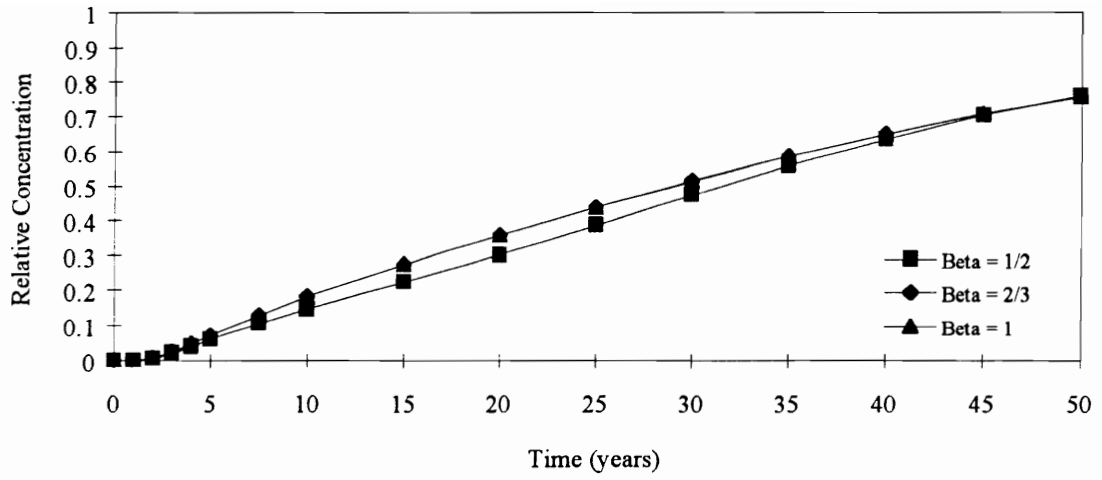

a) Break Through Curves

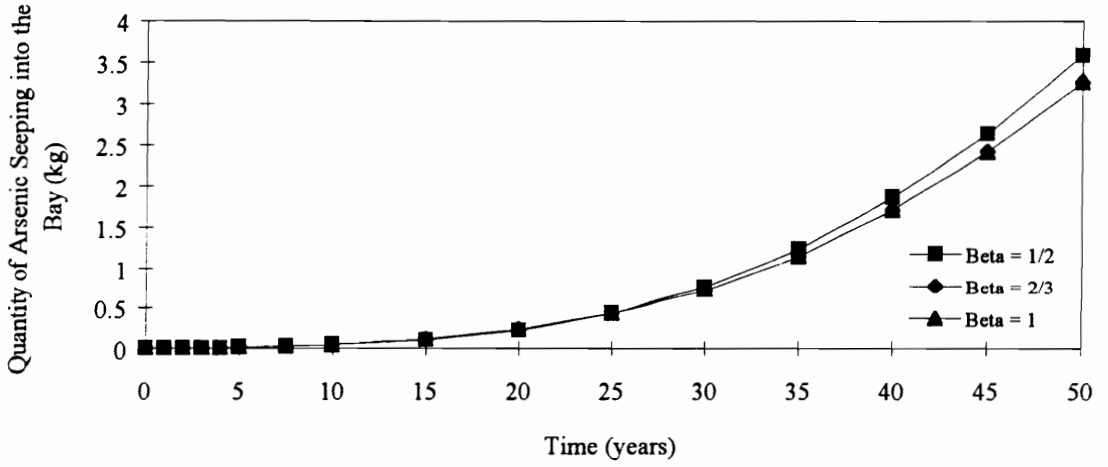

b) Mass Loading Curves

FIGURE 5-11: Effect of Beta Time Factor on the Break Through and Mass Loading Curves.

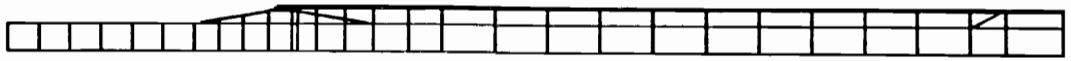

a) Coarse Mesh

b) Medium Mesh

c) Fine Mesh

FIGURE 5-12: Finite Element Meshes Used in the Sensitivity Analyses.

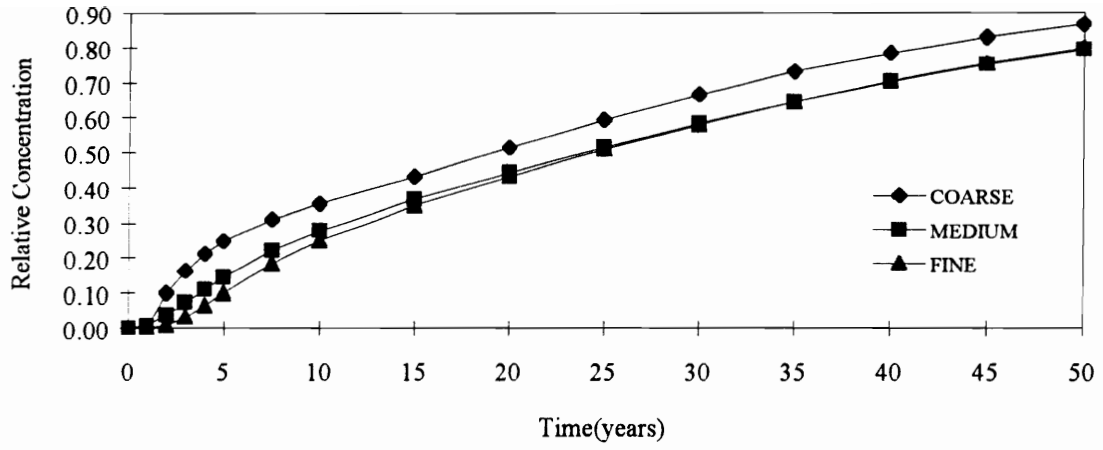

a) Break Through Curves

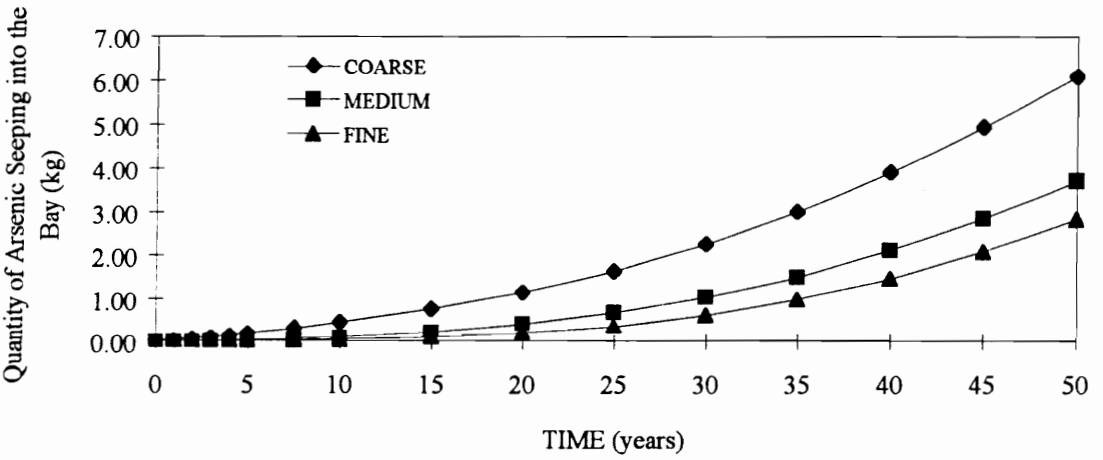

b) Mass Loading Curves

FIGURE 5-13: Effect of Mesh Size on Break Through and Mass Loading Curves.

The hydraulic conductivity of the contaminated dredge material was found to have only a minimal effect on the transport of arsenic as indicated in the break through and mass loading curves shown in Figure 5-14. There is, however, a general trend indicating that higher hydraulic conductivity results in greater arsenic transport.

The influence of the hydraulic conductivity of the dike constructed to close off the slip was evaluated by considering the imported fill and dredged fill material portions seperately. Figure 5-15a shows the break through curves obtained by varying the hydraulic conductivity of the imported fill. As expected, a higher coefficient of hydraulic conductivity results in a quicker break through time and increased arsenic loading to the bay. Note, however, that a significant increase in arsenic transport occurs when the hydraulic conductivity is an order of magnitude higher than the original value of 10^{-3} cm/sec. A hydraulic conductivity one order of magnitude lower than the original value predicts only a slighlty smaller amount of arsenic loading into the bay.

The hydraulic conductivity of the dredged fill portion of the dike was also varied one order of magnitude higher and lower than the original permeability value. The break through and mass loading curves are shown in Figure 5-16. The same general trend as discussed above for the imported fill can be seen in the mass loading curves. However, the variation of the hydraulic conductivity values does not have a significant impact on arsenic transport.

The effect of the hydraulic conductivity of the foundation soils on arsenic transport was also studied. All of the above analyses were performed using the permeability values given by the Corps of Engineers which varied between 1×10^{-2} and 3×10^{-2} cm/sec. An analysis was performed by assuming a value of 3×10^{-2} cm/sec for all of the foundation soils. This small increase in hydraulic conductivity had a negligable effect on the break through and mass loading curves. Two additional analyses were

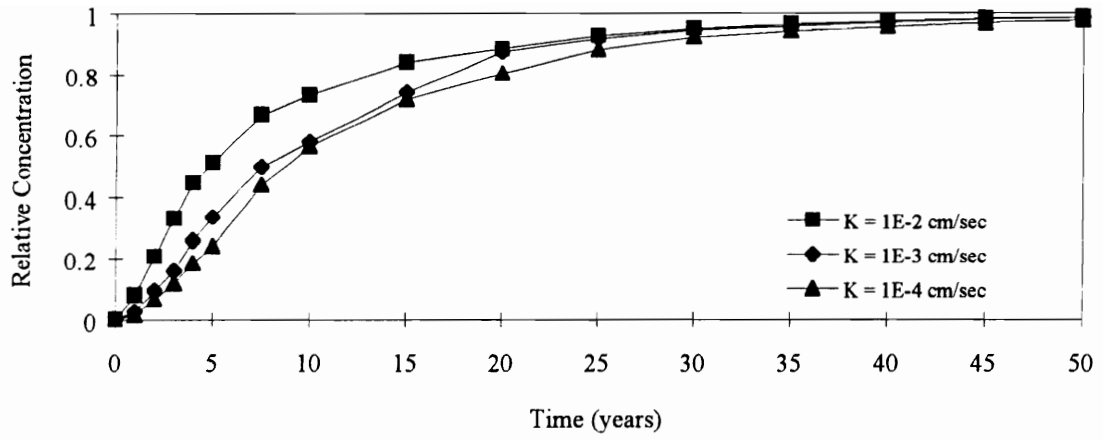

a) Break Through Curves

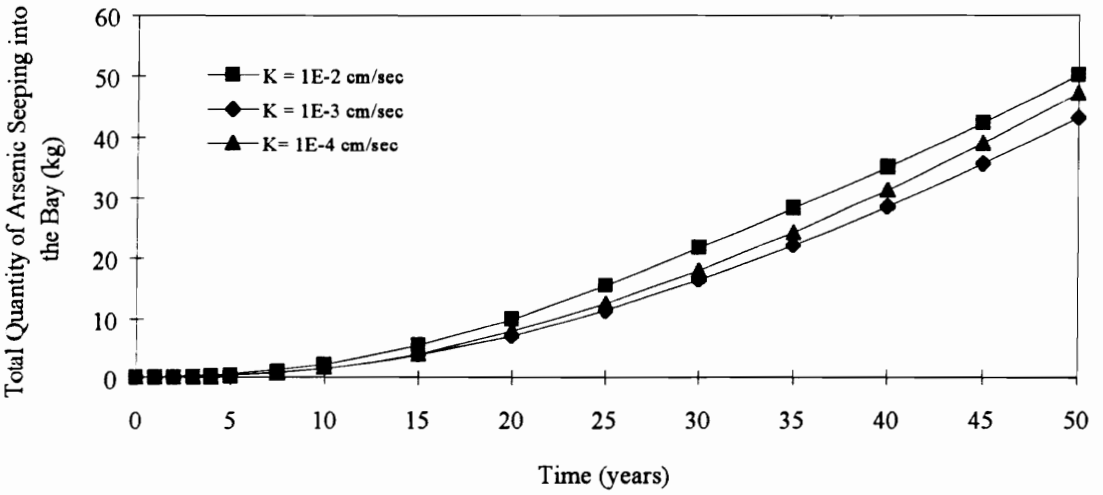

b) Mass Loading Curves

FIGURE 5-14: Effect of the Hydraulic Conductivity of the Dredge Material on the Break Through and Mass Loading Curves.

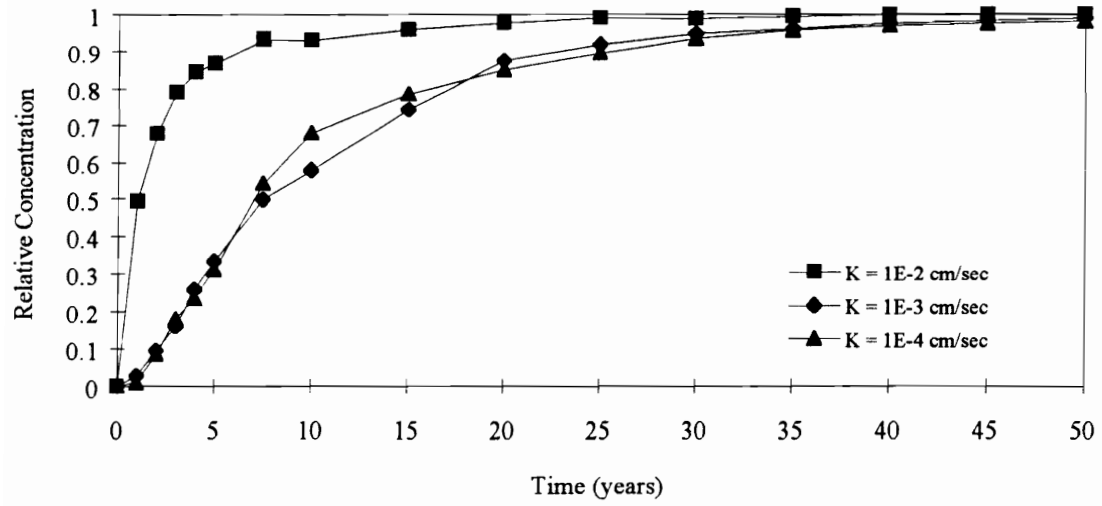

a) Break Through Curves

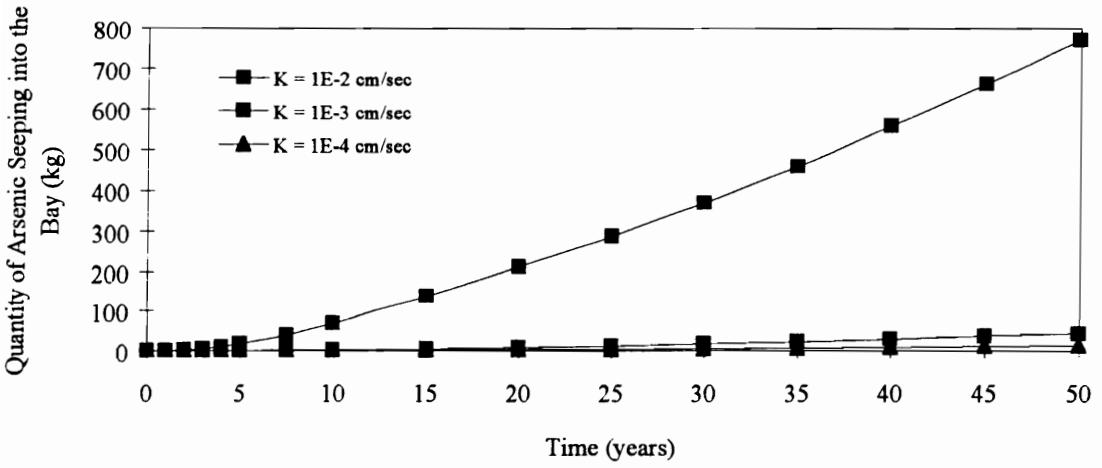

b) Mass Loading Curves

FIGURE 5-15: Effect of the Hydraulic Conductivity of the Imported Dike Fill on the Break Through and Mass Loading Curves.

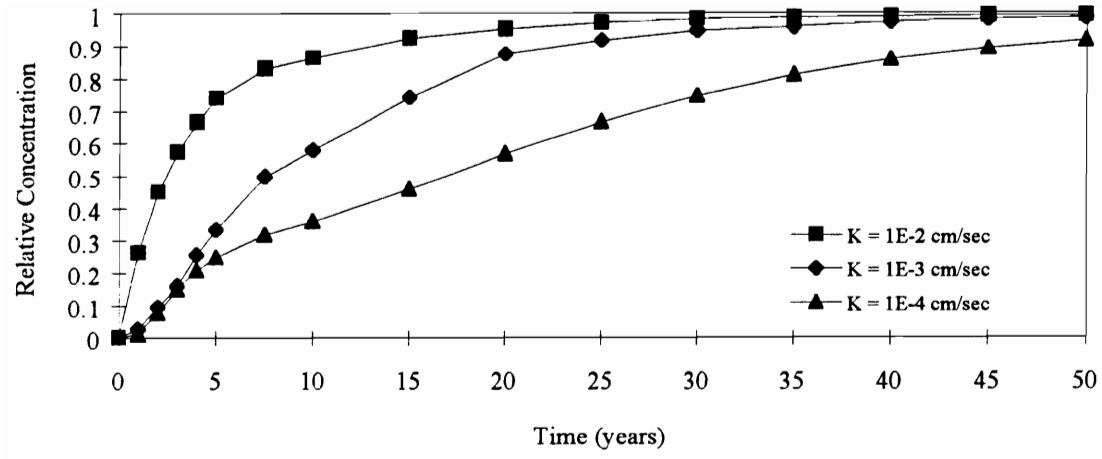

a) Break Through Curves

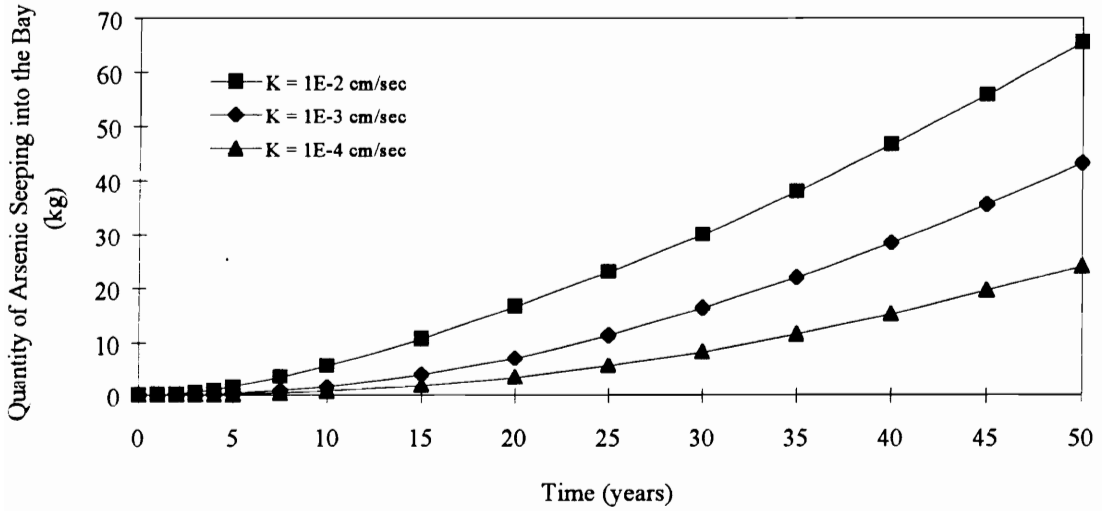

b) Mass Loading Curves

FIGURE 5-16: Effect of the Hydraulic Conductivity of the Dredged Dike Fill on the Break Through and Mass Loading Curves.

performed using hydraulic conductivity values of 3×10^{-1} and 3×10^{-3} cm/sec for all of the foundation soils. The break through and mass loading curves for these three conditions are shown in Figure 5-17. Note that the higher permeablility value has a signigicant effect on the total amount of arsenic that seeps into the bay.

5.6.6 Adsorption

The Corps of Engineers indicated that the distribution coefficient could vary between 0.5 and 2.0 l/kg for all of the soil types. The results reported above are for the low end (0.5 l/kg) of this range. Thus an additional analysis was performed to evaluate arsenic transport using the higher K_d value for all of the soil types. In addition, an analysis was performed ignoring adsorption altogether. The break through and mass loading curves for these conditions are shown in Figure 5-18. These curves indicate that higher distribution coefficients retard the rate of contaminant transport into the bay. This can be expected since a higher adsorption capacity would have the effect of removing arsenic from the groundwater. Note that disregarding adsorption ($K_d = 0$) has the opposite effect. The break through rate is more rapid and more arsenic leaches into the bay. About 23% more arsenic will leach into the bay after 50 years if adsorption is not considered as compared to the original analysis ($K_d = 0.5$). Thus, a conservative estimate of arsenic transport can be obtained by neglecting adsorption. This approach would probably not be too conservative for this problem since the original distribution coefficient is not very large to begin with. Sensitivity analyses were also performed by varying the distribution coefficient for each of the different soil types. The results indicated that the distribution coefficient of the contaminated dredge material had no

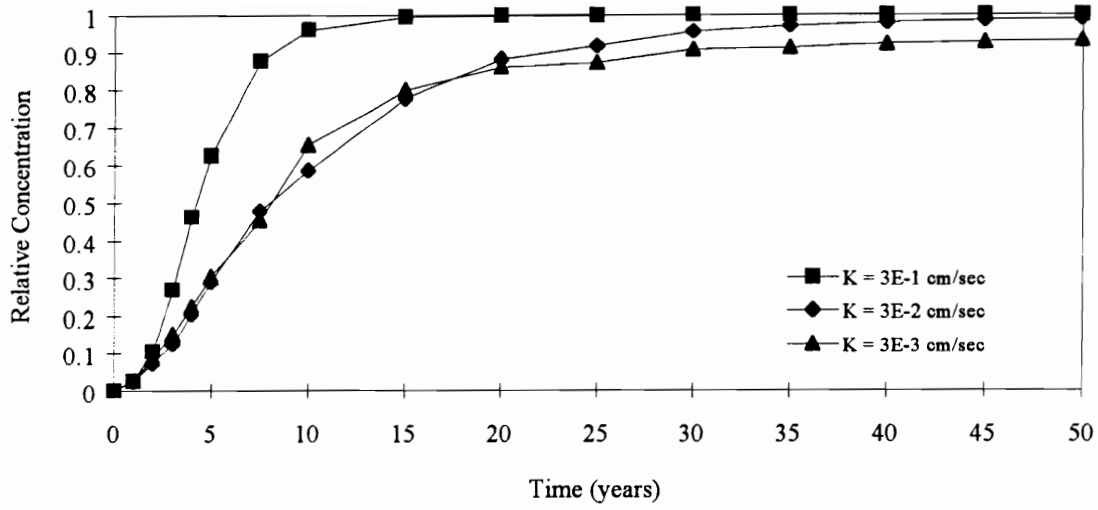

a) Break Through Curves

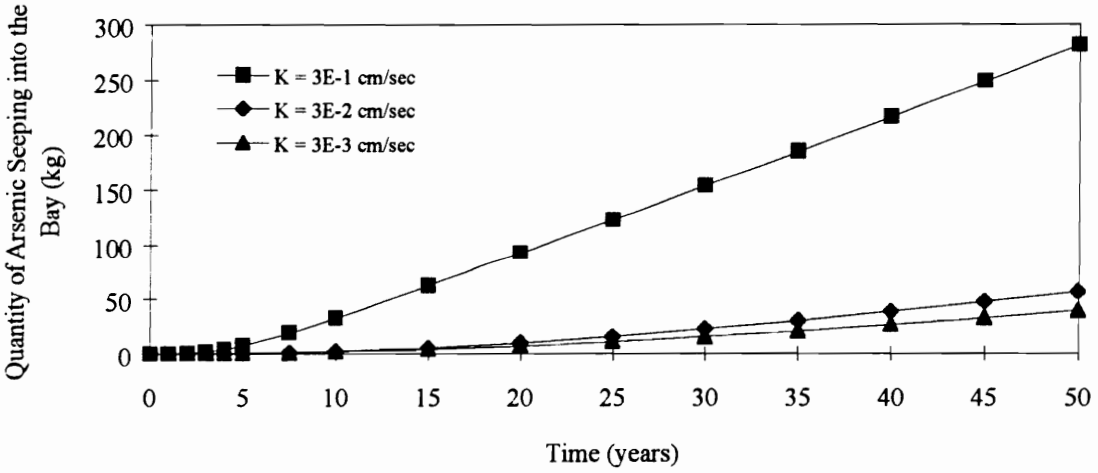

b) Mass Loading Curves

FIGURE 5-17: Effect of the Hydraulic Conductivity of the Foundation Soil on the Break Through and the Mass Loading Curves.

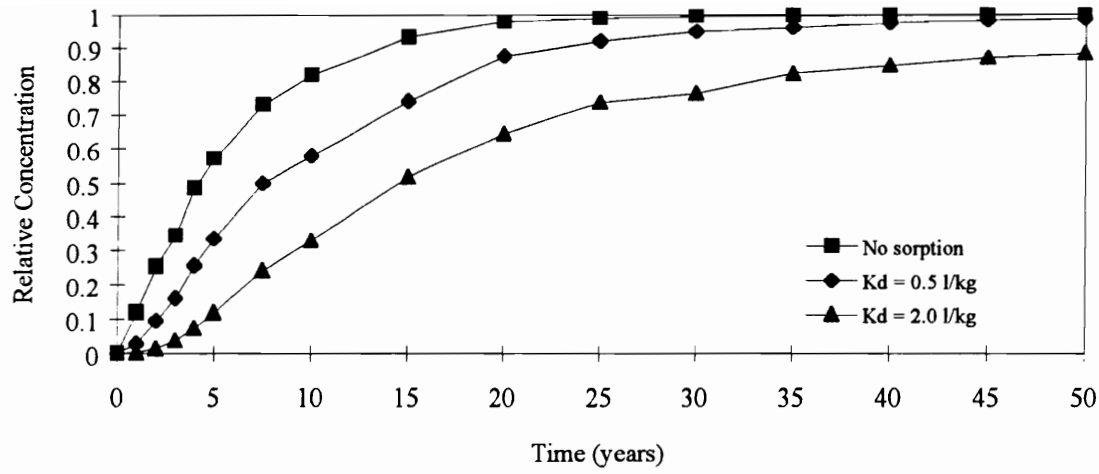

a) Break Through Curves

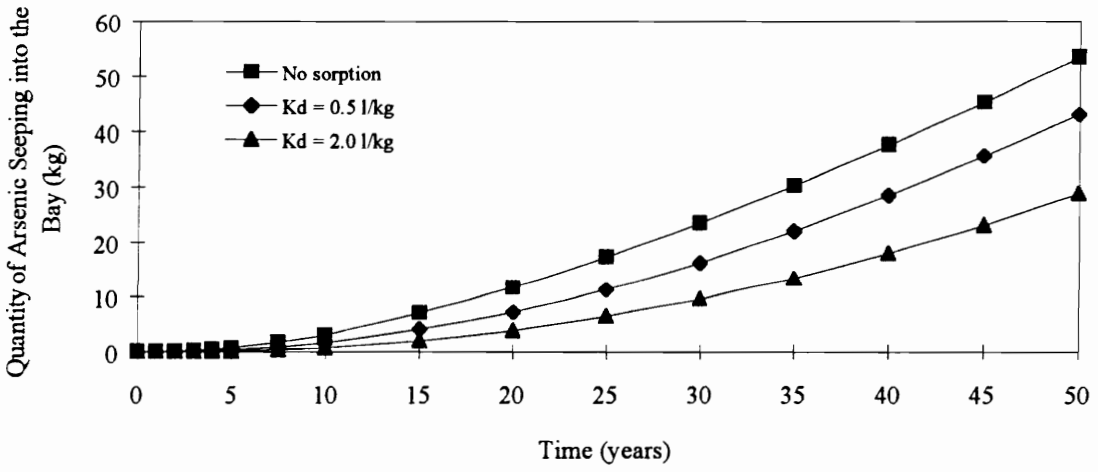

b) Mass Loading Curves

FIGURE 5-18: Effect of the Distribution Coefficient on the Break through and Mass Loading Curves.

effect on the break through or mass loading curves even when no adsorption was considered. The K_d value for the imported dike fill had only a negligible effect on the amount and rate of arsenic transport. A similar effect was observed for the dredged dike fill material. The only material that displayed any noticeable reaction to the different K_d values was the foundation soil. The break through and mass loading curves are shown in Figure 5-19. As expected, higher K_d values resulted in slower transport rates and lower quantities of arsenic seeped into the bay. Note the similarity between the mass loading curves in Figures 5-18b and 5-19b. It is apparent that the distribution coefficient of the foundation soil plays a more significant role in contaminant transport than the K_d values of the other soils in this problem. This can probably be attributed to the larger volume of foundation soil as compared to the dike fill materials.

5.6.7 Molecular Diffusion

The molecular diffusion coefficient was set equal to zero in all of the above analyses because it was assumed that the overall contribution of molecular diffusion to arsenic transport would be negligible if advection and mechanical dispersion dominated. This assumption was tested by performing analyses using molecular diffusion coefficients of 1×10^{-8} and 1×10^{-7} ft^2/day for all of the soil types. These values are considered to be representative for the given soil types and arsenic contaminant. No appreciable difference in arsenic transport was observed using either of these values. Break through and mass loading curves are not shown for these analyses because the data plot essentially on top of each other and are not distinguishable. Thus, the original assumption of disregarding molecular diffusion was correct for this problem.

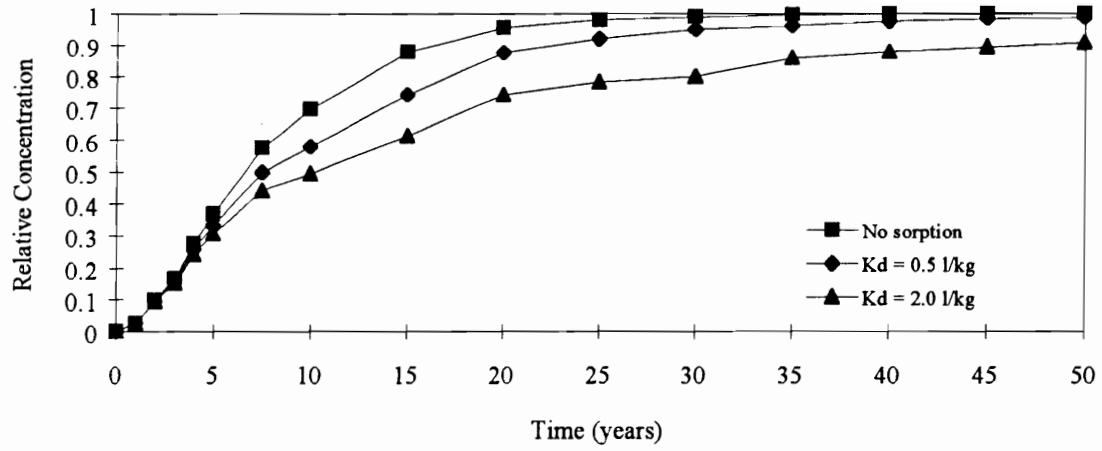

a) Break Through Curves

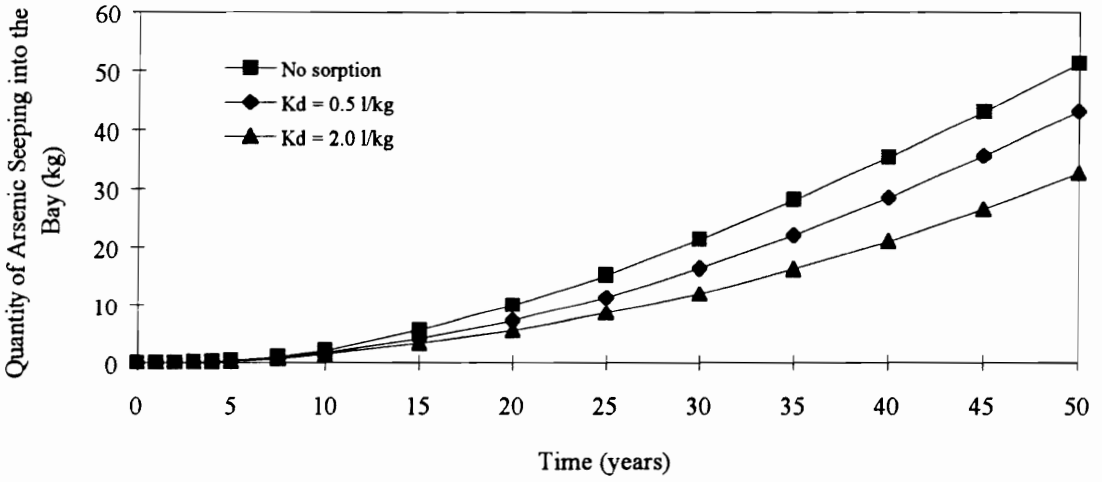

b) Mass Loading Curves

FIGURE 5-19: Effect of the Distribution Coefficient of the Foundation Soil on the Break Through and Mass Loading Curves.

5.6.8 Dispersivity

The values of both the longitudinal and transverse dispersivities used in all of the above analyses (50 and 10 feet, respectively) were estimated based on the soil classification. Sensitivity analyses were performed to evaluate the effect of variations in these values. Preliminary analyses were performed using transverse dispersivities of 1 to 10 feet while holding the longitudinal dispersivity constant. The results indicated that transverse dispersivity has a very small effect on mass transport. These results were consistent with other research (Freeze and Cherry, 1979). Next, several analyses were performed using longitudinal dispersivity values of 10, and 250 feet. These dispersivity values represent typical upper and lower bound field values for the sandy soil types of this problem. The value of the transverse dispersivity was allowed to vary such that the ratio $\alpha_L/\alpha_T = 5$ was always maintained. This ratio is generally consistent with published field data (Gelhar, et al., 1992). Thus, the sensitivity analyses was performed using the following dispersivity values (in feet):

α_L	α_T
10	2
50	10
250	50

The results of the analyses for the different material types are given below.

Analyses were performed using the above dispersivity values for the contaminated dredge material. The results showed no difference in the amount or rate of arsenic transport using any of these dispersivity values.

Figure 5-20a shows the break through curves obtained by varying the dispersivity of the imported dike fill material. As expected, higher values of dispersivity result in a faster rate of contaminant transport and a quicker break through time. For example, a relative concentration value of 0.5 is reached after about 3.5 years for the dispersivity ratio (α_L/α_T) of 250/50, whereas it takes about 12 years to reach this relative

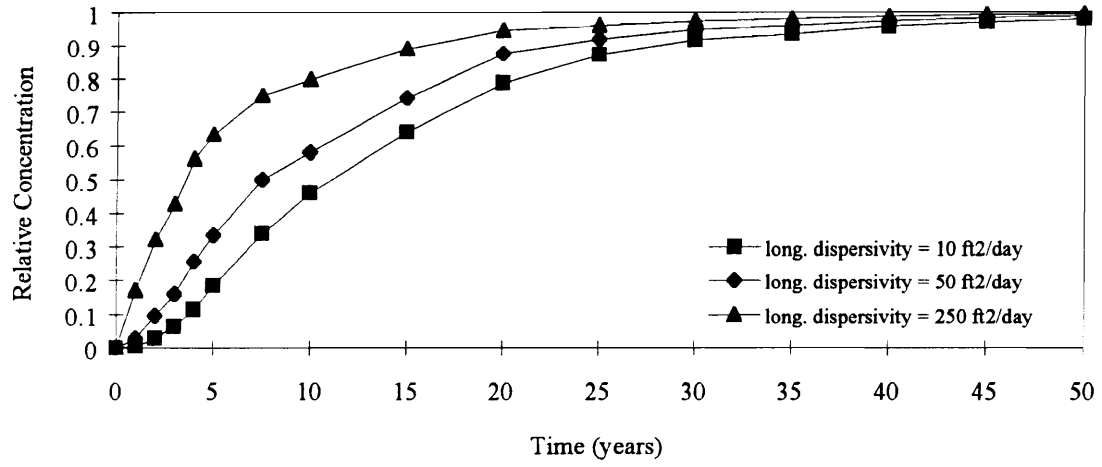

a) Break Through Curves

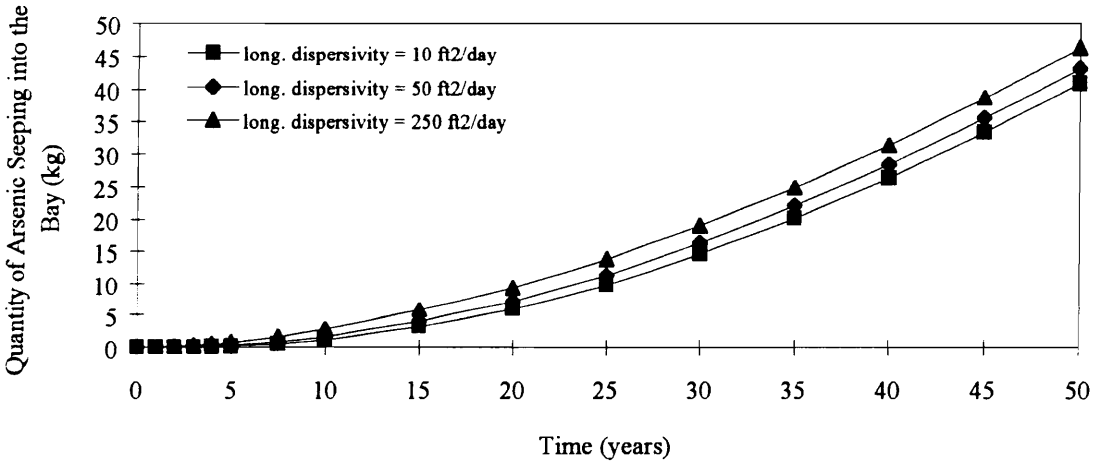

b) Mass Loading Curves

FIGURE 5-20: Effect of Dispersivity of the Imported Dike Fill on the Break Through and Mass Loading Curves.

concentration for the dispersivity ratio of 10/2. However, the overall effect of these differences in the dispersivity ratio of the imported fill is very small as shown by the mass loading curve (Figure 5-20b).

Similar results were obtained for the dredged dike fill and foundation materials. Thus, it can be concluded that the dispersivity values evaluated in these analyses had only a minimal effect on arsenic transport.

5.6.9 Unit Weight and Saturated Volumetric Water Content (Porosity)

The dry unit weight and saturated volumetric water content (porosity) of the imported dike fill material used in the above analyses were given in Table 5-1 as 115 pcf and 0.33, respectively. Additional analyses were performed using dry unit weights of 105 and 125 pcf. The porosity of the fill material corresponding to these unit weights are given below:

Dry Unit Weight (pcf)	Porosity
105	0.38
115	0.33
125	0.26

Porosity values were calculated using a specific gravity of 2.65 as given by the Corps of Engineers. The results shown in Figure 5-21 indicate that the above values of dry unit weight and porosity have only a slight influence on arsenic transport. As the dry unit weight increased (and the porosity decreased), the amount of arsenic seeping into the bay also increased. This is a reasonable conclusion since lower porosities cause higher seepage velocities.

It is apparent that the above analyses includes the effect of both dry unit weight and porosity. To eliminate the effect of the unit weight, the analyses were repeated with the additional condition that adsorption was zero. This condition eliminates the effect of

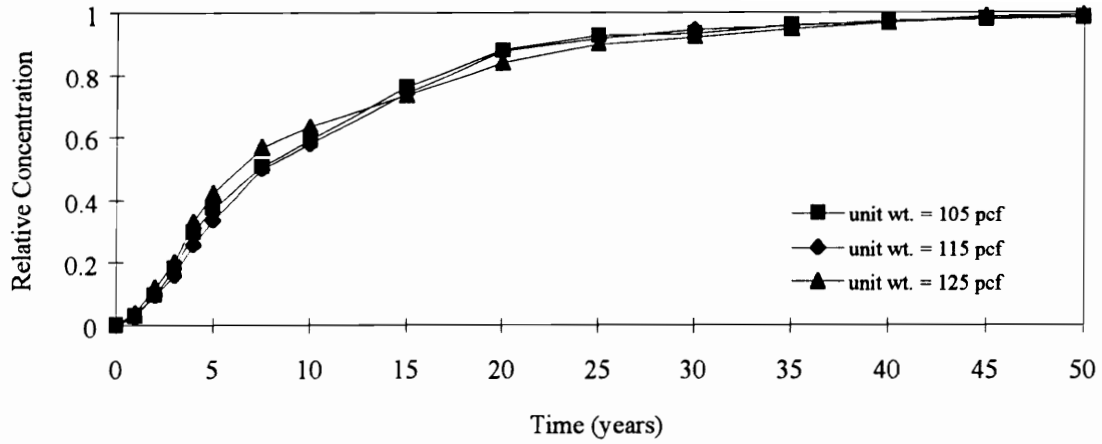

a) Break Through Curves

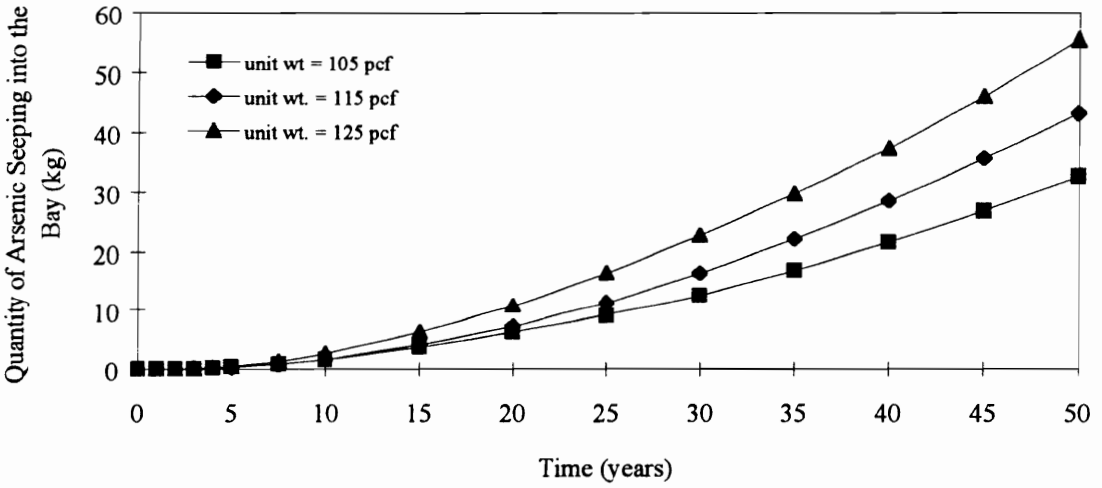

b) Mass Loading Curves

FIGURE 5-21: Effect of Dry Unit Weight and Porosity of the Imported Dike Fill on the Break Through and Mass Loading Curves. (K_d = 0.5 l/kg)

unit weight since the unit weight only effects the adsorption term. Figure 5-22 shows the break through and mass loading curves for this condition. The results are almost identical as those shown in Figure 5-21 which indicates that the dry unit weight has essentially no effect on arsenic transport for this problem.

Similar analyses were performed using values of 73 and 93 pcf for the dry unit weight and 0.56 and 0.44 for the porosity of the foundation soils. The results indicated that these values had very little effect on the break through and mass loading curves.

5.6.10 Residual Volumetric Water Content

The residual volumetric water content (θ_r) is a parameter used in determining the coefficient of moisture capacity (C_m) in the flow equation. Thus it only effects the unsaturated portion of the flow domain. The soil-water retention curve for the imported dike fill material is shown in Figure 5-23a where θ_r takes on the values of 0.0, 0.05 and 0.1. Note that these residual moisture content values do not influence the hydraulic conductivity of this soil (Figure 5-23b). Consequently the results shown in Figure 5-24 indicate that there is only a minor change in the amount of arsenic transport using these residual water content values.

5.6.11 Van Genuchten Parameters m and α

The van Genuchten model described in Section 3.2.4 requires the curve fitting parameters m and α to describe the shape of the soil water retention curve and to calculate the coefficient of hydraulic conductivity in the unsaturated zone. Since these

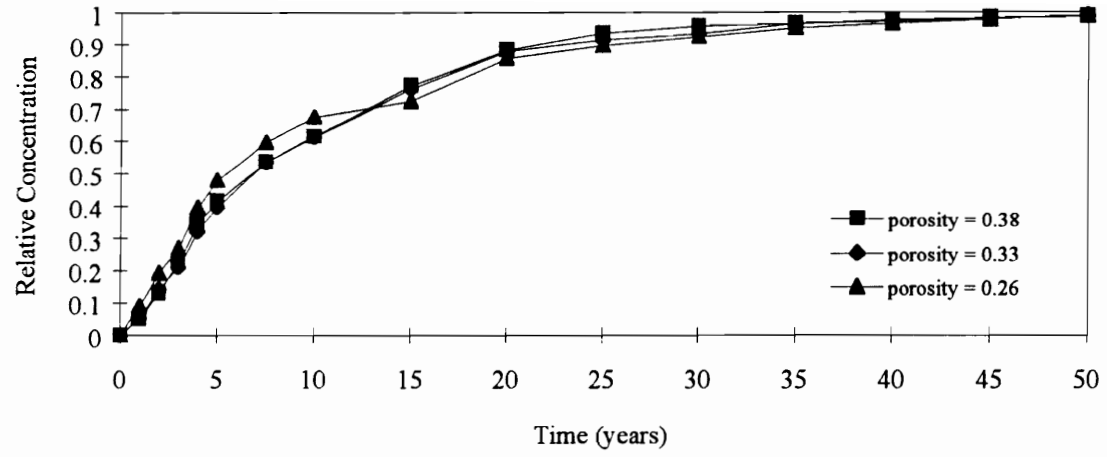

a) Break Through Curves

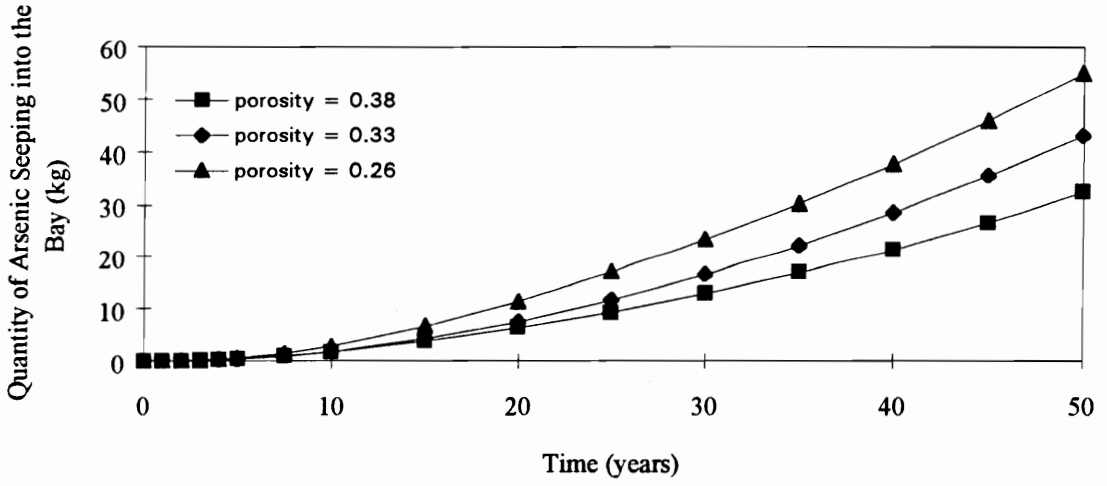

b) Mass Loading Curves

FIGURE 5-22: Effect of the Porosity of the Imported Dike Fill on the Break Through and Mass Loading Curves. (No adsorption)

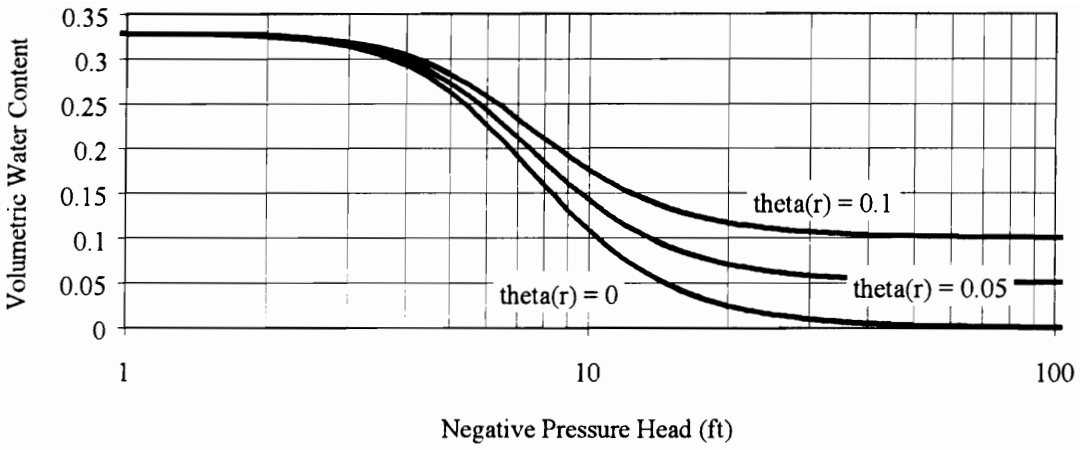

a) Soil-water Retention Curve

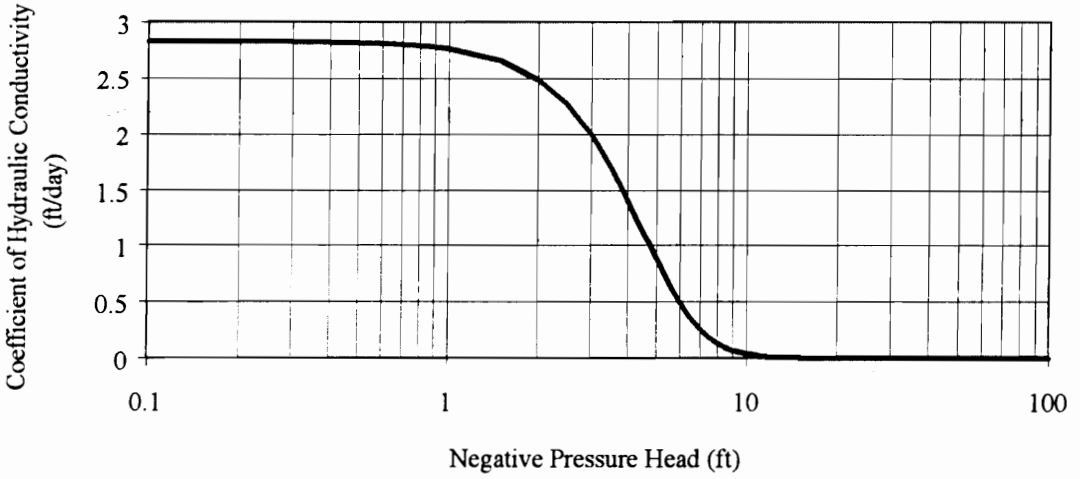

b) Hydraulic Conductivity as a Function of Pressure Head

FIGURE 5-23: The Influence of θ_r on the Soil-water Retention Curve and Hydraulic Conductivity.

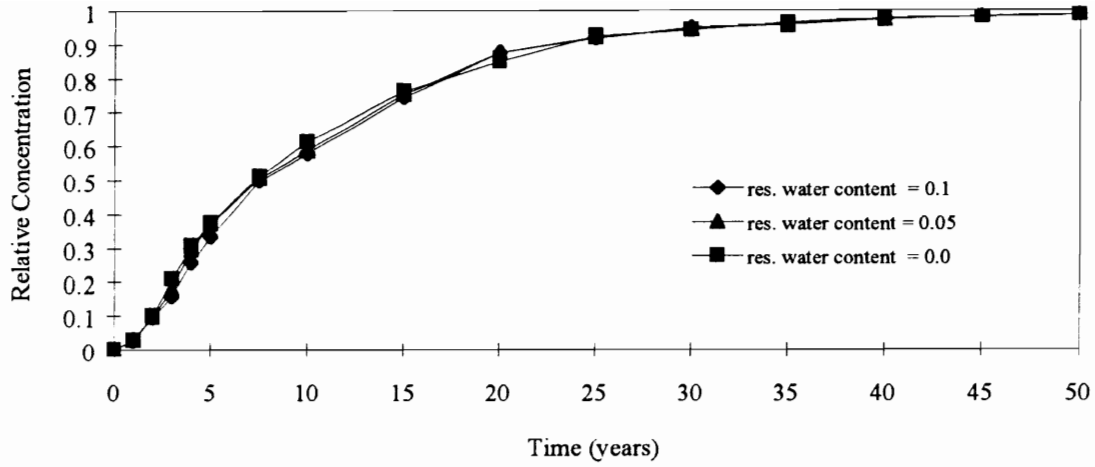

a) Break Through Curves

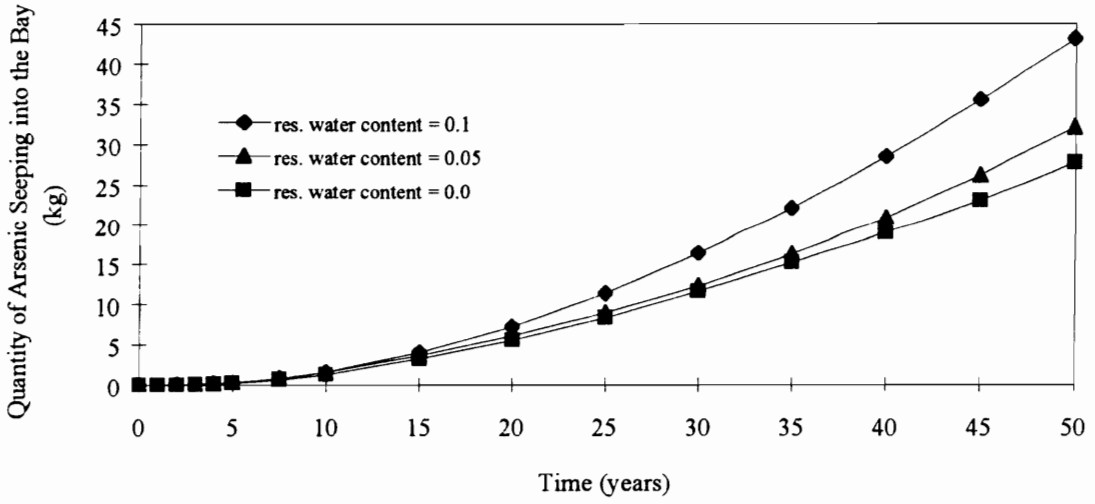

b) Mass Loading Curves

FIGURE 5-24: Effect of Residual Moisture Content of the Imported Dike Fill on the Break Through and Mass Loading Curves.

parameters may not be known, sensitivity analyses were performed to evaluate the effect of each of these parameters. Figure 5-25 shows the effect that m has on the soil water retention curve and on the coefficient of hydraulic conductivity for m values of 0.4, 0.6 and 0.8. Generally, the hydraulic conductivity decreases as m decreases for a given pressure head. The results of the analyses using these m values are shown in Figure 5-26. Note that the difference between these values of parameter m have no significant effect on arsenic transport.

The van Genuchten α parameter was varied from 0.5 to 1.1 ft^{-1}. The effect of these values on the soil water retention curve and the hydraulic conductivity are shown in Figure 5-27. The influence of these values is not significant, and as shown in Figure 5-28, there is little variation in the output between these.

5.7 Source Concentration Varies with Time

The results reported above were all based on the assumption that there was no arsenic transport until the CDF is completely filled with contaminated sediments. Thus, at time equal to zero, the arsenic concentration in the dredge material was 0.027 mg/l and the arsenic concentration everywhere else was zero. In an attempt to model a more realistic field condition, the arsenic concentration in the dredge sediments was assumed to be 0 mg/l initially, but was allowed to increase with time up to the final concentration of 0.027 mg/l. The rate at which this increase was modeled is Figure 5-29. Cases B and C simulate continuous gradual filling of the CDF with contaminated sediments. Case D represents dredging operations in colder climates where filling is only performed during 8 months of the year. Case E simulates a condition where filling in the CDF is discontinued for a year. It should be noted that these simple construction simulations are only approximate since the CDF is assumed to be filled with dredge

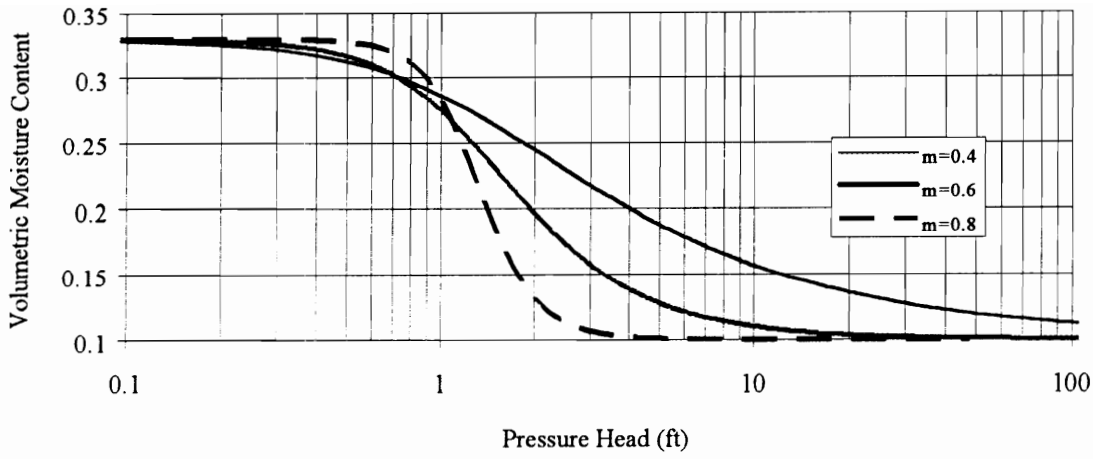

a) Soil-water Retention Curve

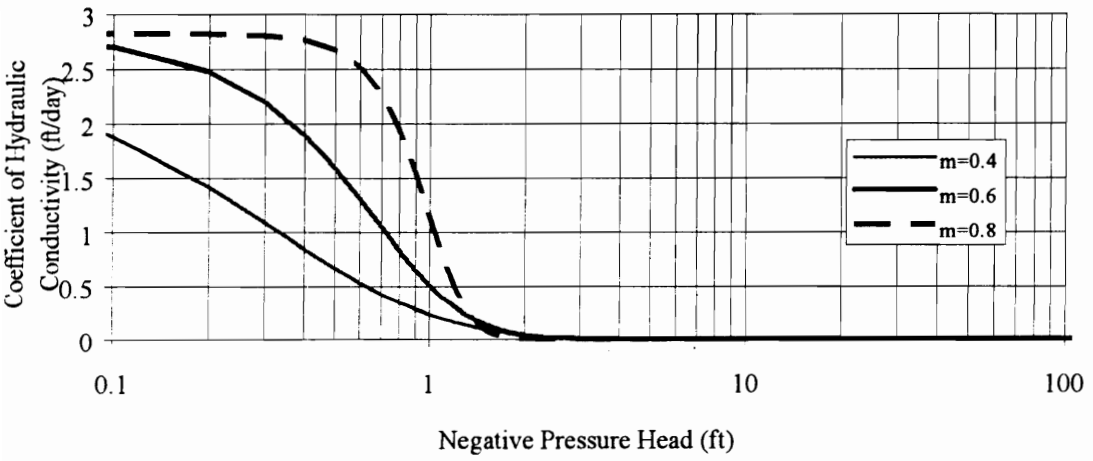

b) Hydraulic Conductivity as a Function of Pressure Head

FIGURE 5-25: The Influence of Van Genuchten m Parameter on the Soil-Water Retention Curve and Hydraulic Conductivity.

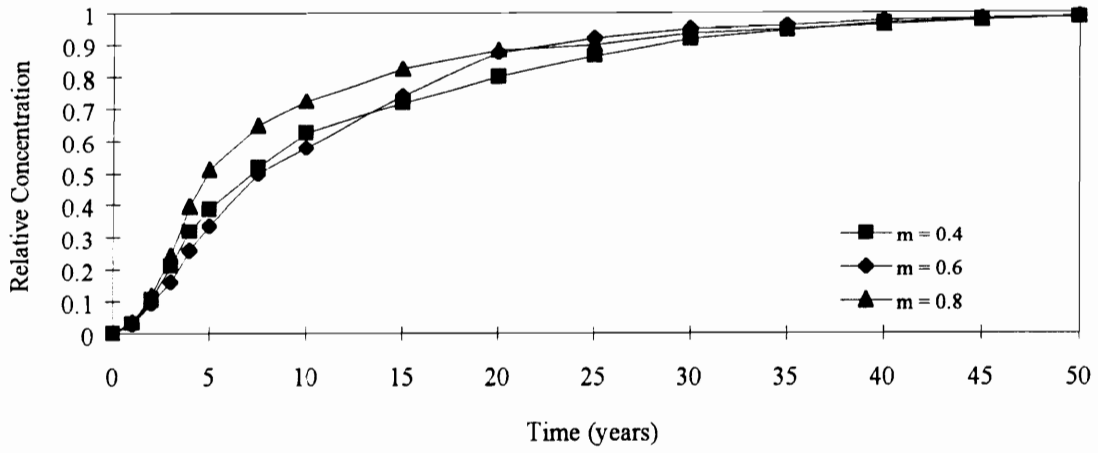

a) Break Through Curves

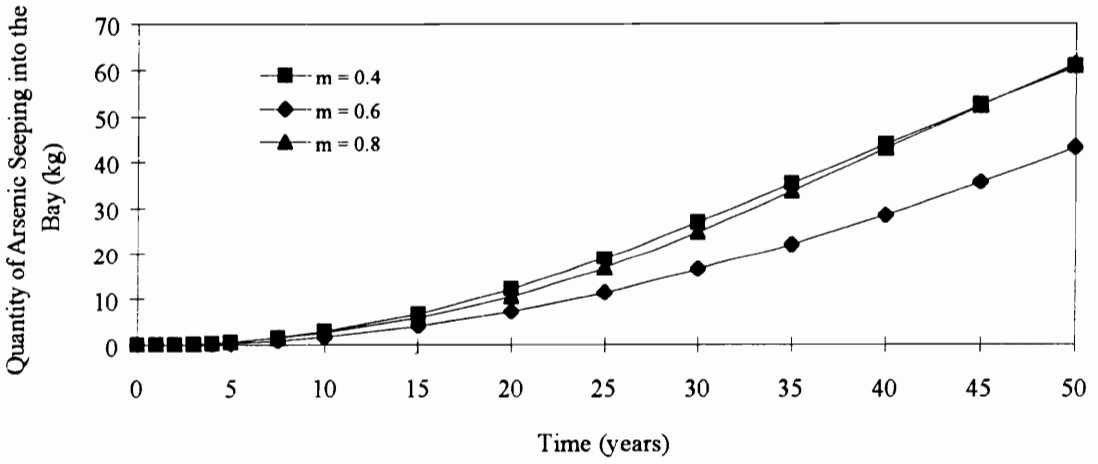

b) Mass Loading Curves

FIGURE 5-26: Effect of Van Genuchten m Parameter of the Imported Dike Fill on the Break Through and Mass Loading Curves.

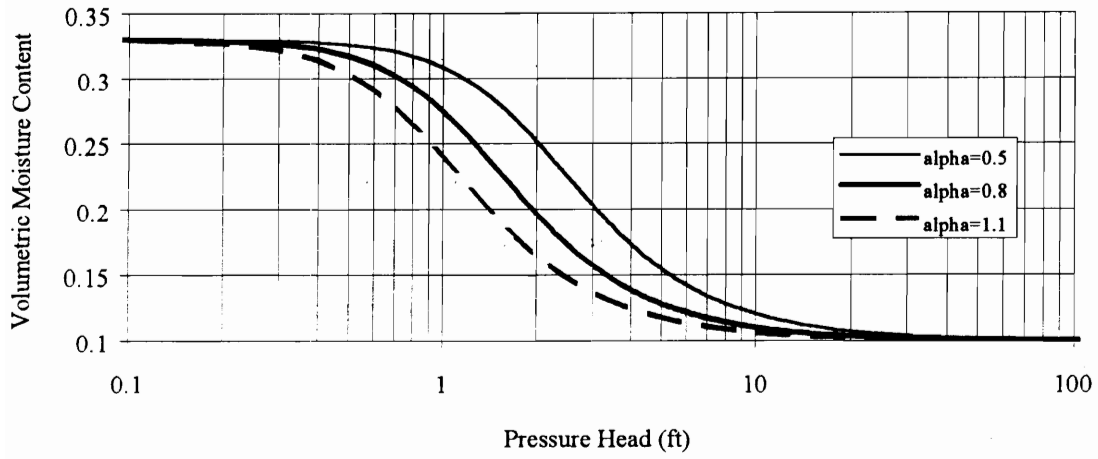

a) Soil-water Retention Curve

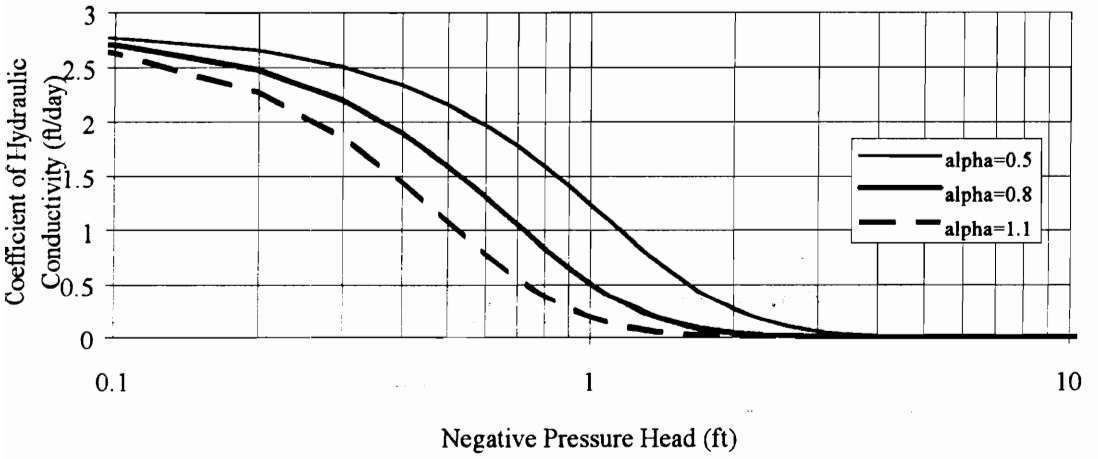

b) Hydraulic Conductivity as a Function of Pressure Head

FIGURE 5-27: The Influence of Van Genuchten α Parameter on the Soil-Water Retention Curve and Hydraulic Conductivity.

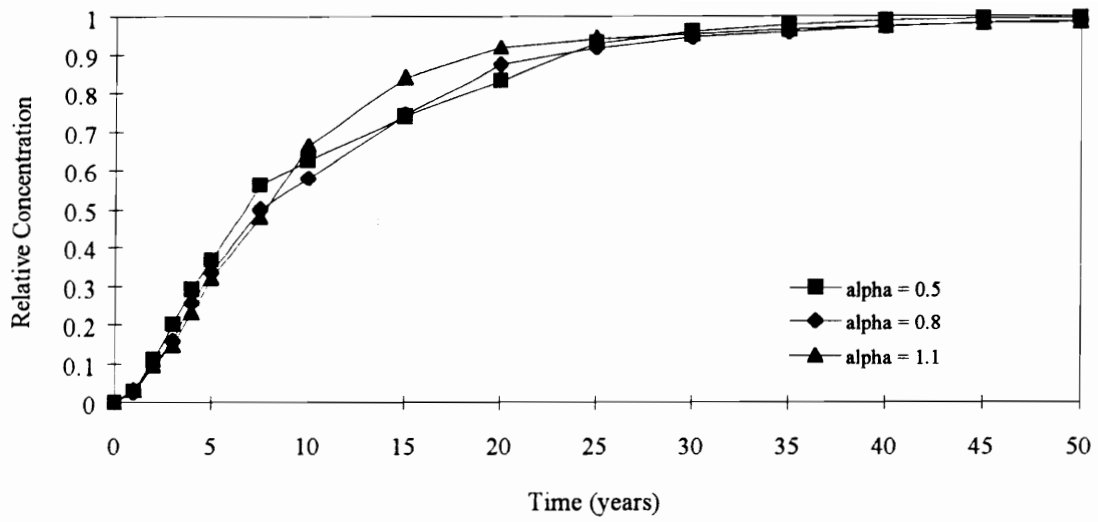

a) Break Through Curves

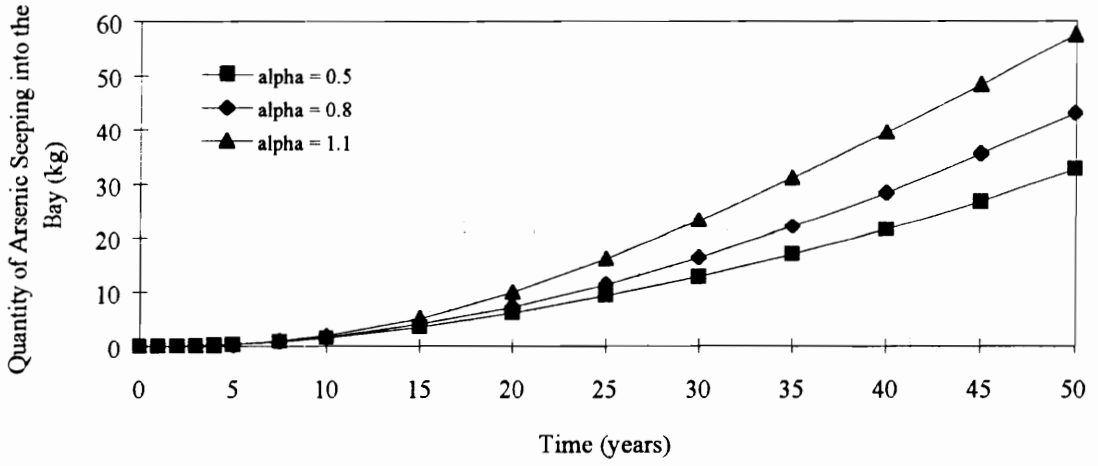

b) Mass Loading Curves

FIGURE 5-28: Effect of Van Genuchten α Parameter of the Imported Dike Fill on the Break Through and Mass Loading Curves.

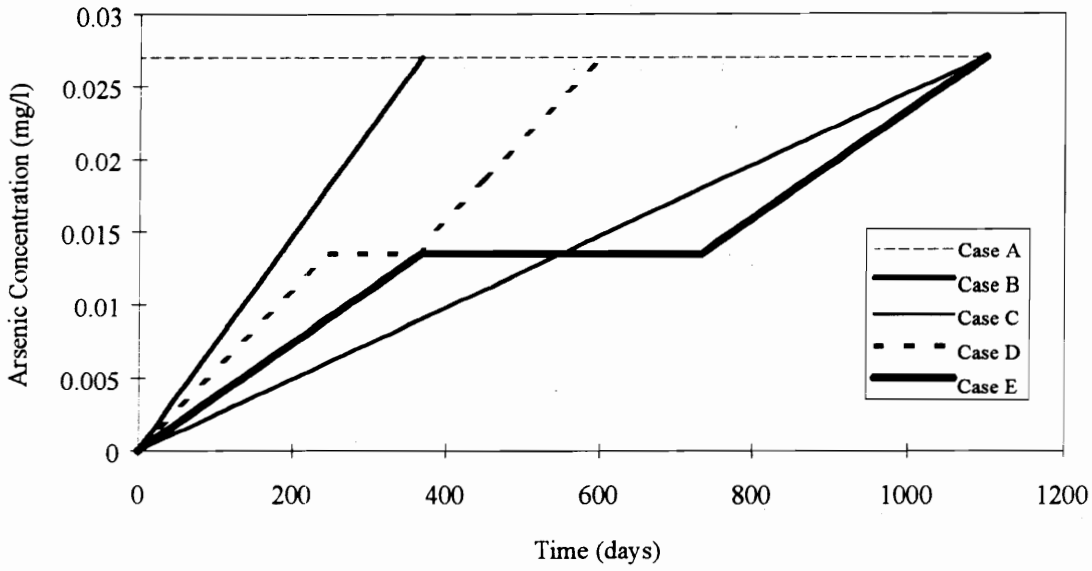

CASE	ARSENIC CONCENTRATION, C
A	C = 0.027 mg/l at time equal to zero (original assumption)
B	C increases linearly for one year
C	C increases linearly for 3 years
D	C increases linearly for 8 months, is constant for 4 months, then increases linearly for 8 more months
E	C increases linearly for one year, is constant for one year, then increases linearly for another year

FIGURE 5-29: Various Source Concentration Schemes Used in the Analyses.

material at the beginning of the simulation time and only the concentration is being varied.

The results shown in Figure 5-30 indicate that the original assumption (Case A) results in only slightly higher arsenic concentrations than any of the other simulations considered, and that this effect is negligible after a time of about 30 years. Thus, the original assumption does not appear to be too conservative for this problem.

5.8 Contaminant Source Boundary Condition

In the previous section, the source arsenic concentration in the dredge material varied with time. In all of the cases, the arsenic concentration would eventually become constant and fixed. Thus, there was a infinite source of arsenic in the dredge material. Although this procedure allows for simple modeling procedures and may be suitable for sensitivity analyses, it does not fully model the field conditions in which there is a finite quantity of arsenic that can actually seep back into the bay. Thus, several analyses were performed using different boundary conditions for the source contaminant concentration in the dredge material. These different analysis methods are summarized in the table and paragraphs below.

METHOD	BOUNDARY CONDITION
A	Original boundary condition. The concentration for all the nodes in the dredge material area is constant with time and equals 0.027 mg/l.
B	Only the top row of nodes located within the dredge material have a constant concentration of 0.027 mg/l. The remainder of the nodes have an initial concentration of 0.027 mg/l.
C	None of the nodes in the dredge material have a constant arsenic concentration. Rather, the analysis is performed using an initial concentration of 0.027 mg/l for these nodes.
D	A quasi-mass balance algorithm is used in which the arsenic concentration in the dredge material decreases with time depending on the amount of arsenic that seeps out of the dredge area.
E	Similar to Case D but only considers the concentration of the top nodes in the dredge material area.

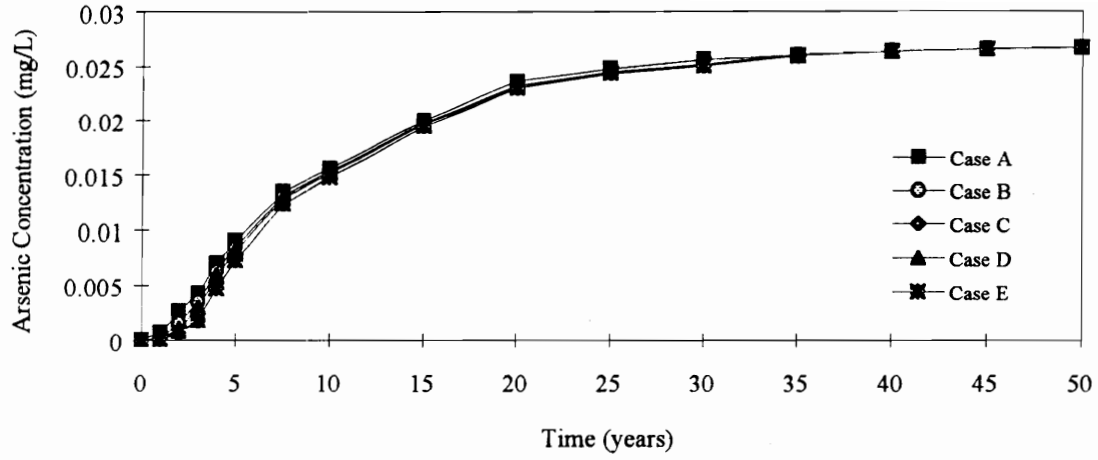

a) Break Through Curves

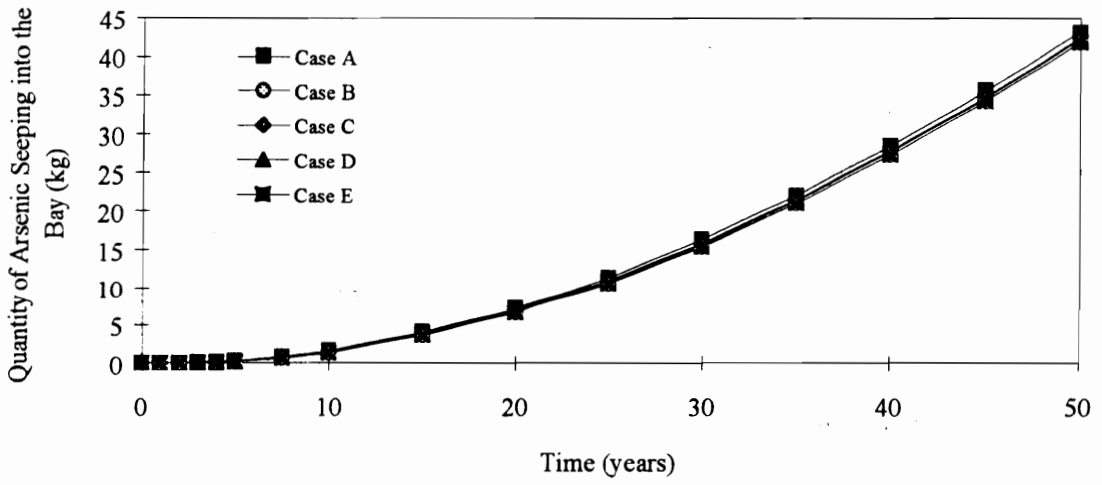

b) Mass Loading Curves

FIGURE 5-30: Effect of the Source Concentration Scheme on the Break Through and Mass Loading Curves.

A new subroutine was developed and incorporated into POLUTIDAL for Method D. To model these conditions, the following algorithm was employed. For the first time step, a concentration of 0.027 mg/l was used for all the nodes within the contaminated dredge material, and the analysis was performed as usual to determine the arsenic concentrations within the remainder of the mesh. Then, the total mass quantity of arsenic in each element in the mesh was determined based on the area and porosity of each element and the average concentration of the nodes in the element. The amount of arsenic that seeped out of the dredged material was then subtracted from the original mass of arsenic that was in the dredged soils. The new concentration of arsenic in the dredge was then calculated, and this value was used as the boundary condition for all of the nodes in the dredge material area for the next time step. This procedure was repeated for every time step during the simulation. In method E, a similar approach was used except that only the top row of nodes was considered. The remainder of the nodes in the dredge material area were not used as a boundary condition, rather, they were given an initial concentration of 0.027 mg/l. It should be noted that adsorption was not considered for any of these analyses.

The results of all of these methods are shown in Figure 5-31. Note that the results tend to lie along one of two sets of curves. Methods A and B, which would be expected to give the greatest contaminant transport, yielded very similar break through and mass loading curves. The remainder of the cases predict about the same concentration and quantity of arsenic transport into the bay. As a comparison, methods C, D and E predict a maximum relative concentration of 0.30 at the end of 50 years, whereas methods A and B predict a relative concentration of about 1 at 50 years. Methods C, D and E also predict about 38% as much arsenic leachate into the bay as methods A and B (Figure 5-31b). These extremes in values may represent upper and lower bound solutions to the problem.

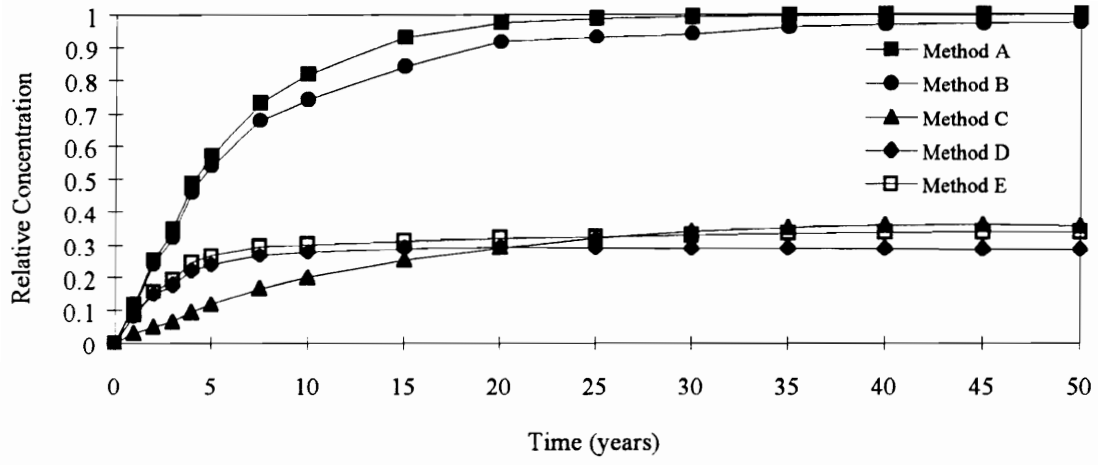

a) Break Through Curves

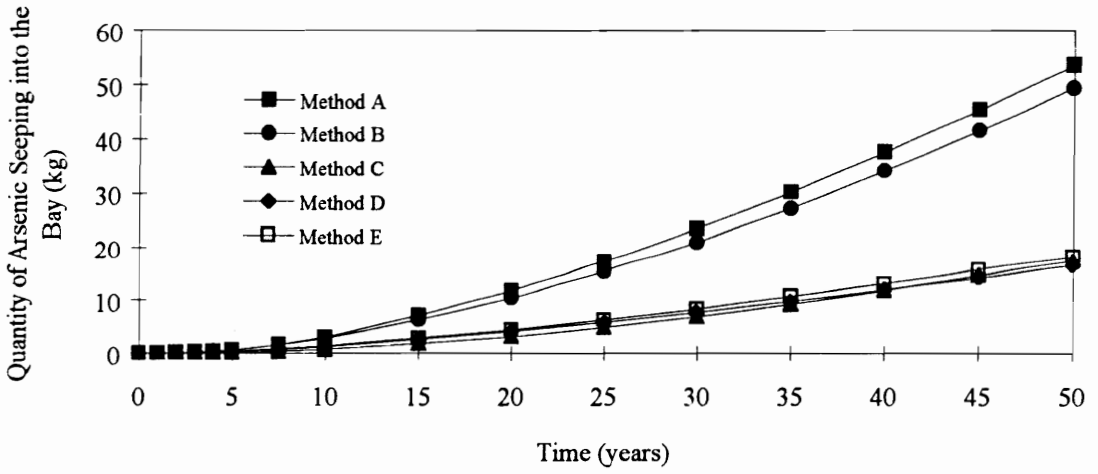

b) Mass Loading Curves

FIGURE 5-31: Effect of the Contaminant Source Boundary Condition on the Break Through and Mass Loading Curves.

5.9 Effect of Sorption Model

The appropriate equilibrium sorption model for a soil-contaminant system is often determined from laboratory batch tests as indicated in Section 3.3.2.2. The Corps of Engineers indicated that the linear Freundlich model was suitable for arsenic for this problem. Since some investigators have found that the Langmuir model is also appropriate for arsenic, an additional analysis was performed to compare the results of this model with the Freundlich model. Figure 5-32 shows an arbitrary laboratory test curve of a plot of the quantity of arsenic adsorbed onto the soil as a function of the arsenic concentration in solution. The Freundlich model has a distribution coefficient of 2 l/kg, while the Langmuir curve fitting parameters are b = 0.0135 l/kg, and k' = 100. As indicated in the figure, the non-linear Langmuir model has an upper limit on the amount of arsenic which can adsorb onto the soil. The Freundlich model predicts an unlimited amount of arsenic adsorption. Figure 5-33 shows the results of analyses performed using these two models. As expected, the Freundlich model predicts the slowest rate of arsenic transport. This occurs because greater adsorption occurs with the Freundlich model than with the Langmuir model resulting in less arsenic in the aqueous phase.

5.10 Methods of Containment

5.10.1 Effect of a Clay Liner

The results presented in the previous sections indicate that arsenic will seep into the bay within a relatively short time frame based on the given soil properties. Therefore, some method of containment method may be required to minimize contamination of the bay. The COE requested that the effect of a 1 foot thick clay liner placed beneath the dredge material be evaluated. This containment method is similar to that of a landfill underlain by a clay liner. The COE indicated that coefficients of hydraulic conductivity for local soils are in the range of 1E-5 to 1E-7 cm/sec. Distribution coefficients of 3 to 10

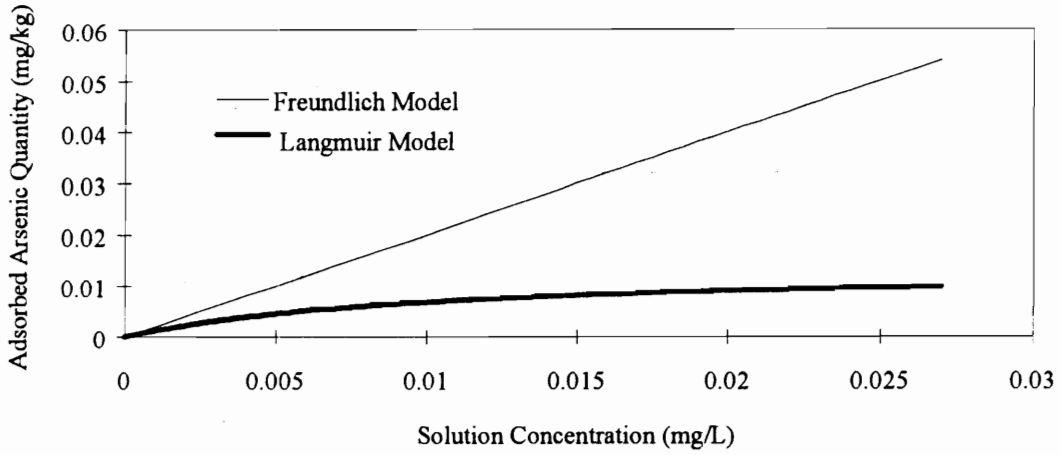

FIGURE 5-32: Laboratory Adsorption Test Curves of Freundlich and Langmuir Models.

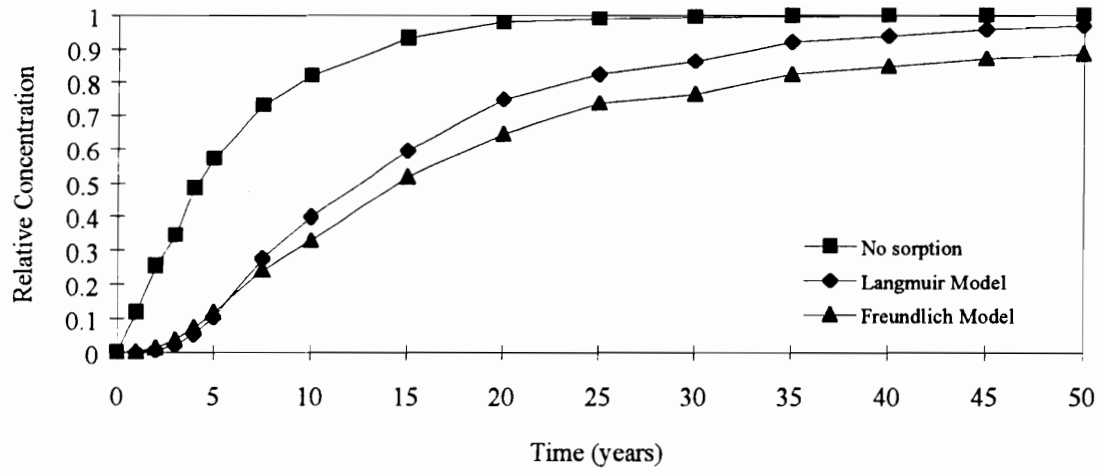

a) Break Through Curves

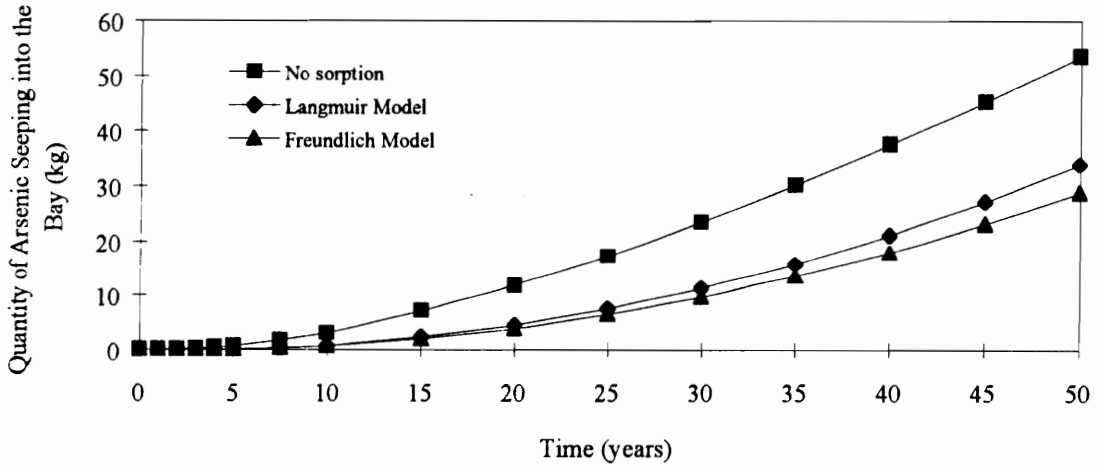

b) Mass Loading Curves

FIGURE 5-33: Effect of Sorption Model on the Break Through and Mass Loading Curves.

l/kg are expected for the clay liner soil. The other soil properties for the liner are listed in Table 5-2.

The initial analyses were performed using hydraulic conductivity values of 1E-5, 1E-6 and 1E-7 cm/sec and a linear distribution coefficient of 3 l/kg. A constant source of arsenic in the dredge was used in the analyses to be conservative. The results shown in Figure 5-34 indicate that the liner is mostly effective if the hydraulic conductivity is 1E-7 cm/sec. Note that a liner with a hydraulic conductivity of only 1E-5 cm/sec provides little arsenic containment. Further analyses were performed which indicated that the value of the distribution coefficient of the liner had negligible effect on the amount of arsenic contained. In addition, molecular diffusion values of 1E-6 ft^2/day and 1E-7 ft^2/day for the clay liner also had no effect on arsenic containment.

The analysis was repeated using a 2 feet thick clay liner with a hydraulic conductivity of 1E-6 cm/sec. The results shown in Figure 5-35 indicate that the thickness of the liner has a fairly significant effect on arsenic transport for this problem.

5.10.2 Effect of a Slurry Trench

A soil cement slurry trench was considered for this problem due to the difficulties that may be encountered in constructing a clay liner. In addition, a slurry trench is a common method of containment remediation. Table 5-3 list the properties of the slurry trench. Hydraulic conductivities were of the same magnitude as those of the clay liner. Adsorption was not considered based on the results of the analyses with the liner. The trench is located through the center line of the embankment and extends through the foundation soils. It is assumed that an impermeable material underlies the silty sand foundation layer. A trench width of 4 feet was assumed in the analyses.

Figure 5-36 shows the effect of the slurry trench on arsenic transport through the CDF. As with a clay liner, the slurry trench is an effective barrier against arsenic transport

TABLE 5-2: Soil Properties Used to Model the Clay Liner.

Soil Property	Value
Longitudinal Dispersivity	50 feet
Transverse Dispersivity	10 feet
Molecular Diffusion	0
Dry Unit Weight	100 pcf
Sat. Volumetric Water Content	0.4
Res. Volumetric Water Content	0.1
van Genuchten Parameter m	0.3
van Genuchten Parameter α	0.05 ft^{-1}

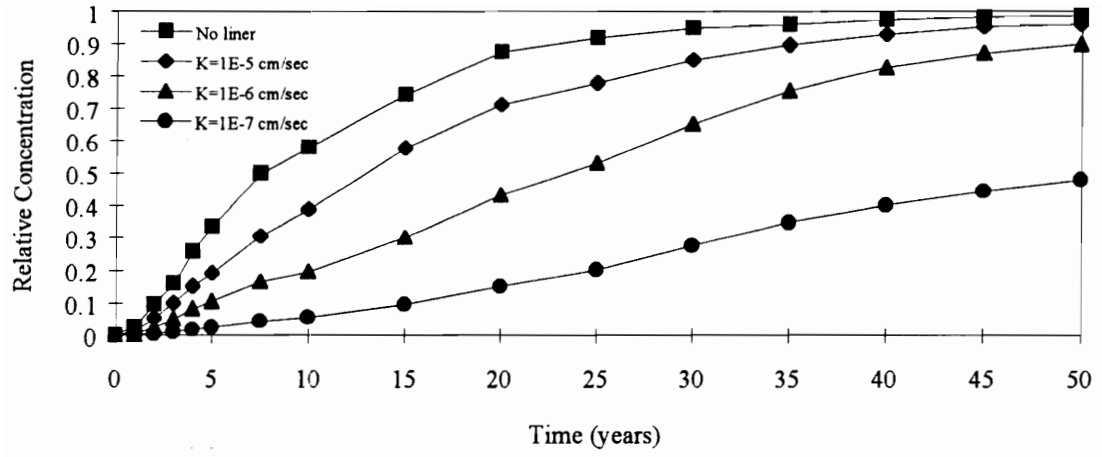

a) Break Through Curves

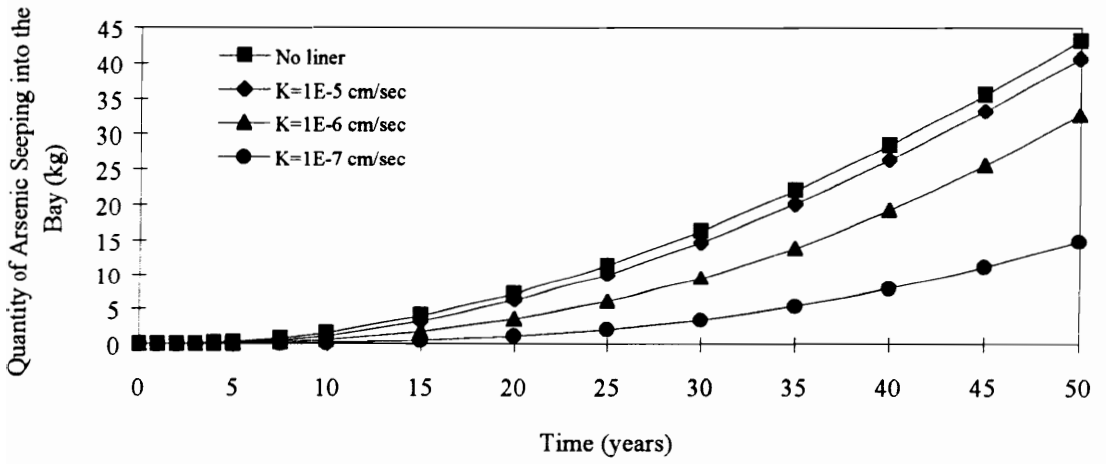

b) Mass Loading Curves

FIGURE 5-34: Effect of a 1 foot thick Clay Liner on the Break Through and Mass Loading Curves.

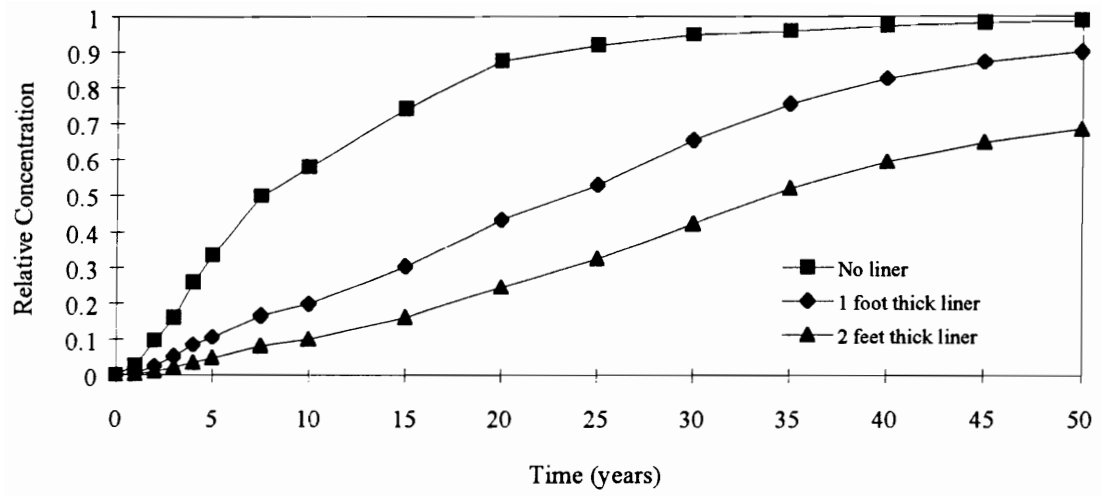

a) Break Through Curves

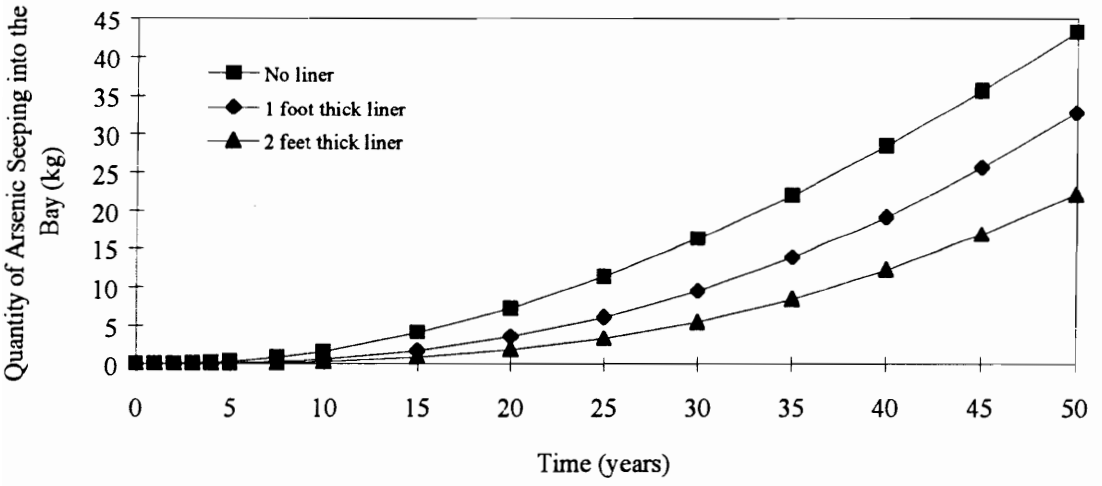

b) Mass Loading Curves

FIGURE 5-35: Effect of a 2 feet thick Clay Liner on the Break Through and Mass Loading Curves (K = 1E-6 cm/sec).

TABLE 5-3: Soil Properties Used to Model the Slurry Trench.

Soil Property	**Value**
Longitudinal Dispersivity	50 feet
Transverse Dispersivity	10 feet
Molecular Diffusion	0
Dry Unit Weight	85 pcf
Sat. Volumetric Water Content	0.41
Res. Volumetric Water Content	0.1
van Genuchten Parameter m	0.3
van Genuchten Parameter α	0.05 ft^{-1}

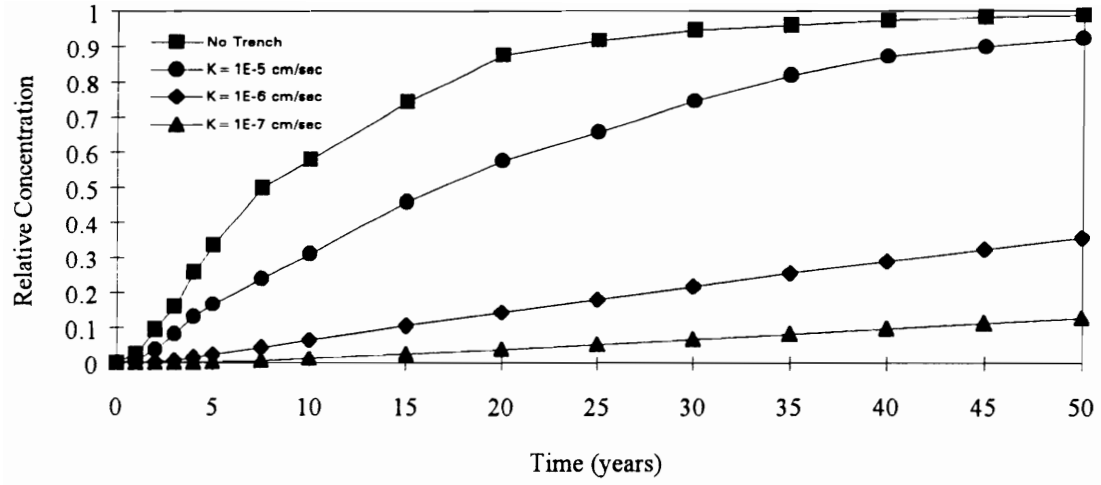

a) Break Through Curves

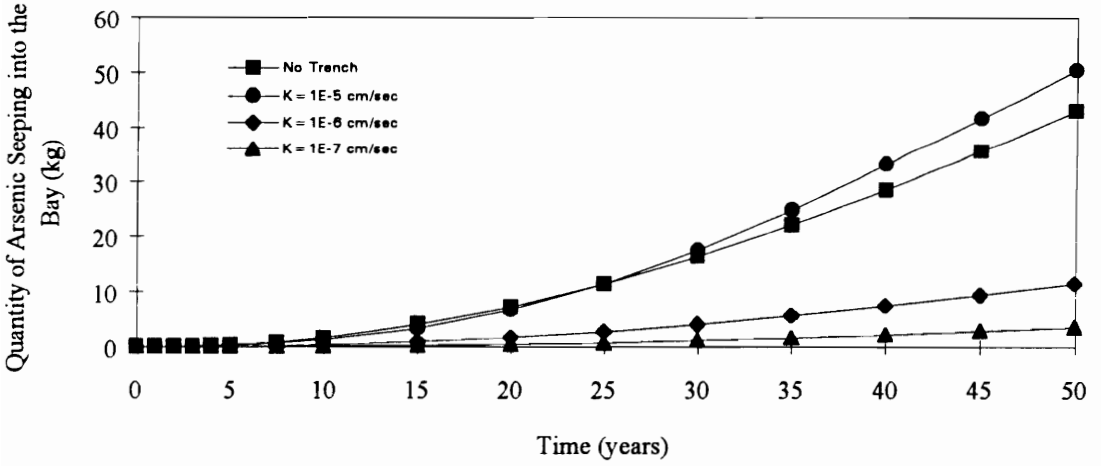

b) Mass Loading Curves

FIGURE 5-36: Effect of a Slurry Trench on the Break Through and Mass Loading Curves.

provided that the hydraulic conductivity is not greater than 1E-6 cm/sec. That results indicate that a slurry trench with an in-place hydraulic conductivity of 1E-7 cm/sec significantly reduces the amount of arsenic that will seep into the bay.

Figure 5-37 compares the break through and mass loading curves for the case where no liner (or slurry trench) is provided, and where a 1 or 2 feet thick clay liner or slurry trench is included. In this comparison, the hydraulic conductivity of the clay liner and slurry trench is 1E-6 cm/sec. Note that the slurry trench provides the most effective means of arsenic containment.

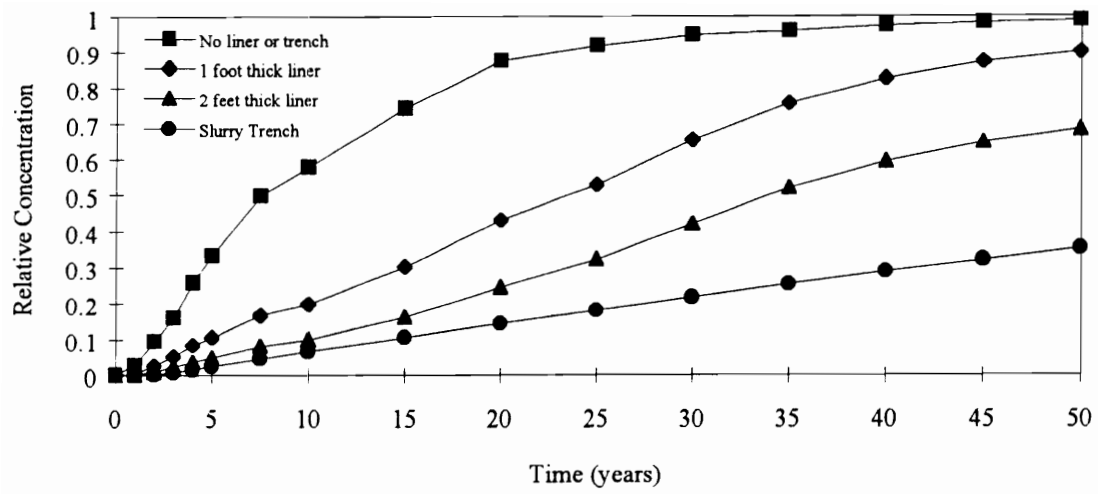

a) Break Through Curves

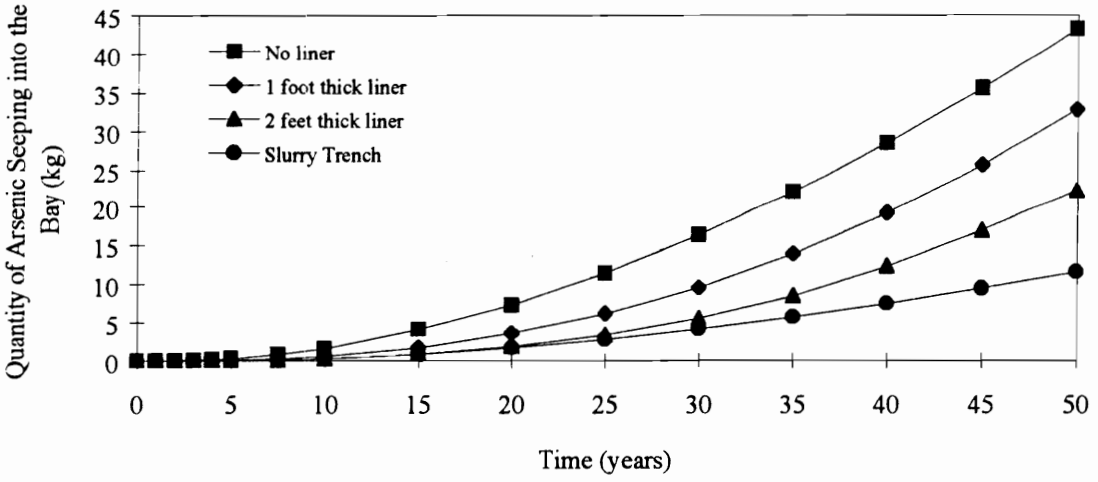

b) Mass Loading Curves

FIGURE 5-37: Comparison of the Two Containment Methods.

CHAPTER 6

Problem 2 - Buffalo Harbor Dike Number 1

6.1 Chapter Overview

In this chapter, a CDF constructed in Lake Erie near Buffalo, New York will be evaluated using POLUTIDAL. This facility, called the Buffalo Harbor Dike Number 1, was constructed in 1967 as part of the initial dike disposal program in the Great Lakes (Myers, 1987). Filling of this CDF with dredge spoils ceased in 1974. In 1986, additional fill soils were placed within the CDF to cap off the facility for eventual use as a parking lot. Monitoring wells were installed within the dredge to evaluate the water quality inside the CDF. Analyses of the water samples indicated that the concentration of several organic and inorganic compounds including cyanide, chlorobenzene and zinc exceeded the federal water quality criteria for fresh water aquatic life (Myers, 1987). The primary purpose of the research presented in this chapter is to estimate the annual loading of chlorobenzene from this facility into Lake Erie. The effect of several remediation methods are also presented. The program POLUTIDAL was modified for this problem to account for infiltration due to snow melt and rain , and to account for the fluctuation of Lake Erie with time.

6.2 Problem Description

6.2.1 Geometry

The Buffalo Harbor Dike Number 1 CDF is approximately 1000 feet long and 1000 feet wide. It is bounded on three sides by Lake Erie, and is adjacent to Fuhrmann Boulevard in Buffalo, New York. The dike constructed to contain the dredge materials is about 20 feet high and was constructed of "slag and rip rap" materials. The original side slope of the dike was about 1.5H:1V, and the crest width was about 10 feet. Plan and profile views of the facility are shown in Figure 6-1.

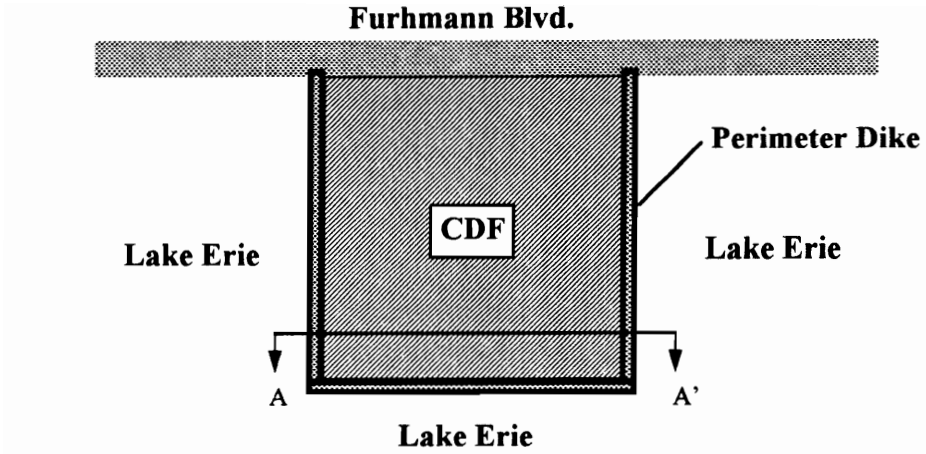

a) Plan View

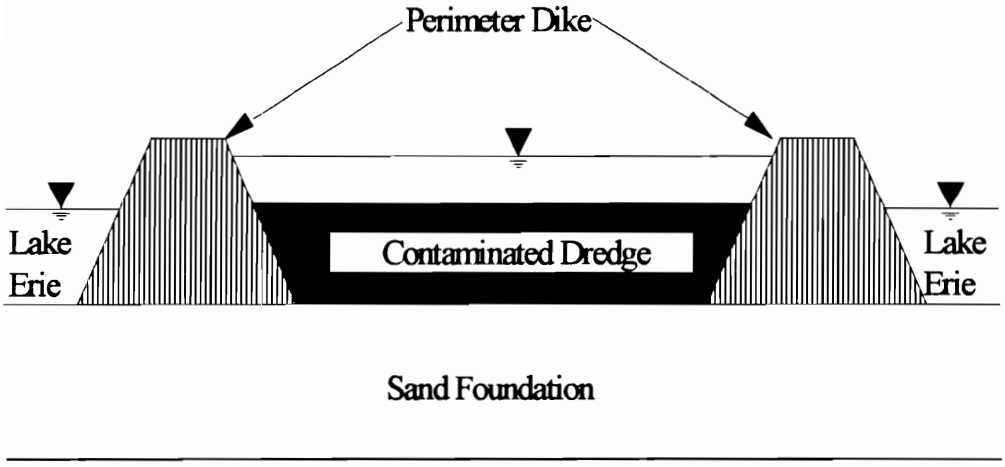

b) Profile View through section A-A'

FIGURE 6-1: Plan and Profile Views of Buffalo Harbor Dike Number 1.

6.2.2 Water Level Conditions

As indicated above, this CDF is bounded on three sides by Lake Erie. The level of Lake Erie has fluctuated slightly since the CDF was built. Figure 6-2 shows the fluctuation of Lake Erie at Buffalo, New York from June 1967 to December 1991. These values are the monthly mean elevation obtained by National Oceanic and Atmospheric Administration (NOAA,1980-1991). The data indicates that the lake level has fluctuated somewhat since the CDF was constructed. However, the total maximum change in elevation has only been about 3 feet.

The elevation of the water table within the CDF in 1986 was evaluated from the monitoring well data. A plot showing the contour of the water table is shown on Figure 6-3. Note that an apparent mound of water exists within the central portion of the CDF at EL 578. The water level at Lake Erie at this time was EL 573.3. Thus, seepage from the CDF into Lake Erie occurs through all 3 sides, as well as towards Furhmann Boulevard.

6.2.3 Contaminant Information

Monitoring wells were installed within the perimeter dikes and within the dredge itself to evaluate the presence of contaminants in the pore water. Some of the contaminants detected in samples take from the wells included cyanide, chromium, zinc, arsenic, heptachlor and chlorobenzene. Of particular interest to the Corps is chlorobenzene which had high concentration levels. Chlorobenzenes are used in the production of pesticides, adhesives, waxes and other chemicals, and have been shown to affect the liver, kidneys and brains in lab animals exposed to acute doses (Meck and Giddings, 1991). Figure 6-4 shows the chlorobenzene concentration levels in mg/liter at the monitoring well locations within the CDF. It should be noted that the initial concentration of chlorobenzene in the pore water in the dredge spoils when filling in the CDF began is not known.

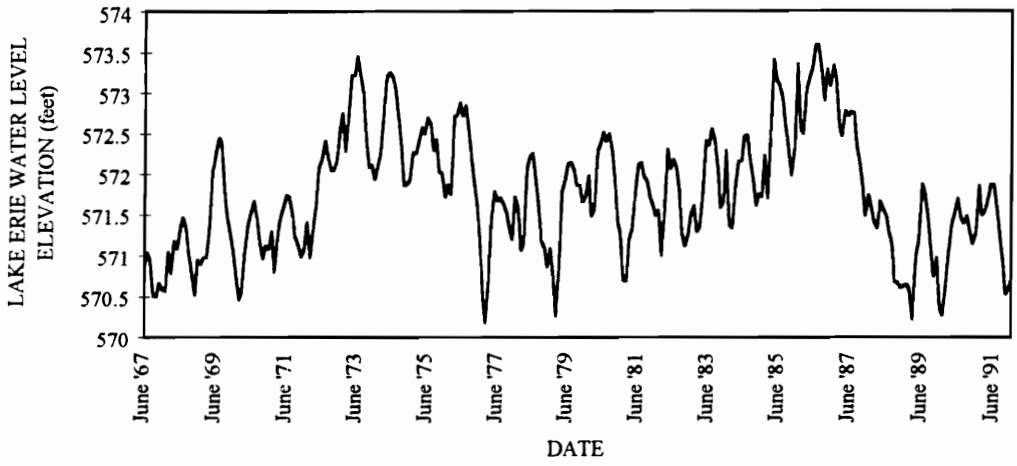

FIGURE 6-2: Fluctuation of Lake Erie from June 1976 to December 1991.

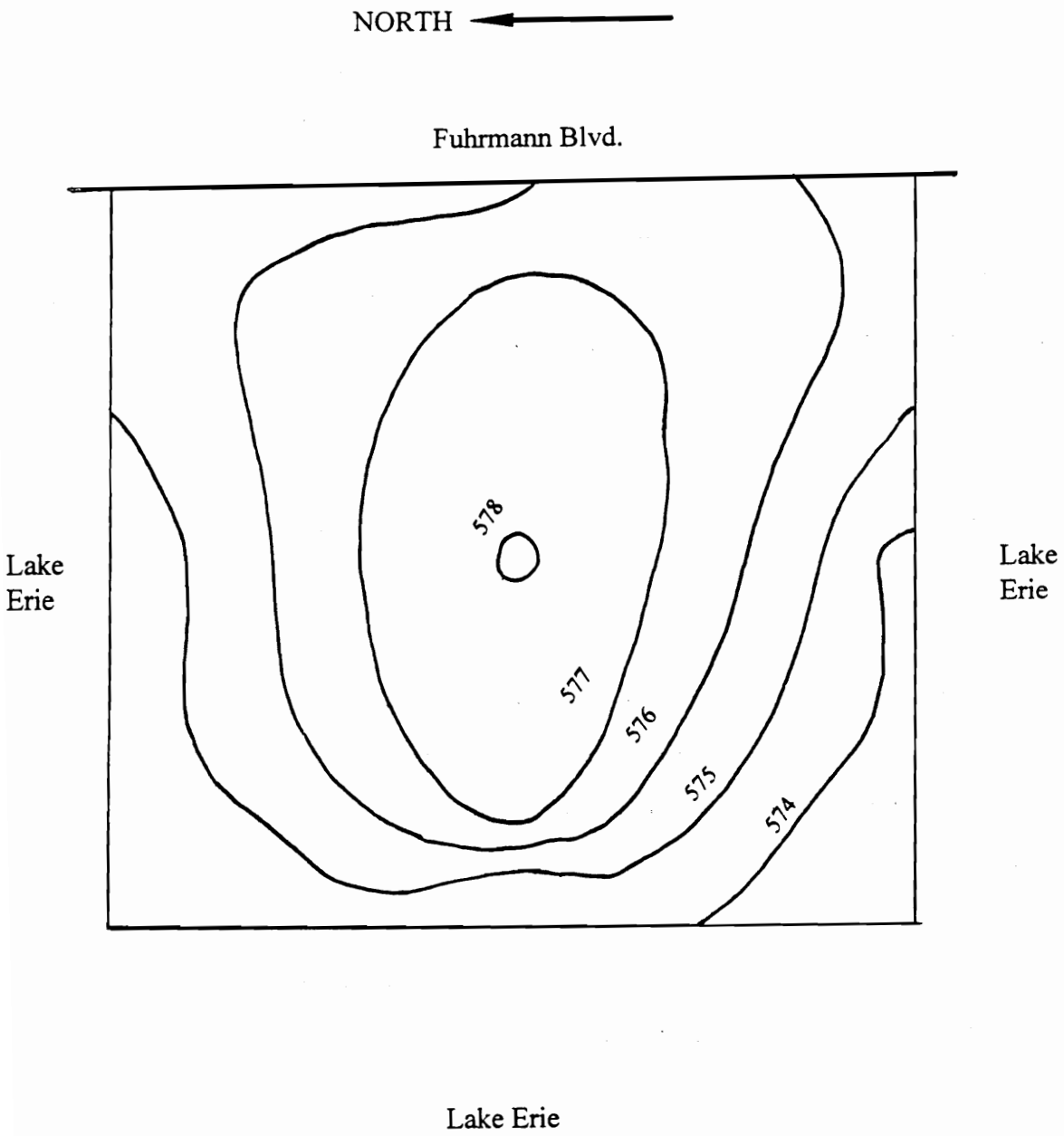

FIGURE 6-3: Ground Water Contours within the CDF.

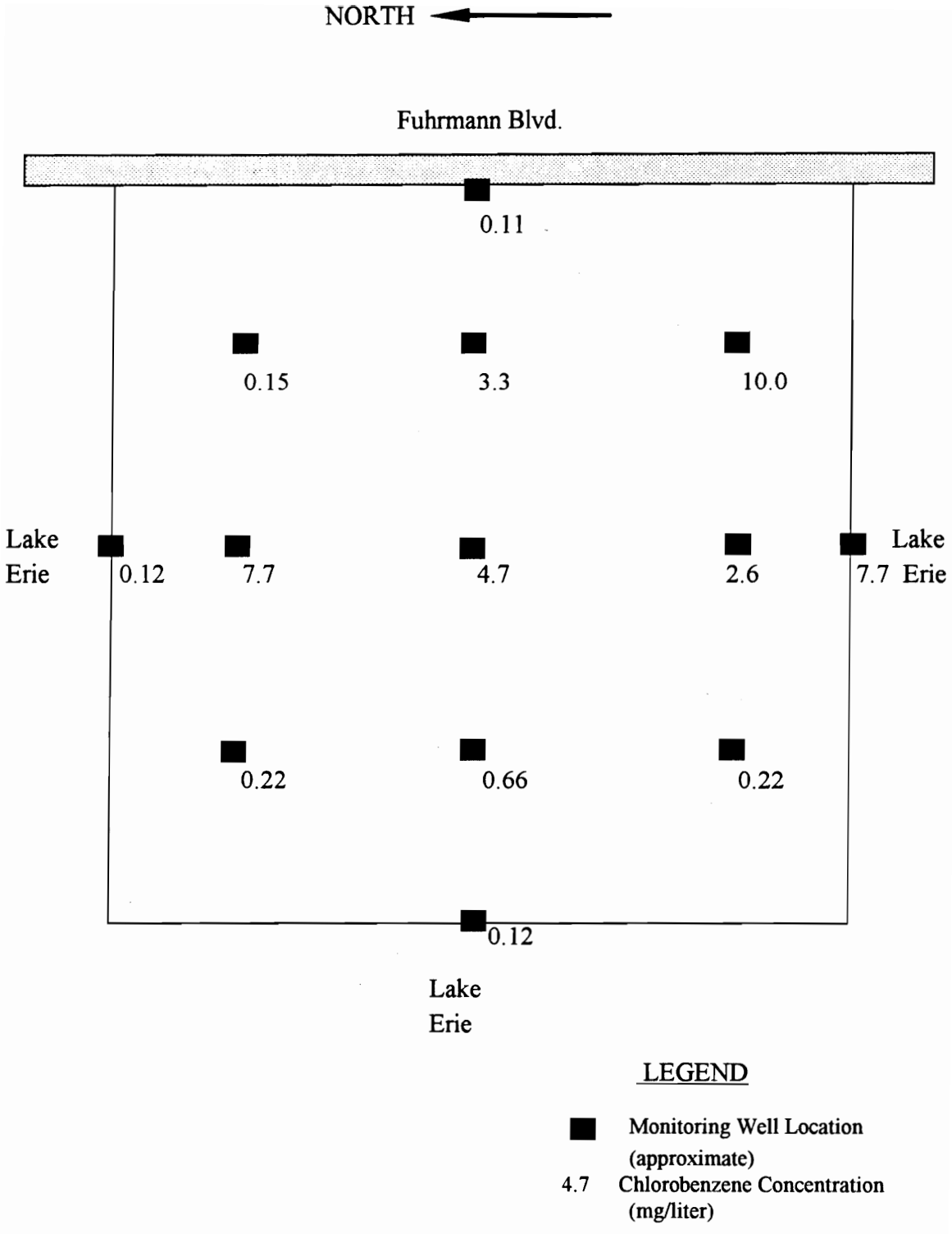

FIGURE 6-4: Chlorobenzene Concentrations within the CDF.

6.2.4 Material Properties

As indicated above in Section 6.2.1, the dike surrounding the CDF was constructed of "slag and rip rap" materials. No other information or laboratory test data is available for this material. Several sieve analyses and Atterberg Limits tests were performed by a private consulting firm on the dredge material contained within the CDF. This soil generally classified as a non-plastic silt (ML). The Corps of Engineers indicated that to the best of its knowledge this facility is underlain by about 50 feet of sand. Beneath this layer is a low permeability layer of unknown thickness. This is the extent of the known soil data available for this research project. The soil properties used in the finite element analyses are presented in Section 6.3.5.

6.3 Finite Element Approximation

6.3.1 Methodology

The primary interest in this problem is to determine how much chlorobenzene is leaching into Lake Erie each year based on the known concentration of chlorobenzene in the pore water of the dredge material measured in 1986. There are several difficulties associated with this problem that make an accurate prediction of this quantity impossible to evaluate. As indicated above, none of the important soil properties (including hydraulic conductivity, porosity, and dispersivity) are known for the dike, dredge or foundation soils. These properties will be assumed based solely on soil classification. Another difficulty occurs because the concentration of chlorobenzene in the sand foundation soils was not measured in 1986. The concentration in the pore water of these soils is needed for the overall solution of the problem. In order to estimate the concentration of the contaminant within these soils in 1986, initial finite element analyses were performed to model the years between 1967 and 1986. From these analyses, the chlorobenzene concentration in the foundation soils was estimated, and additional analyses were

performed to evaluate the quantity of chlorobenzene seeping into Lake Erie each year after 1986. The details of this procedure are explained below.

6.3.2 Finite Element Meshes

As indicated in Figure 6-3, seepage from the CDF into Lake Erie occurs from all 3 sides of the structure. Thus, transport of chlorobenzene in this problem is a 3-dimensional phenomena. To evaluate this problem with 2-dimensional analyses, the CDF was divided into 3 cross-sections as shown in Figure 6-5. The north (N-N') and south (S-S') sections were taken at about the center of the CDF where the water table is mounded. The west (W-W') section was taken from the land side of the facility toward the west face of the dike. Thus, the migration of chlorobenzene into Lake Erie from the north, south and west faces of the CDF was evaluated using the N-N', S-S' and W-W' cross-sections, respectively.

The finite element mesh used to model the north and south sections consisted of 287 nodes and 241 elements, and had horizontal and vertical dimensions of 650 feet and 70 feet, respectively. The mesh for the west cross-section consisted of 337 nodes and 283 elements and had horizontal and vertical dimensions of 1150 feet and 70 feet, respectively. These meshes are shown in Figure 6-6.

6.3.3 Boundary Conditions

The seepage boundary conditions are shown in Figure 6-7. The actual Lake Erie water levels were used as a "fixed" head boundary condition for the sides of the CDF bounded by the lake. Note that the value of this fixed head was allowed to vary with time as shown in Figure 6-2. No flow boundary conditions were assumed for the bottom nodes of the mesh and for the nodes along the central section of the CDF. Infiltration of rain water and snow melt into the CDF was modeled using a known seepage quantity boundary condition for the nodes located along the top of the mesh as shown on Figure 6-

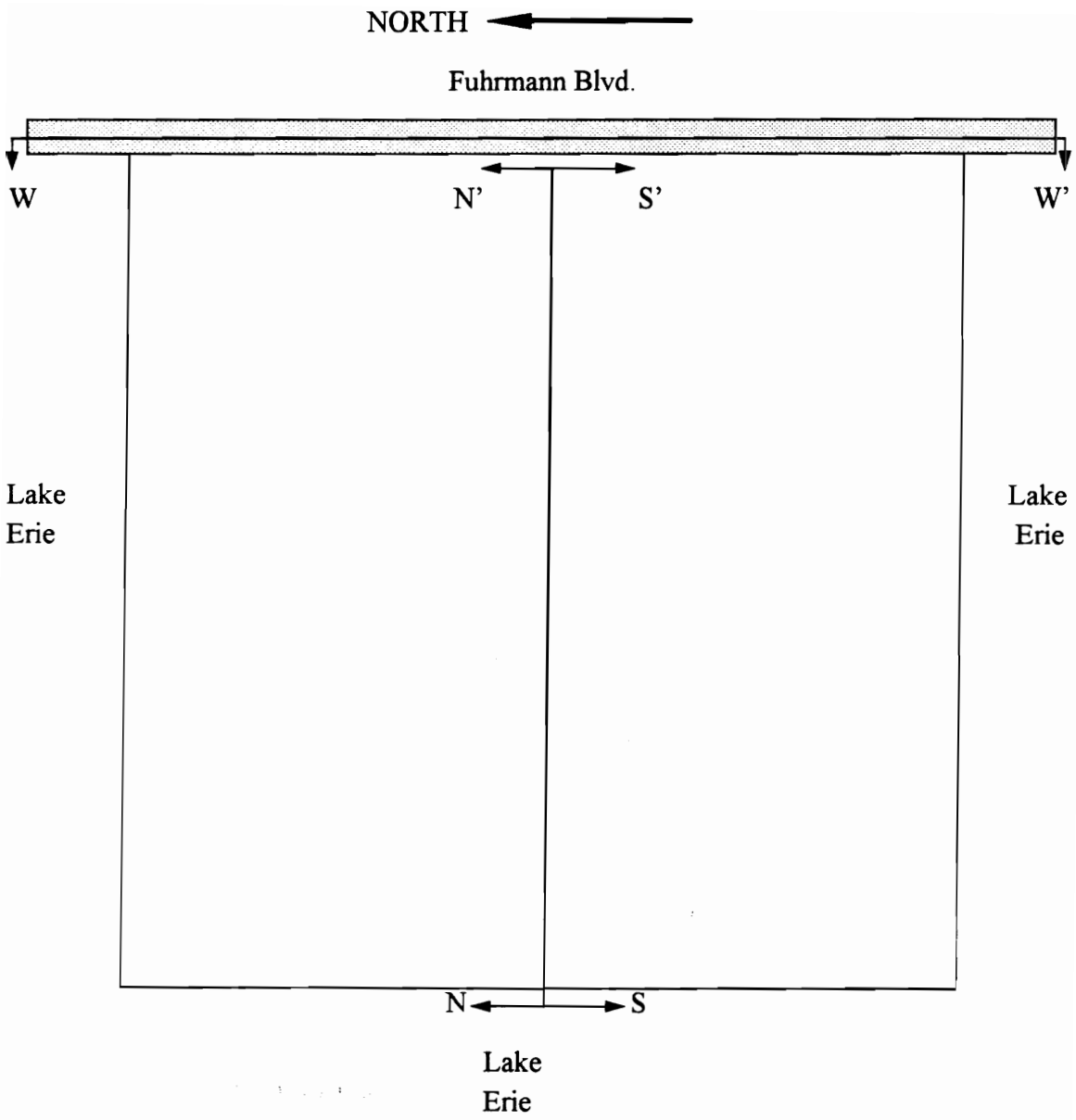

FIGURE 6-5: Cross-Sections Used to Analyze the CDF with a 2-D Model.

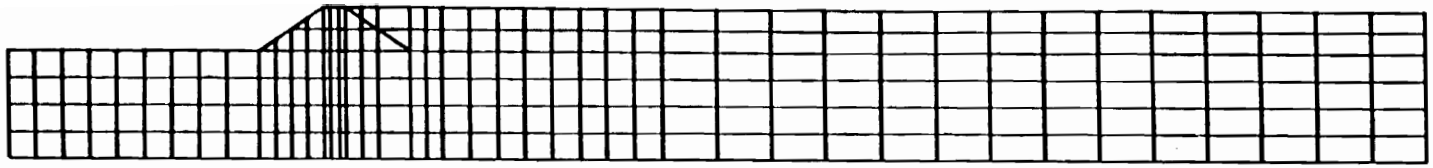

a) North and South Mesh

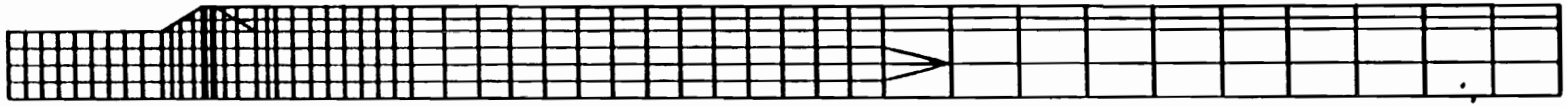

b) West Mesh

FIGURE 6-6: Finite Element Meshes Used to Evaluate Buffalo Harbor Dike Number 1.

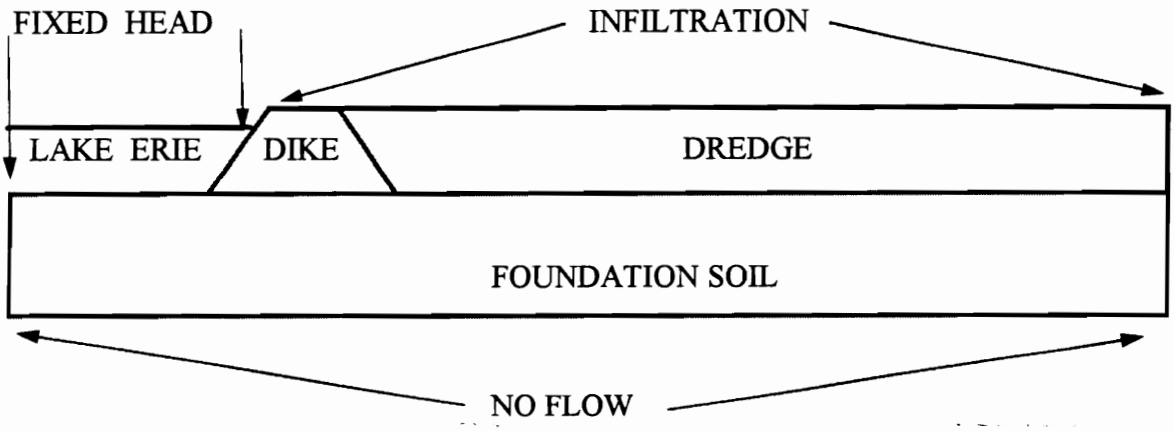

FIGURE 6-7: Seepage Boundary Conditions used for the Analyses.

7. The Corps of Engineers previously performed a water balance analysis for this structure using the HELP program in order to evaluate the amount of infiltration that could be expected at this site (Myers, 1987). They estimated that between 15 to 23 percent of the annual precipitation at this site percolates into the CDF. These numbers correspond to 5.4 and 8.3 inches of water per year, respectively. The program POLUTIDAL was modified by the author to incorporate this seepage boundary condition. These boundary conditions were used for both the pre-1986 and post-1986 analyses.

The chlorobenzene concentration within the dredge was assumed to be fixed with time for each of the analyses performed. However, different concentration values were used for the different cross-sections and for the pre-1986 and post-1986 analyses. These boundary conditions are shown in Figures 6-8 through 6-10. The post-1986 analyses concentration values were taken from the measured concentration data of 1986 as shown in Figure 6-4. The pre-1986 values were obtained by normalizing the post-1986 values using the highest concentration for the cross-section. Using these chlorobenzene concentrations, the corresponding relative concentration in the foundation soils were obtained using the program POLUTIDAL for 1986. These concentrations were then multiplied by the maximum actual concentration to obtain the estimated contaminant concentration in the foundation soils for the post-1986 analysis.

6.3.4 Initial Conditions

For the seepage portion of the analyses, an initial head was given for each node based on the water level of Lake Erie at the time the analysis was started and on the location of the ground water table within the CDF in 1986.

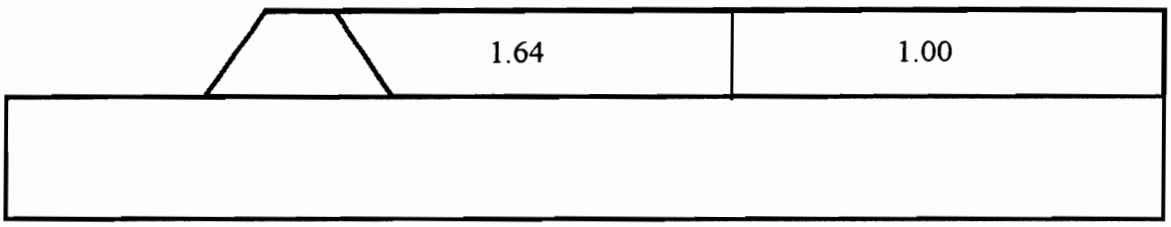

a) pre-1986

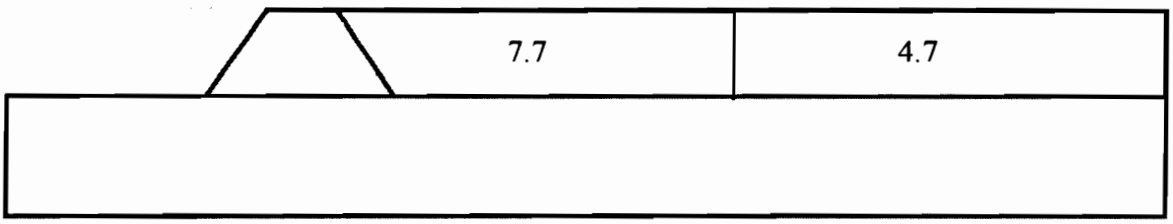

b) post-1986

FIGURE 6-8: Fixed Chlorobenzene Concentration Boundary Conditions used for the Analyses in the North Cross-Section (mg/l).

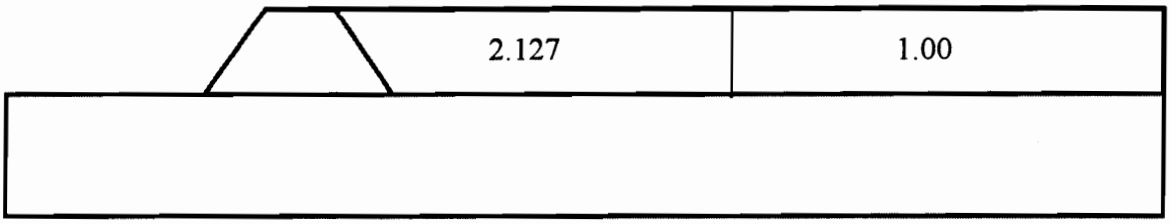

a) pre-1986

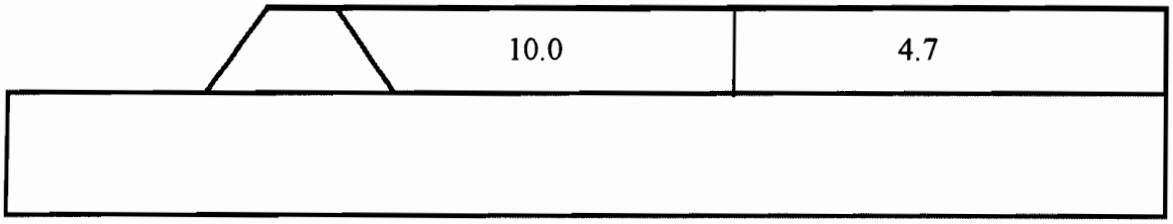

b) post-1986

FIGURE 6-9: Fixed Chlorobenzene Concentration Boundary Conditions used for the Analyses in the South Cross-Section (mg/l).

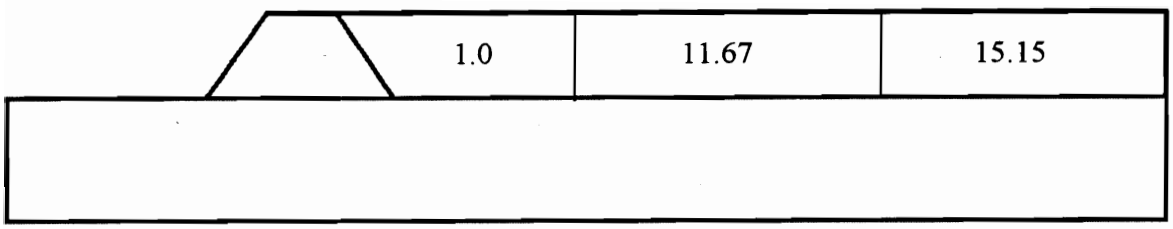

a) pre-1986

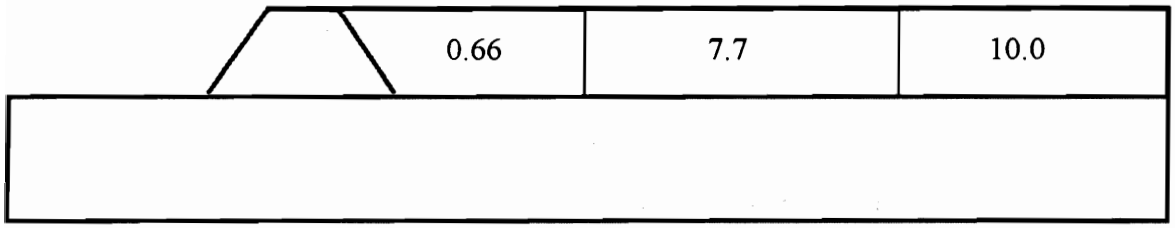

b) post-1986

FIGURE 6-10: Fixed Chlorobenzene Concentration Boundary Conditions used for the Analyses in the West Cross-Section (mg/l).

For the pre-1986 analyses, the initial concentration of chlorobenzene within the dredge was set equal to the values shown in Figures 6-8 (a) through 6-10 (a), whereas the concentration in the dike and foundation soils was assumed to be zero. The analyses were performed and the relative concentration of chlorobenzene at each node in the foundation and dike soils was obtained. These values were then adjusted (to correct for normalization) and used as the initial concentration in the foundation and dike soils for the post-1986 analyses. The initial concentration of chlorobenzene within the dredge for the post-1986 analyses was set equal to the values shown in Figures 6-8 (b) through 6-10 (b).

6.3.5 Soil Properties

As previously indicated, very little is known about the soil properties for this problem. Consequently, these properties where estimated based on soil classification. A summary of the soil properties used in the analyses is shown in Table 6.1. A linear adsorption model was used, and a value of 50 l/kg was considered for the dredge and foundation soils as recommended by the Corps of Engineers. Adsorption was not considered for the porous dike.

6.4 Results of the Analyses

6.4.1 Effect of the Infiltration Rate

Using the soil properties and the boundary and initial conditions described above, POLUTIDAL was used to evaluate the quantity of chlorobenzene that will seep annually into Lake Erie from the Buffalo Harbor Dike Number 1 facility. Initial analyses were performed to obtain an estimate of the chlorobenzene concentration in the dike and

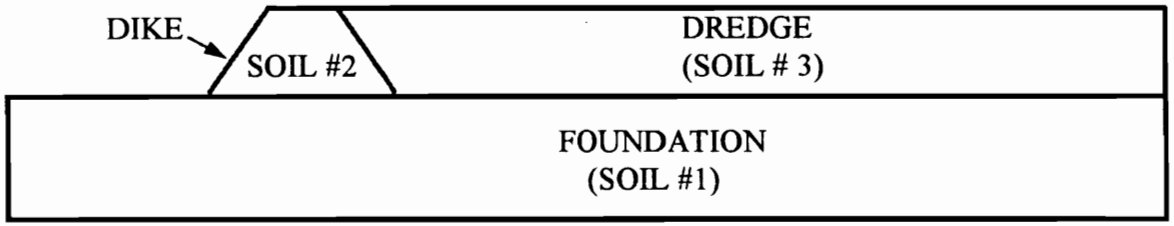

TABLE 6.1: Material Properties Used in the Analyses.

Soil #	Location	K_x (cm/sec)	Longitudinal Dispersivity (ft)	Transverse Dispersivity (ft)	Dry Unit Weight (pcf)	K_d (l/kg)	Sat. Water Content	Res. Water Content	van Genuchten α (ft^{-1})	van Genuchten m
1	Foundation	1E-3	50	10	83	50	0.5	0.1	0.8	0.6
2	Dike	1E-1	80	16	100	0	0.4	0.0	0.8	0.6
3	Dredge	1E-5	50	10	80	50	0.52	0.16	0.14	0.65

NOTE: K_y equals $\frac{1}{4}$ K_x

foundation soils in 1986. The final analyses were run using these results to obtain the quantity of chlorobenzene seeping into the lake from 1986 to 1991. The annual chlorobenzene loading quantity was obtained by averaging the results for these 5 years.

As indicated in Section 6.3.3, the infiltration rate of rain water and snow melt into the CDF was estimated by the Corps of Engineers to vary between 5.4 and 8.3 inches per year. The first set of analyses was performed using the smaller infiltration rate. The average annual chlorobenzene loading into Lake Erie from the north, south and west face of the structure using this infiltration rate are summarized below:

Face	Average Annual Loading (kg/yr)
North	18.1
South	23.2
West	3.5

The difference in the values between the faces of the CDF is attributed to the differences in the chlorobenzene concentration in the dredge material as indicated in Figures 6-8 (b) through 6-10 (b). Thus, the program predicts a total of 44.8 kilograms of chlorobenzene per year will seep into Lake Erie from this facility.

The effect of the infiltration rate was evaluated by repeating the above analyses using an infiltration rate of 8.3 inches per year and no infiltration. The results of these analyses are shown in Figure 6-11. This figure shows the important effect that infiltration can have on contaminant transport. The total annual loading of chlorobenzene into Lake Erie was reduced to 4.9 kg/year (a reduction by a factor of about 9) if no infiltration was considered. The results also show an increase in the annual loading to 86.3 kg/year (an

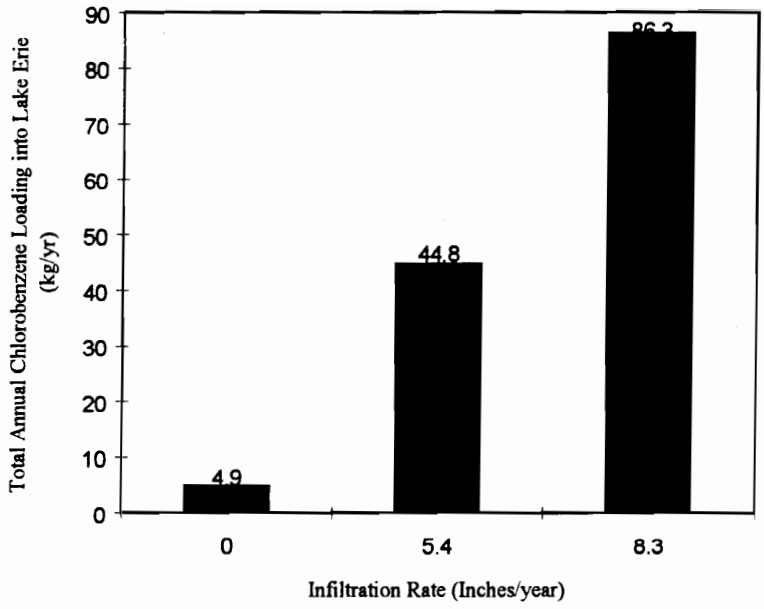

FIGURE 6-11: Plot Showing the Effect of Infiltration Rate on the Amount of Chlorobenzene Loading into Lake Erie.

increase by a factor of about 1.9) for an infiltration rate of 8.3 inches per year (an increase in the infiltration rate by a factor of 1.5).

6.4.2 Effect of Hydraulic Conductivity

Since the hydraulic conductivity of the dike, foundation and dredge soils was estimated based soley on material classification, a paramertic study was performed to evaulate the sensitivity of the values used in the previous analyses. The results reported in Chapter 5 indicated that the hydraulic conductivity of the dredge material itself did not strongly affect contaminant transport. Therefore, the influence of just the dike and foundation soils will be considered in this section.

Two anlayses were performed to evaluate the effect of the hydraulic conductivity of the dike on chlorobenzene transport. The hydraulic conductivity value was increased and decreased by a factor of 10 from the original assumed value. As shown in Figure 6-12, the amount of chlorobenzene that seeps into Lake Erie decreases as the hydraulic conductivity of the dike decreases. Notice, however, that the effect is not very pronounced. A decrease in hydraulic conductivity by 2 orders of magnitude only caused a 15% decrease in the amount of chlorobenzene loading into the lake.

A different trend is observed in Figure 6-13 which shows the effect of the hydraulic conductivity of the foundation soil on chlorobenzene transport. As the hydraulic conductivity decreased, the amount of chlorobenzene that seeped into Lake Erie increased. These results can be attributed to the fact that the seepage pattern changes as the hydraulic conductivity changes. As the foundation soil becomes less permeable, more seepage occurs through the dike rather than the foundation. Thus, chlorobenzene reaches the lake at a faster rate as the foundation soil becomes less permeable.

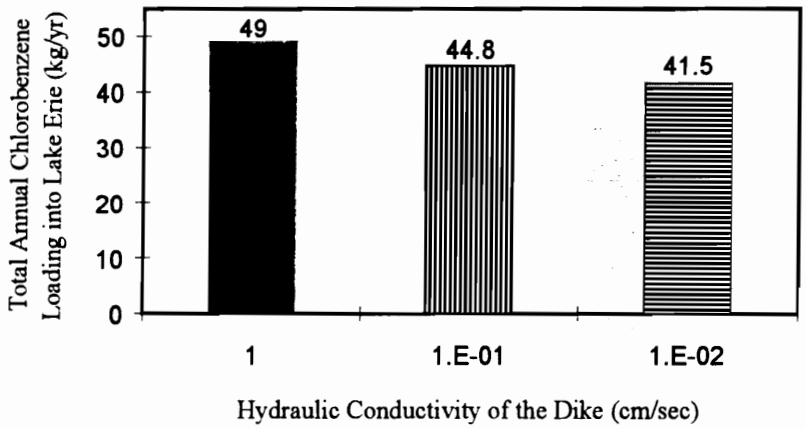

FIGURE 6-12: Effect of the Hydraulic Conductivity of the Dike on the Amount of Chlorobenzene Loading into Lake Erie.

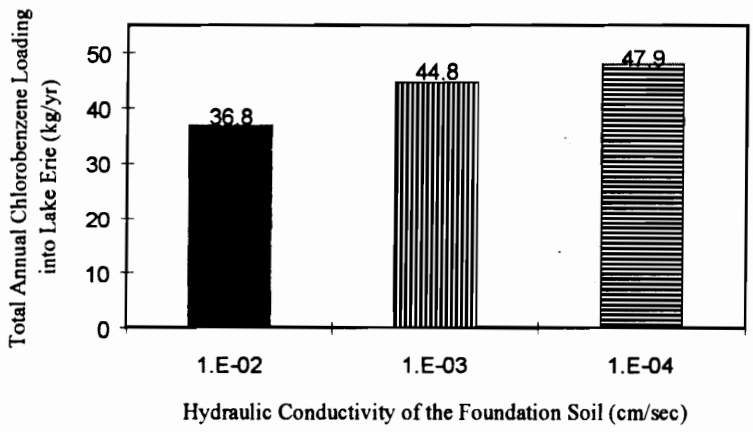

FIGURE 6-13: Effect of the Hydraulic Conductivity of the Foundation Soil on the Amount of Chlorobenzene Loading into Lake Erie.

6.4.3 Effect of Contaminant Boundary Condition

All of the above analyses were performed using a fixed concentration boundary condition inside the contaminated dredge zone. As indicated in Section 5.8 for the coastal CDF, this methodology would be expected to give an upper bound (most conservative) solution for the problem. The problem was reanalyzed to give a lower bound solution by specifying only the initial concentration of chlorobenzene within the pore water of the dredge. Thus, no fixed concentration values were given for any of the nodes in the finite element mesh. Figure 6-14 shows the results of the analyses and indicates that the amount of chlorobenzene that reaches the lake decreases from 44.8 kg/year using the fixed concentration approach to 29 kg/year using only the initial concentration approach. Thus, it does not appear to be too conservative to model the concentration of the contaminant within the dredge pore water as constant with time.

6.4.4 Effect of Containment Methods

As indicated in Section 5.10, one of the primary benefits of using POLUTIDAL is the ability to evaluate the effectiveness of various containment schemes in minimizing contaminant transport from confined disposal facilities into surrounding waters. To this end, the program was used to evaluate the amount of chlorobenzene that would seep into Lake Erie if a slurry trench was constructed through the perimeter dike and/or a soil cover was placed across the entire surface of the CDF. Each of these containment methods is described below.

6.4.4.1 Slurry Trench

The CDF was re-analyzed to evaluate the effect that a slurry trench would have on minimizing the amount of chlorobenzene migration into Lake Erie. The trench was 4 feet wide and was located along the centerline of the perimeter dikes. The trench was modeled as extending completely through the dike and sand foundation and into the underlying

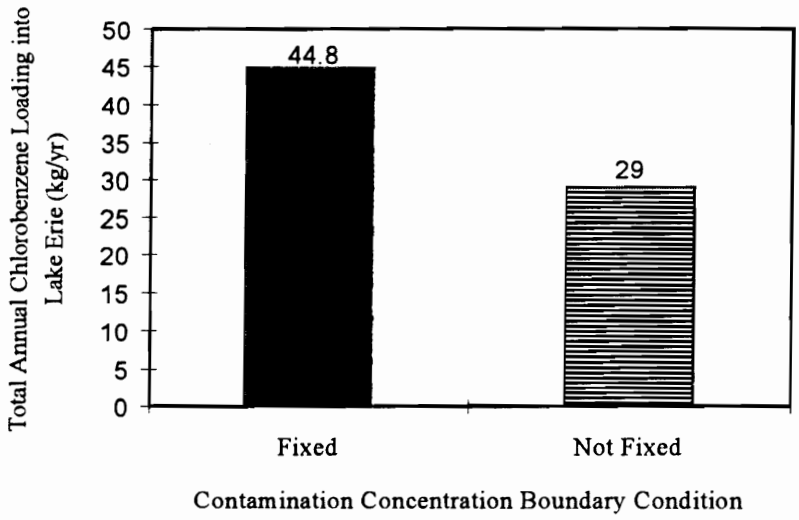

FIGURE 6-14: Effect of Contaminant Boundary Condition on Chlorobenzene Loading.

low permeability material as shown in Figure 6-15. Two analyses were performed using hydraulic conductivity values of 1E-5 and 1E-6 cm/sec for the trench. A constant infiltration rate of 5.4 inches per year was used in the analysis. The results of these analyses are shown in Figure 6-16. The slurry trench reduced the amount of chlorobenzene loading from 44.8 kg/year (if no trench is present) to about 29 kg/year. Note that the hydraulic conductivity of the slurry trench did not have much impact on the overall results.

6.4.4.2 Soil Cover

The above results indicated that a slurry trench would not significantly reduce the amount of chlorobenzene that will seep from the CDF into the lake. In addition, previous analyses (Section 6.4.1) indicated that infiltration of rain water and snow melt into the CDF had a significant effect of chlorobenzene transport. Thus, the effect of a soil cover placed across the entire surface of the CDF was evaluated. This containment method is quite common and is required for solid and hazardous waste landfill facilities. In the initial analyses, a two feet thick layer of low permeability soil was used as the cover material. The finite element meshes were slighlty modified by adding another row of elements across the top of the original meshes. Three analyses were performed using three different hydraulic conductivities for the cover soil, those being 1E-5, 1E-6 and 1E-7 cm/sec. To evaluate the effect of the soil cover, the chlorobenzene concentration at each node in 1986 was obtained using the pre-1986 analyses which did not include a cover. The new meshes were used with the cover material in place, and the problem was re-analysed for 5 years to determine how much chlorobenzene would seep into the lake.The results of these analyses are shown in Figure 6-17. Note that the cover did not have a significant effect on minimizing chlorobenzene migration into Lake Erie. There is a trend

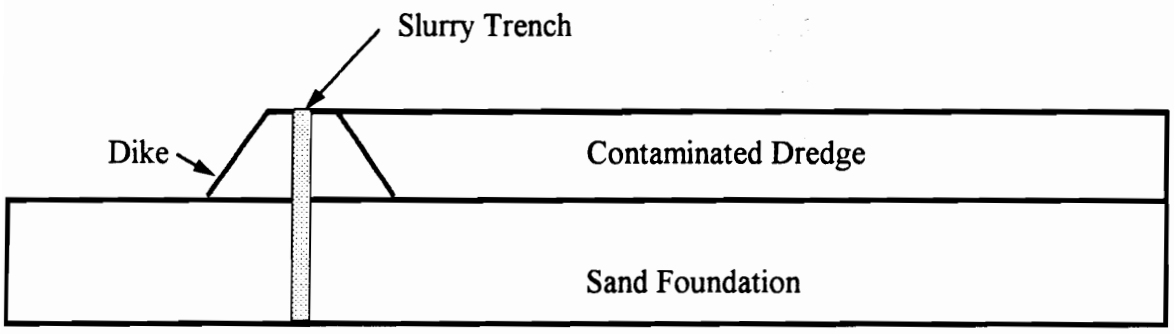

FIGURE 6-15: Location of Slurry Trench within the CDF.

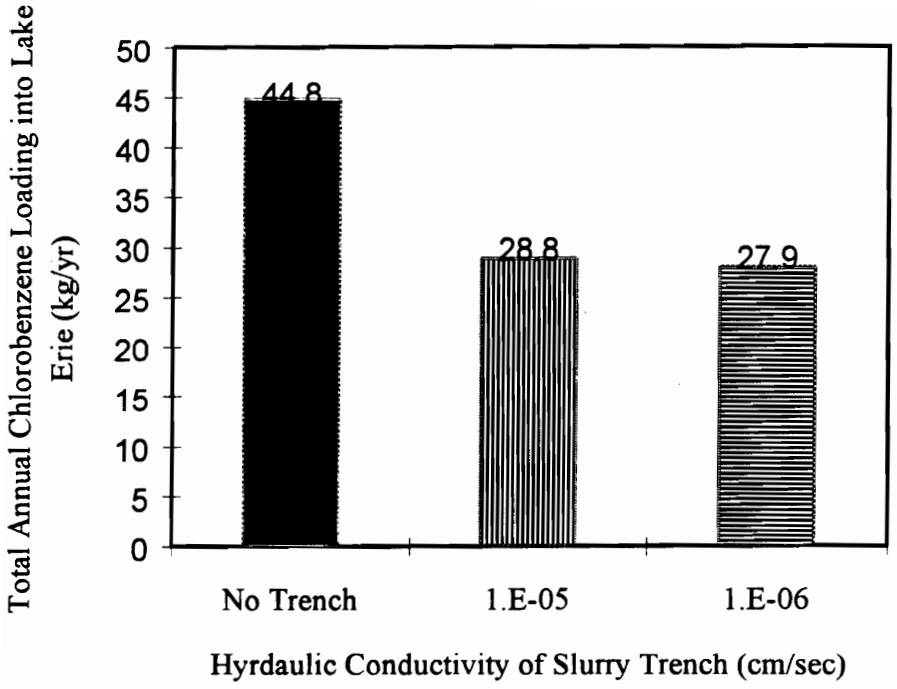

FIGURE 6-16: Effect of Slurry Trench on Chlorobenzene Loading.

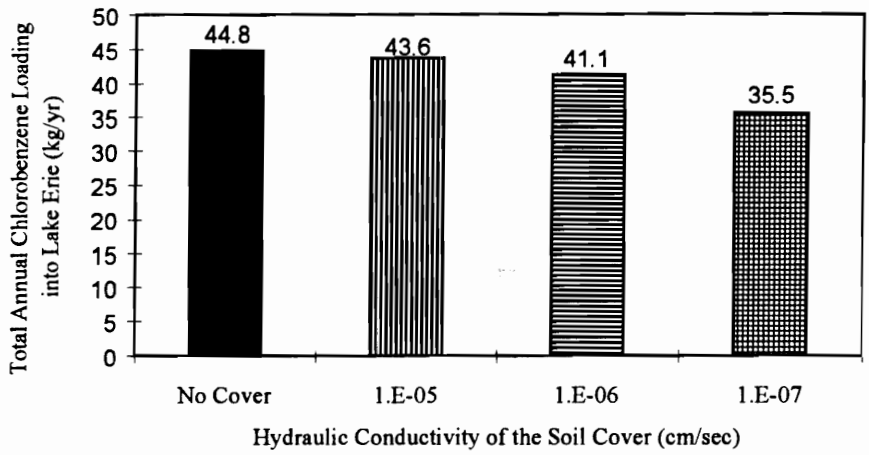

FIGURE 6-17: Effect of Soil Cover on Chlorobenzene Loading.

indicating that contaminant transport decreases as the hydraulic conductivity of the soil cover decreases.

6.4.4.3 Combined Slurry Trench and Soil Cover

It is apparent from the previous results that a slurry trench or soil cover alone are not very effective containment measures for this problem. Thus, additional analyses were performed to evaluate the combined effect of a slurry trench and a soil cover. In all of the analyses, the hydraulic conductivity of the slurry trench and soil cover were assumed to be 1E-6 and 1E-7 cm/sec, respectively. In addition, the width of the slurry trench was considered to be 4 feet as in the pervious analyses, however, the thickness of the cover material varied from 2 to 5 feet. The results of these analyses are shown in Figure 6-18. It can be seen that the combination of a slurry trench and cover can significantly decrease the amount of chlorobenzene that will seep into Lake Erie from the CDF. A slurry trench and 2 feet thick soil cover reduces the loading rate by about one-half. The thickness of the cover material also effects the amount of chlorobenzene loading. As the thickness of the cover increases, the amount of contaminant that is transported into the lake decreases. It is apparent from this set of analyses that a combined slurry trench and soil cover is the best containment method. Note, however, that there will still be chlorobenzene seeping into Lake Erie. The chlorobenzene that is in the pore water of the foundation and dike soils on the lake side of the slurry trench will still seep into the lake regardless of the containment method that is used.

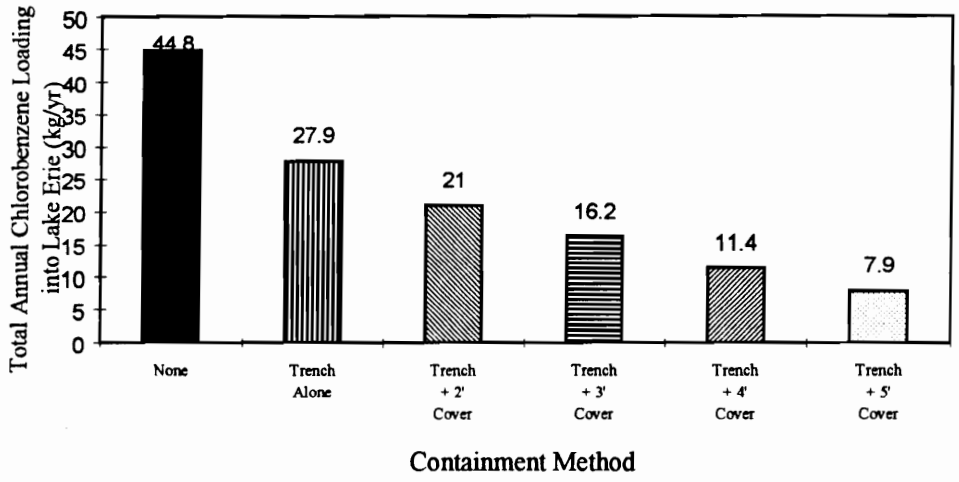

FIGURE 6-18: Effect of the Containment Method on Chlorobenzene Loading.

CHAPTER 7

Summary and Conclusions

7.1 Chapter Overview

In this chapter, the scope of the research and the results of the analyses are summarized. The general overall results for each of the two field problems are presented first, followed by a discussion of the effect that the soil properties, boundary conditions, and other variables had on contaminant transport from CDFs. Conclusions that can be made from this research are also discussed, as well as recommendations for future research for finite element modeling of contaminant transport through confined disposal facilities.

7.2 Summary of the Research Project

7.2.1 Purpose

The purpose of this research project was to modify the existing computer program POLUT2D such that the transport of contaminants associated with confined disposal facilities could be evaluated. Confined disposal facilities are structures built by the U.S. Army Corps of Engineers to contain sediments dredged from harbors and shipping channels. These sediments often contain contaminants such as heavy metals and organic compounds that can seep back into the waters from which the sediments were dredged. To evaluate contaminant transport through CDFs, the following modifications were made to the original computer program:

- a general beta time integration scheme was added,
- an algorithm was incorporated to account for the effect of tidal variations,
- the ability to specify a given head at any node at any time was incorporated to simulate the effect of the fluctuation of the water level of the Great Lakes,
- an infiltration seepage boundary condition was added to account for seepage due to precipitation and snow melt,

- a subroutine was added to include the effect of linear Freundlich and non-linear Langmuir adsorption on contaminant transport, and
- algorithms were incorporated to simulate gradual filling of the CDF with contaminated sediments and the effect of a finite contaminant capacity.

These changes were made, and the modified program was called POLUTIDAL. Using this program, two actual field problems were modeled and analyzed to evaluate the transport of contaminants through the CDF and foundations soils. The first field problem that was studied was a facility located in coastal waters, and the primary contaminant of concern was arsenic. For this problem, the effect of the tide on arsenic transport was examined. In addition, extensive sensitivity analyses were performed to evaluate the effect of the soil properties, sorption model, and boundary conditions on arsenic transport. The other field problem was the Buffalo Harbor Dike Number 1 located on Lake Erie, and the primary contaminant considered in the analyses was chlorobenzene. The effect of seepage due to infiltration from rain water and snow melt on chlorobenzene migration was evaluated. The impact of several remediation measures to minimize chlorobenzene seepage into Lake Erie was also investigated. The results of all these analyses are summarized in the sections below.

7.2.2 General Results for Problem No. 1: Coastal CDF

The geometry for this problem was shown in Figures 5-1 and 5-2. The estimated concentration of arsenic in the pore water of the dredge material was given by the Corps of Engineers as 0.027 mg/l. The primary objective for this problem was to evaluate the rate of arsenic transport and the total quantity of arsenic that will seep from the CDF into the bay. Using the soil properties given in Table 5-1 and the approximation for the fluctuation of the tide shown in Figure 5-4, the program predicts that an arsenic plume will migrate away from the disposal area and into the bay at the rate shown in Figure 5-8. The results indicated that it will only take about 7.5 years for the maximum relative concentration of arsenic that seeps into the bay to reach 50% of the original arsenic concentration in the dredge pore water. After 30 years the relative concentration will be

about 95%. The program also predicted that a cumulative total of 43 kilograms of arsenic will seep into the bay at the end of 50 years.

7.2.3 General Results for Problem No. 2: Buffalo Harbor Dike #1

The geometry for this problem was shown in Figure 6-1, and the actual measured concentration of chlorobenzene in the pore water of the dredge material in 1986 was shown in Figure 6-4. The objective for this problem was to evaluate the annual amount of chlorobenzene that is seeping into Lake Erie from this facility. As indicated in Section 6.3.1, the problem was solved using 3 finite element meshes, and two series of analyses. The first set of analyses were performed to obtain an estimate of the chlorobenzene concentration in the dike and foundation soils. The second set of analyses were performed using these estimated chlorobenzene concentrations and the measure data from 1986. Using this procedure and the soil properties given in Table 6-1, 44.8 kilograms of chlorobenzene is expected to seep from this facility into Lake Erie each year.

7.2.4 Effect of Soil Properties on Contaminant Transport

Sensitivity analyses were performed to evaluate which soil properties had the greatest effect on contaminant transport through CDFs. The influence of these soil properties is summarized below beginning with the soil properties which had the least overall effect and continuing with those which had the most overall effect on contaminant transport. Note that most of the soil property sensitivity analyses were performed for the coastal CDF (Problem No.1).

The results indicated that the coefficient of molecular diffusion (D_d) had no impact on arsenic transport through the CDF. Identical break through and mass loading curves were obtained for values of D_d of 0, 1E-7 and 1E-8 ft^2/day. These results are consistent with other findings which show that diffusion plays a very small role in mass transport problems where advection and dispersion govern. Thus, molecular diffusion can be ignored for problems where seepage is readily occurring.

The unit weight of the dike fill soil was varied between 105 and 125 pcf. The results show that these values had essentially no effect on arsenic transport as indicated by comparing Figures 5-21 and 5-22. This soil property only affects the adsorption term in the mass transport equation. However, the porosity did have a moderate effect on the mass loading curves (Figure 5-22b). As the porosity decreased from 0.38 to 0.26 (corresponding to 105 and 125 pcf, respectively), the program predicted a 80% increase in the total quantity of arsenic that will seep into the bay at the end of 50 years simulation time. This increase in mass loading is attributed to an increase in the seepage velocity of the arsenic plume.

The transverse dispersivity value was varied from 1 to 10 feet with essentially no impact on the rate or amount of arsenic transport. However, the longitudinal dispersivity did impact arsenic transport. The value of the longitudinal dispersivity was varied between 10 and 250 feet for each of the soil types in the coastal CDF problem. There was no difference in the results using these longitudinal dispersivity values for the soil within the contaminated dredge zone. The longitudinal dispersivity of the dike soils was also varied between 10 and 250 feet. The higher longitudinal dispersivity values produced a faster break through curve than the lower values. For example, at a simulation time of 10 years, the relative concentration obtained using a longitudinal dispersivity of 10 feet was 0.45, whereas a longitudinal dispersivity value of 250 feet predicted a relative concentration of 0.8. This behavior is expected since the longitudinal dispersivity directly impacts the hydrodynamic dispersion term in the mass transport equation. Similar results were obtained when the longitudinal dispersivity of the other soil types were varied between 10 and 250 feet.

The van Genuchten soil parameters (θ_r, m, and α), used to evaluate the unsaturated hydraulic conductivity and coefficient of moisture capacity, had almost no influence on the break through curves as shown previously in Figures 5-24a, 5-26a, and 5-28a. However, these parameters did have an impact on the total quantity of arsenic that was predicted to seep into the bay at the end of 50 years as seen in the mass loading

curves. Of the van Genuchten terms, the α parameter had the most significant impact on arsenic transport. The program predicted an 87 % increase in the amount of arsenic that will seep into the bay at the end of 50 years simulation time when α increased from 0.5 to 1.1 ft^{-1}.

Sorption of the contaminant onto the soil retarded the rate and amount of transport as clearly demonstrated in the results of the sensitivity analyses. As shown in Figure 5-48, at a simulation time of 10 years, a relative arsenic concentration of 0.81 was obtained when sorption was not considered in the analysis, whereas a relative arsenic concentration of 0.31 was obtained using a K_d of 2.0 l/kg. Thus, the arsenic plume moved about 2.6 times faster when sorption was ignored. At a simulation time of 50 years, the model predicted that about 97% more arsenic will seep into the bay when sorption was ignored as compared to including the mechanism of sorption in the analysis. The results also indicated that sorption does not have much impact on contaminant transport in soil layers of little volume.

The soil property which had the most significant impact on contaminant transport through confined disposal facilities was the coefficient of hydraulic conductivity. Analyses were performed using values for the hydraulic conductivity of each soil that were one order of magnitude higher and lower than the value used in the original analyses. Thus, a total range of 2 orders of magnitude were considered in the sensitivity analyses. All of the analyses except one indicated that the rate and quantity of contaminant transport increases as the hydraulic conductivity of the soils increase. The only exception to this trend was observed for the foundation soil of the Buffalo Harbor Dike facility. In this instance, the annual chlorobenzene loading into Lake Erie was observed to increase by about 30% when the hydraulic conductivity of the foundation soil decreased by 2 orders of magnitude. This response is attributed to a change in the flow pattern of the chlorobenzene plume. The lower hydraulic conductivity values for the foundation soil forced most of the chlorobenzene to seep through the dike rather than into the underlying foundation soils.

The hydraulic conductivity of the imported fill section of the dike for the coastal CDF had the most significant impact on contaminant transport as shown in Figure 5-15. The results indicated that the arsenic plume moved about 2.8 times faster when the hydraulic conductivity was increased by 2 orders of magnitude. Even more significant is the total quantity of arsenic that the program predicted will seep into the bay after a simulation time of 50 years. A hydraulic conductivity of 1E-4 cm/sec for the dike soil yields about 12.6 kilograms of arsenic at the end of 50 years. However, if the hydraulic conductivity is increased by 2 orders of magnitude, the model predicts that 770 kilograms of arsenic will seep into the bay at the end of 50 years.

7.2.5 Effect of Boundary Conditions on Contaminant Transport

7.2.5.1 Fluid Flow Boundary Conditions

The two field problems that were evaluated had slightly different boundary conditions. The coastal CDF is bounded on one sided by a fluctuating tide, whereas the Buffalo Harbor facility is subjected to fluctuating lake levels and infiltration due to precipitation. To evaluate the effect of the tidal boundary condition on arsenic transport, analyses were performed using the tidal simulation algorithm discussed in Section 5.2.2 and constant head boundary conditions. The results shown in Figure 5-9 indicated that the low tide model (Head = 2 feet) overpredicted, and the average tide model (Head = 7 feet) underpredicted the rate and quantity of arsenic migration through the CDF as compared to the tidal model.

For the Buffalo Harbor, the analyses indicated that infiltration due to percolation of rainwater and snow melt water had a significant impact on chlorobenzene migration into Lake Erie as shown in Figure 6-11. The program predicted a 97% increase of chlorobenzene into the lake due to a 54% increase in the infiltration rate (from 5.4 inches/year to 8.3 inches/year). In addition, the predicted 17.6 times less chlorobenzene loading into the lake when infiltration was not considered at all.

7.2.5.2 Contaminant Concentration Boundary Conditions

In Section 5.8, results were presented for analyses where the concentration of arsenic in the pore water of the dredge material varied with time to simulate gradual filling of the CDF with contaminated dredge. The results indicated that this simulation technique had only a slight impact on the break through curve in the early stages of the simulation time (up to about 10 years). After this time, there was almost no impact on the rate or quantity of arsenic transport through the CDF as seen in Figure 5-30.

Other analyses were performed using boundary conditions to model the contaminant in the dredge as a quasi-finite quantity. Several methods were proposed and analyzed which gave an apparent upper and lower bound solution for the mass transport problem. As shown in Figure 5-31, the methods which give an upper bound predicted that an average of 50 kilograms of arsenic will seep into the bay after 50 years, whereas the lower bound methods predicted that an average of 15 kilograms of arsenic will seep into the bay after 50 years.

7.2.6 Effect of Containment Method on Contaminant Transport

Several analyses were performed to evaluate the effectiveness of different types of containment methods on minimizing contaminant transport from confined disposal facilities. The first containment method investigated for the coastal CDF consisted of a low permeability soil liner placed along the inside of the CDF prior to placement of contaminated dredge. The effect of the liner thickness and hydraulic conductivity were investigated. As previously shown in Figure 5-34, both the rate and quantity of arsenic migration from the dredge zone decreased as the hydraulic conductivity of the liner decreased from 1E-5 to 1E-7 cm/sec. The data in the figure also indicates that the rate of arsenic migration from the dredge zone decreased as the thickness of the liner increases.

In the event that a soil liner would be difficult to construct inside the CDF, a slurry trench was also considered as a possible containment method. The analyses indicated that a slurry trench would be more effective than the 2 feet thick soil liner in containing the arsenic as indicated in Figure 5-37. Note also that the slurry trench reduces the relative

concentration and quantity of arsenic that will seep into the bay at the end of 50 years by a factor of 3 and 4, respectively, as compared to no type of containment method.

A slurry trench was also considered to minimize further spreading of chlorobenzene from the existing Buffalo Harbor facility into Lake Erie. The trench was shown to reduce the annual quantity of chlorobenzene loading into the lake from 44.8 kg/year without the trench to 27.9 kg/year with the trench installed completely around the perimeter of the facility (Figure 6-16). As an additional means of minimizing chlorobenzene seepage into Lake Erie, a low hydraulic conductivity soil cover placed across the entire surface of the CDF was modeled. Figure 6-18 showed how this combination of slurry trench and soil cover reduced the annual loading of chlorobenzene into the lake.

7.2.7 Effect of Finite Element Modeling Parameters on Contaminant Transport

Sensitivity analyses performed on some of the finite element modeling parameters such as time increment, beta time factor and mesh size indicated that none of these parameters had a significant influence on contaminant migration from CDF's for the values investigated in this research.

7.3 Conclusions

7.3.1 Accuracy/Usefulness of the Program POLUTIDAL

The results presented in this project show that POLUTIDAL is an accurate and useful program for modeling contaminant transport through confined disposal facilities. The analyses performed in Section 4.7 indicated that the program gave results that were identical to closed form solutions for simple problems, and that were in good agreement with solutions obtained by other workers for more complex problems. However, the accuracy of the solution of mass transport problems using numerical methods is dependent on the Peclet and Corount Numbers as indicated in Section 4.5. The importance of these criteria cannot be overemphasized. The solution may be in error if the finite element grid or time increment is too large due to numerical oscillations. The meshes and time

increments used in this project were adjusted to avoid these types of errors. Since there is currently no general agreement on how to avoid numerical oscillations, adjustment of the mesh and time increment is probably the best solution.

This research project demonstrated that a major benefit of the program is its use as a tool for the design or remediation of CDFs. The effect of soil properties and other uncertainties on containment of the contaminant can be readily evaluated. Different containment methods can be analyzed and compared to assist in the final design of a new facility or the remediation of an existing structure.

Another benefit of the program is that it can analyze CDFs located in both coastal and non-coastal environments. In addition, the program can be used to evaluate contaminant transport through porous media where sorption is a factor.

7.3.2 Significance of the Soil Properties

The results indicated that some soil properties do not have much impact on the migration of contaminants through confined disposal facilities. Some of these properties include unit weight, molecular diffusion, and transverse dispersivity. Other properties, such as the distribution coefficient, the van Genuchten parameters, and the longitudinal dispersivity, have only a slight to moderate impact on contaminant transport. However, the solution did not vary significantly when values were used which were fairly typical for the given soil type.

The results indicated that the value of the coefficient of hydraulic conductivity can have a significant impact on contaminant transport though CDFs. The quantity of contaminant that seeps from the facility can be severely underestimated if the hydraulic conductivity varies by only 1 order of magnitude. This was particularly the case for the dike soils. Consequently, accurate values of this soil property are needed in order to arrive at an accurate solution of the problem. Sensitivity analyses on this parameter should always be performed for the design or remediation of CDFs.

Although the mechanism of sorption was shown to retard movement of contaminants through confined disposal facilities, its influence may be neglected without

introducing too much conservatism. This is especially true in light of all the uncertainties regarding the other soil parameters.

7.3.3 Significance of the Boundary Conditions

The algorithm developed to model the fluctuations of the tide should be used when evaluating coastal CDFs. The input data is easy to obtain, and the model gives different results if the effect of the tide is not considered.

The results showed that precipitation falling on a CDF has a significant effect on the rate at which contaminants seep through the facility. The influence of infiltration should be considered in the analysis and design of these CDFs. Infiltration from precipitation may be extremely important for facilities where flow from other sources, i.e. groundwater, tides etc., is small. In some situations, infiltration may be the driving force behind contaminant transport.

Different approaches were performed to model the concentration of the source contaminant in the pore water of the dredge soils. The simplest approach used constant concentration values at all of the nodes in dredge zone. Although this method does not represent the actual field conditions, it is useful for performing parametric studies and for comparing the results of different containment methods. This approach is expected to give an upper bound solution to the problem. The finite capacity model that was developed is more representative of field conditions and would be better for predicting actual concentration values. It may be reasonable to analyze CDF problems using both approaches in order to obtain a range of solution values.

The analyses that were performed to simulate gradual filling of the CDF with contaminated dredge indicated that this technique may not be necessary. Short term solutions were only slightly effected by using this approach while long term results showed no change in the rate or quantity of contaminant transport into the bay when this option was considered.

7.3.4 Contaminant Containment Methods

A slurry trench was found to be more effective in containing arsenic than a 2 feet thick soil liner. In addition, a trench would almost certainly be easier to construct than a compacted clay liner. For the case of remediation, a trench alone may not be sufficient as shown in the analyses of the Buffalo Harbor facility. In this problem, a soil cover used in conjunction with a trench was most effective. This observation demonstrates the significance of infiltration on contaminant transport as discussed above.

7.4 Recommendations for Future Research

One of the major difficulties of numerical models is program verification. Some verification was performed in this study, however, closed form solutions for the complicated field problems that were actually solved are not available. The author suggests that further research in this area should include laboratory and/or small scale field simulations to verify the computer code.

The Buffalo Harbor facility required three 2-D finite element meshes because the problem actually involved 3-D flow and mass transport. This effort could be minimized if a 3-D version of POLUTIDAL was developed. The algorithms used to solve the problem would not change significantly. However, the computational effort and the amount of input data would certainly increase.

Further refinement to the program should include the ability to incorporate other types of sorption models such as the kinematic models discussed in Section 3.3.2.2. In addition, this study did not include the effect of desorption. Desorption often occurs as the concentration in the pore water becomes lower than the solid phase concentration.

For coastal confined disposal facilities, the effect of the salinity of the coastal waters may have an impact in contaminant transport. Salinity effects were not considered in this study.

Another containment method which would be useful to consider would be the use of a geomembrane rather than soil as the liner or cover material. Although a geomembrane is not really a porous material (except for the presence of defects), equivalent hydraulic

conductivity and molecular diffusion values could be obtained for modeling the geomembrane as a very thin "soil" layer.

Finally, additional research is needed to handle the problem of numerical oscillations which occur if the grid of time increment is too large. Care should be taken, however, such that the new procedure does not introduce too much dispersion into the solution of the problem.

REFERENCES

Aggour, M., Lentz, J., and Tayel, M., "Design Methodology of Dredged Material Containment Areas", ***Proceedings of the World Dredging Conference 1983***, Paper N1, pp. 557-567.

Ahmad, F., ***Numerical Modelling of Transport of Pollutants through Soils***, Thesis, Virginia Polytechnic Institute and State University, Blacksburg, VA, 1991.

Alther, G., Evans, J., Fong, H-Y, and Witner, K., "Influence of Inorganic Permeants upon the Permeability of Bentonite", in ***Hydraulic Barriers in Soil and Rock***, ed. by A. Johnson, R. Frobel, N. Cavalli and C. Pattersson, ASTM, Philadelphia, PA, pp 64-73, 1985.

Anderson, D., Crawley, W., and Zabcik, J., "Effects of Various Liquids on Clay Soil: Bentonite Slurry Mixtures", in ***Hydraulic Barriers in Soil and Rock***, ed. by A. Johnson, R. Frobel, N. Cavalli and C. Pattersson, ASTM, Philadelphia, PA, pp 93-103, 1985.

Bahr, J., and Rubin, J., "Direct Comparison of Kinetic and Local Equilibrium Formulations for Solute Transport Affected by Surface Reactions," ***Water Resources Research***, Vol. 23, No. 3, pp. 438-452, 1987.

Bar-Yosef, B., "pH-Dependent Zinc Adsorption by Soils," ***Soil Science Society of America, Journal***, Vol. 43, pp. 1095-1099, 1979.

Bear, J., ***Hydraulics of Groundwater***, McGraw-Hill Inc., 1979.

Bowders, J., and Daniel, D., "Hydraulic Conductivity of Compacted Clay to Dilute Organic Chemicals," ***Journal of Geotechnical Engineering***, ASCE, Vol. 113, No. 12, pp. 1432-1448, December, 1987.

Bradley, J., "Dredging and the Environmental Policy Act of 1969", ***Dredging and its Environmental Effects***, P. Krenkel, J. Harrison, and J. C. Burdick III (Eds.), ASCE, New York, pp. 39-48, 1976

Bray, R., ***Dredging: A Handbook for Engineers***, Edward Arnold Ltd., 1979.

Brooks R., and Corey, T., "Hydraulic Properties of Porous Media", ***Hydrology Paper No. 3***, Colorado State University, Fort Collins, Colorado, March 1964.

Brooks, R., and Corey, A., "Properties of Porous Media Affecting Fluid Flow", ***Journal of the Irrigation and Drainage Division***, ASCE, Vol. 92, No. IR2, pp. 61-88, June, 1966.

Brooks, A., and Hughes, T., "Streamline Upwind/Petrov-Galerkin Formulation for Convective Dominated Flows with Particular Emphasis on the Incompressible Navier-Stokes Equations," ***Computer Methods in Applied Mechanics and Engineering***, Vol. 32, pp. 199-259, 1982.

Bruce, R., "Hydraulic Conductivity Evaluation of the Soil Profile from Soil Water Retention Relations", ***Soil Science Society of America Proceedings***, Vol. 36, No. 4, pp. 555-561, 1972.

Brunelle, T., Pell, L., and Meyer, C., "Effect of Permeameter and Leachate on a Clay Liner", in ***Geotechnical Practice for Waste Disposal '87***, ed. R. Woods, ASCE, pp 347-361, 1987.

Brutsaert, W., "Probability Laws for Pore-Size Distributions", ***Soil Science***, Vol. 101, No. 2, February 1966, pp. 85-92.

Brutsaert, W., "Some Methods of Calculating Unsaturated Permeability", ***Transactions of the American Society of Agricultural Engineers***, Vol. 10, No. 3, pp. 400-404, 1967.

Budhu, M., Giese Jr., R., Campbell, G., and Baumgrass, L., "The Permeability of Soils with Organic Fluids", ***Canadian Geotechnical Journal***, vol. 28, No. 1, pp 140-147, 1991.

Burdine, N., "Relative Permeability Calculations from Pore Size Distribution Data", ***Petroleum Transactions***, American Institute of Mining and Metallurgical Engineers, Vol. 198, pp. 71-78, 1953.

Burrett, R., and Frind, E., "Simulation of Contaminant Transport in Three Dimensions 2. Dimensionality Effects", ***Water Resources Research***, Vol. 23, No. 4, pp. 695-705, 1987.

Cameron, D., and Klute, A., "Convective-Dispersive Solute Transport with a Combined Equilibrium and Kinetic Adsorption Model," ***Water Resources Research***, Vol. 13, No. 1, pp 183-188, 1977.

Cantekin, M., and Westerink, J., "Non-Diffusive N+2 Degree Petrov-Galerkin Methods for Two-Dimensional Transient Transport Computations," ***International Journal for Numerical Methods in Engineering***, Vol. 30, pp. 397-418, 1990.

Childs, E., and Collis-George, N., "The Permeability of Porous Materials", ***Proceedings of the Royal Society of London***, Series A, Vol. 201, pp. 392-405, May 1950.

Christie, I., Griffith, D., Mitchell, A., and Zienkiewicz, O., "Finite Element Methods for Second Order Differential Equations with Significant First Derivatives," ***International Journal for Numerical Methods in Engineering***, Vol. 10, pp 1389-1396, 1976.

Crooks, V., and Quigley, R., "Saline Leachate Migration through Clay: A Comparative Laboratory and Field Investigation", ***Canadian Geotechnical Journal***, Vol. 21, No. 2, pp. 349-362, May, 1984.

Dane, J., "Comparison of Field and Laboratory Determined Hydraulic Conductivity Values", ***Soil Science Society of America Journal***, Vol. 44, No. 2, pp. 228-231, 1980.

Daniel, D., "Clay Liners", in ***Geottechnical Practice for Waste Disposal***, Ed Daniel, D, pp 135-163, Chapman and Hall, London, 1993.

Daniel, D., Anderson, D., and Boynton, S., "Fixed-wall versus Flexible-wall Permeameters", in ***Hydraulic Barriers in Soil and Rock***, ed. by A. Johnson, R. Frobel, N. Cavalli and C. Pattersson, ASTM, Philadelphia, PA, pp 107-126, 1985.

Daus, A., Frind, E., and Sudicky, E., "Comparative Error Analysis in Finite Element Formulations of the Advection-Dispersion Equation," ***Advances in Water Resources***, Vol. 8, pp 86-95, 1985.

Dhatt, G., and Touzet, G., ***The Finite Element Method Displayed***, John Wiley and Sons, 1984.

Elkhatib, E., Bennett, O.,and Wright, R. "Arsenite Sorption and Desorption in Soils", ***Soil Science Society of America Journal***, vol. 40, pp 1025-1030, 1984.

Elprince, A., "Effect of pH on the Adsorption of Trace Radioactive Cesium by Sediments",***Water Resources Research***, vol. 14, No. 4, pp 696-698, 1978.

Elrashidi, M., and O'Connor, G., "Boron Sorption and Desorption in Soils," ***Soil Science Society of America, Proceedings***, Vol. 46, No. 1, pp. 27-31, 1982.

Enfield, C., Harlin, Jr. C., and Bledsoe, B., "Comparison of Five Kinetic Models for Orthophosphate Reactions in Mineral Soils," ***Soil Science Society of America Journal***, Vol. 40, pp. 243-249, 1976.

Fetter, C.W., ***Contaminant Hydrogeology***, MacMillan Publishing Company, New York, NY, 1993.

Fernandez, F., and Quigley, R., "Hydraulic Conductivity of Natural Clays Permeated with Simple Liquid Hydrocarbons", ***Canadian Geotechnical Journal***, vol. 22, pp 205-214, 1985.

Fireman, M., "Permeability Measurements on Disturbed Soil Samples", ***Soil Science***, vol. 58, pp 337-353, 1944.

Fishel, V., "Further Tests of Permeability with Low Hydraulic Gradients", ***American Geophysical Union,_Transactions***, 16th Annual Meeting, pp. 499-503, April 1935.

Foreman, D., and Daniel, D., "Permeation of Compacted Clay with Organic Chemicals", ***Journal of Geotechnical Engineering***, Vol. 112, No. 7, pp 669-681, 1986.

Fowler, B., "Arsenical Metabolism and Toxicity to Fresh Water and Marine Species," ***Biological and Environmental Effects of Arsenic***, Ed. B. Fowler, Elsevier, pp. 155-170, 1983.

Freeze, R., and Cherry, J., ***Groundwater***, Prentice-Hall, Inc., Englewood Cliffs, NJ, 1979.

Fried, J., ***Groundwater Pollution***, Elsevier Scientific Publishing Company, Amsterdam, 1975.

Frind, E., and Hokkanen, G., "Simulation of the Borden Plume Using the Alternating Direction Galerkin Technique," ***Water Resources Research***, Vol. 23, No. 5, pp. 918-930, 1987.

Gaber, H., Comfort, S., Insteep, W., and El-Attar, H., "A Test of the Local Equilibrium Assumptiom for Adsorption and Transport of Picloram," ***Soil Science Society of America, Proceedings***, Vol. 56, No. 5, pp. 1392-1400, 1992.

Gates, J., and Leitz, W., "Relative Permeabilities of California Cores by the Capillary-Pressure Method", ***Drilling and Production Practice***, American Petroleum Institute, pp. 285-298, 1950.

Gelhar, L., Welty, C., and Rehfeldt, K., "A Crititcal Review of Data on Field-Scale Dispersion in Aquifiers," ***Water Resources Research***, Vol. 28, No. 7, pp. 1955-1974, 1992.

Gipson, JR. A., "Permeability Testing on Clayey Soil and Silty Sand-Bentonite Mixture using Acid Liquor", ***Hydraulic Barriers in Soil and Rock***, ed. by A. Johnson, R. Frobel, N. Cavalli and C. Pattersson, ASTM, Philadelphia, PA, pp 140-154, 1985.

Green, R., Ahuja, L., and Chong, S., "Hydraulic Conductivity, Diffusivity, and Sorptivity of Unsaturated Soils: Field Methods", ***Methods of Soil Analysis Part 1: Physical and Mineralogical Methods***, A. Klute (Ed.), 2nd Edition, Number 9, American Society of Agronamy, Inc., Madison Wisconsin, pp. 771-798, 1986.

Gren, G., "Hydraulic Dredges, Incuding Boosters", in ***Dredging and its Environmental Effects***, P. Krenkel, J. Harrison, and J. C. Burdick III (Eds.), ASCE, New York, pp. 115-124, 1976.

Greshno, P., and Lee, R., "Don't Supress the Wiggles - They're Telling You Something!," ***Finite Element Methods for Convection Dominated Flows***, Ed. T. Hughes, AMD, Vol 34, pp. 37-61, 1979.

Griffin, R., and Av, A., "Lead Adsorption by Montmorillonite Using a Competitive Longmuir Equation," ***Soil Science Society of America, Journal***, Vol. 41, pp. 880-882, 1977.

Hammer, D., and Blackburn, E., "Design and Construction of Retaining Dikes for Containment of Dredged Material" ***Technical Report D-77-9***, US Army Engineer Waterways Experiment Station, Vicksburg, MS. 1977.

Hansbo, S., "Consolidation of Clay, with Special Reference to Influence of Vertical Sand Drains", ***Swedish Geotechnical Institute Proceedings***, No. 18, 1960.

Harr, M., ***Groundwater and Seepage***, McGraw-Hill Book Company, Inc., New York, 1962.

Harter, R., "Adsorption of Copper and Lead by Ap and B2 Horizons of Several Northeastern United States Soils," ***Soil Science Society of America, Journal***, Vol. 43, pp. 679-683, 1979.

Harter, R., "Curve-fit Errors in Langmuir Adsorption Maxima," ***Soil Science Society of America, Journal***, Vol. 48, pp. 749-752, 1984.

Harter, R., and Baker, D., "Applications and Misapplications of the Longmuir Equation to Soil Adsorption Phenomena," ***Soil Science Society of America, Journal***, Vol. 41, pp. 1077-1080. 1977.

Harter, R., and Smith, G., "Langmuir Equation and Alternate Methods of Studying "Adsorption" Reactions in Soils", pp. 167-182, In R. H. Dowdy, et al. (Editors), ***Chemistry in the Soil Environment***, special publication No 40, American Society of Agronomy, Madison, Wisconsin, 1981.

Heinrich, J., Huyakorn, P., Zienkiewicz, O., and Mitchell, A., "An 'Upwind' Finite Element Scheme for the Two-Dimensional Convective Transport Equation," ***International Journal for Numerical Methods in Engineering***, Vol. 11, pp 131-143, 1977.

Ho, Yl, and Pufahl, D., "The Effects of Brine Contamination on the Properties of Fine-grained soils", in ***Geotechnical Practice for Waste Disposal '87***, ed. R. Woods, ASCE, pp 547-561, 1987.

Hollis, C., "Legislative Impacts on Dredging: General Regulatory Functions", ***Dredging and its Environmental Effects***, P. Krenkel, J. Harrison, and J. C. Burdick III (Eds.), ASCE, New York, pp. 1-9, 1976.

Hopmans, J., and Dane, J., "Temperature Dependence of Soil Hydraulic Properties", ***Soil Science Society of American Journal***, Vol. 50, No.1, 1986, pp. 4-9.

Hubbert, M., "Darcy's Law and the Field Equations of the Flow of Underground Fluids", ***Transactions of the American Institute of Mining, Metallurgical, and Petroleum Engineers***, Vol. 207, pp. 222-239, 1956.

Hughes, T., and Brooks, A., "A Multi-Dimensional Upwind Scheme with No Crosswind Diffusion," ***Finite Element Methods for Convection Dominated Flows***, Ed. T. Hughes, AMD, Vol 34, pp. 19-35, 1979.

Hutton, M., "Human Health Concerns of Lead, Mercury, Cadmium, and Arsenic," in ***Lead, Mercury Cadmium and Arsenic in the Environment***, Eds. Hutchinson, T., and Meema, K., pp. 53-68, John Wiley and Sons, 1987.

Huyakorn, P., "Solution of Steady-State Convective Transport Equations Using an Upwind Finite Element Scheme," ***Applied Mathematical Modelling***, Vol. 1, pp. 187-195, 1977.

Huyakorn, P., and Nilkuha, K., "Solution of Transient Transport Equation Using an Upstream Finite Element Scheme," ***Applied Mathematical Modelling***, Vol. 3, pp. 7-17, 1979.

Huyakorn, P., and Pinder, G., ***Computational Methods in Subsurface Flow***, Academic Press, New York, 1983.

Irmay, S., "On the Hydraulic Conductivity of Unsaturated Soils", ***Transactions of the American Geophysical Union***, Vol, 35, No. 3, pp. 463-467, June 1954.

Istok, J., ***Groundwater Modeling by the Finite Element Method***, American Geophysical Union, Water Resource Monograph #13, 1989.

Kandil, H., Miller, C., and Skaggs, R., "Modeling Long-Term Solute Transport in Drained Unsaturated Zones", ***Water Resources Research***, Vol. 28, No. 10, pp 2799-2809, 1992.

Karickhoff, S., Brown, P., and Scott, T., "Sorption of Hydrophobic Pollutants on Natural Sediments", ***Water Research***, vol. 13, pp 241-248, 1979.

Kelly, D., Nakazaw, S., Zienkiewicz, O., and Heinrich, J., "A Note on Upwinding and Anisotropic Balancing Dissipation in Finite Element Approximation to Convective Diffusion Problems," ***International Journal for Numerical Methods in Engineering***, Vol. 15, pp. 1705-1711, 1980.

Kirda, C., Nielsen, D., and Biggar, J., "Simultaneous Transport of Chloride and Water During Infiltration", ***Soil Science Society of America Proceedings***, Vol. 37, No. 3, pp. 339-345, 1973.

Klute, A., "Water Retention: Laboratory Models", ***Methods of Soil Analysis Part 1: Physical and Mineralogical Methods***, A. Klute (Ed.), 2nd Edition, Number 9, American Society of Agronamy, Inc., Madison Wisconsin, pp. 635-662, 1986a.

Klute, A., and Dirksen, C., "Hydraulic Conductivity and Diffusivity: Laboratory Models", ***Methods of Soil Analysis Part 1: Physical and Mineralogical Methods***, A. Klute (Ed.), 2nd Edition, Number 9, American Society of Agronamy, Inc., Madison Wisconsin, pp. 687-734, 1986b.

Kool, J., Parker, J., and van Genuchten, M., "Determining Soil Hydraulic Properties from One-Step Outflow Experiments by Parameter Estimation: I, Theory and Numerical Studies", ***Soil Science Society of America Journal***, Vol. 49, No. 6, pp. 1348-1354, 1985.

Klutz, D., and Moser, H., "Hydrodynamic Dispersion as Aquifer Characteristic: Model Experiments with Radioactive Tracers", ***Isotope Techniques in Groundwater Hydrology***, Vol. 2, pp. 341-355, 1974.

Krizek, R., Gallagher, B., and Karadi, G., **Water Quality Study for a Dredgings Disposal Area**, Technical Report No. 4, Northwestern University, September, 1974.

Krizek, R., and Salem, A., "Behavior of Dredged Materials in Diked Containment Areas", ***Technical Report No. 5,*** Northwestern University, Evanston Illinois, 1974.

Kuo, S., and Lotse, E., "Kinetics of Phospate Adsorption and Desorption by Hematite and Gibbsite," ***Soil Science***, Vol. 116, No. 6, pp.----1973.

Kuo, S., "Application of a Modified Langmuir Isotherm to Phosphate Sorption by some Acid Soils," ***Soil Science Society of America, Journal***, Vol. 52, pp. 97-102, 1988.

Kuppusamy, T., and Ahmad, F., ***POLUT2D -- A Finite Element Program for Vertical 2-D Advective Dispersive Pollutant Transport Problems User's Manual***, Department of Civil Engineering, VPI & SU, June 1991.

Kuppusamy, T. and Tyler, T. "User's Manual for Program POLUTIDAL" *Report for the Development of CDF Dike Seepage and Transport Model Using the Computer Program POLUT2D*, Virginia Polytechnic Institute and State University, Blacksburg VA, 1993..

Lai, S., and Jurinak J., "Cation Adsorption in One-Dimensional Flow through soils: A Numerical Solution," ***Water Resources Research***, Vol. 8, No. 1, pp. 99-107, 1972.

Langmuir, I., "The Adsorption of Gases on Plane Surfaces of Glass, Mica, and Platinum," ***Journal of the Americal Chemical Society***, Vol. 40, pp. 1361-1402, 1918.

Lapidus, L., and Amundson, N., "Mathematics of Adsorption in Beds. VI. The Effect of Longitudinal Diffusion in Ion Exchange and Chromatographic Columns," ***Journal of Physical Chemistry***, Vol. 56, pp. 984-987, November, 1952.

Leonard, B., "A Survey of Finite Differences of Opinion on Numerical Muddling of the Incomprehensible Defective Confusion Equation," ***Finite Element Methods for Convection Dominated Flows***, Ed. T. Hughes, AMD, Vol 34, pp. 1-7, 1979.

Lentz, R., Horst, W., and Uppot, J., "The Permeability of Clay to Acidic and Caustic Permeants", ***Hydraulic Barriers in Soil and Rock***, ed. by A. Johnson, R. Frobel, N. Cavalli and C. Pattersson, ASTM, Philadelphia, PA, pp 127-139, 1985.

Locke, M., "Sorption-Desorption Kinetics of Alachor in Surface Soil from Two Soybean Tillage Systems," ***Journal of Environmental Quality***, Vol. 21, No. 4, pp. 558-566, 1992.

Low, P., "Physical Chemistry in Clay-Water Interaction"_***Advances in Agronomy***, Vol. 13, pp. 269-327, 1961.

Lutz, J. and Kemper, W., "Intrinsic Permeability of Clay as Affected by Clay-Water Interaction", ***Soil Science***, Vol. 88, No. 2, pp. 83-90, August 1959.

Mallawatontri, A., and Mullo, D., "Herbicide Adsorption and Organic Carbon Contents on Adjaunt Low Input Versus Conventional Farms," ***Journal of Environmental Quality***, Vol. 21, No. 4, pp. 546-551, 1992.

Mansell, R., Selim, H., Kanchanasut, P., Davidson, J., and Fiskell, J., "Experimental and Simulated Transport of Phosphorus through Sandy Soils", ***Water Resources Research***, vol. 13, No. 1, pp 189-194, 1977.

Marshall, T., "A Relation between Permeability and Size Distribution of Pores", ***The Journal of Soil Science***, Vol. 9, No. 1, pp. 1-8, March 1958.

McNeal, B., and Coleman, N., "Effect of Solution Composition on Soil Hydraulic Conductivity", ***Soil Science Society of America, Proceedings***, vol. 30, pp 308-312, 1966.

Meck, M., and Giddings, M., ***Chlorobenzenes other than Hexachlorobenzene***, Environmental Health Criteria #128, World Health Organization, Geneva, 1991.

Milks, R., Fonteno, W., and Larson, R., "Hydrology of Horticulture Substrates: I. Mathematical Models for Moisture Characteristics of Horticultural Container Media", ***Journal of the American Society for Horticultural Science***, Vol.114, No. 1, pp. 48-52, January, 1989.

Miller, R., and Low, P., "Threshold Gradient for Water Flow in Clay Systems", ***Soil Science Society of America Proceedings***, Vol. 27, No. 6 pp. 605-609, 1963.

Millington, R. & Quirk, J., "Permeability of Porous Solids", ***Transaction of the Faraday Society***, Vol. 57, Part 7, pp. 1200-1207, July 1961.

Mitchell, J., and Younger, J. S., "Abnormalities in Hydraulic Flow through Fine-Grained Soils", ***Paper No. 185***, Department of Civil Engineering, University of California, Berkeley, 1966.

Mitchell, J., and Madsen, F., "Chemical Effects on Clay Hydraulic Conductivity", in ***Geotechnical Practice for Waste Disposal '87***, ed. R. Woods, ASCE, pp 87-116, 1987.

Mohr, A., "Mechanical Dredges", in ***Dredging and its Environmental Effects***, P. Krenkel, J. Harrison, and J. C. Burdick III (Eds.), ASCE, New York, pp. 125-138, 1976.

Moloney, L., and O'Bryan, M., "Construction of Monroe Harbor Confined Disposal Facility", in ***Dredging and Dredged Material Disposal***, R. Montgomery and J. Leach (Eds.), Volume 2, ASCE, pp. 793-801, 1984.

Moltyaner, G., "Dispersion of Contaminants in Saturated Porous Media: Validation of a Finite Element Model," ***Computational Methods in Water Resources: Volume 2 - Numerical Methods for Transport and Hydrologic Processes***, Eds. Celia, Ferrand, Brebbir, Gray and Pinder, Elsevier, U.K., pp 201-206, 1988.

Mualem, Y., "A New Model for Predicting the Hydraulic Conductivity of Unsaturated Porous Media", ***Water Resources Research***, Vol. 12, No. 3, pp. 513-522, June 1976.

Mualem Y., "Hydraulic Conductivity of Unsaturated Soils: Prediction and Formulas", ***Methods of Soil Analysis Part 1: Physical and Mineralogical Methods***, A. Klute (Ed.), 2nd Edition, Number 9, American Society of Agronamy, Inc., Madison Wisconsin, pp. 771-798, 1986.

Muskat, M., ***The Flow of Homogenous Fluids Through Porous Media***, McGraw-Hill Book Company, Inc., New York, 1937.

Myers, T. E., *Memorandum for Record*, Internal US Army Corps of Engineers Report, 1987.

National Research Council, ***Ground Water Models: Scientific and Regulatory Applications***, National Academy Press, Washington, D.C., 1990.

NOAA, *Great Lakes Water Levels*, NOAA, Lake Survey Center, Detroit, Michigan, 1980-1991.

O'Conner, T., "Investigation of the Elutriate Test", ***Dredging and its Environmental Effects***, P. Krenkel, J. Harrison, and J. C. Burdick III (Eds.), ASCE, New York, pp. 299-318, 1976.

Palermo, M., "Dredge Material Disposal", in *Handbook of Coastal and Ocean Engineering*, Herbich, J., (Ed.), Volume 3, Gulf Publishing Co., pp. 393-464, 1992.

Parker, Kool and van Genuchten, "Determining Soil Hydraulic Properties from One-Step Outflow Experiments by Parameter Estimation: II, Experimental Studies", ***Soil Science Society of America Journal***, Vol. 49, No. 6, pp. 1354-1359.

Patterson, R., and Spoel, T., "Laboratory Measurements of the Strontium Distribution Coefficient KdSr for Sediments from a Shallow Sunk Aquifer", ***Water Resources Research***, vol. 17, No. 3, pp 513-520, 1981.

Pershagen, G., "The Epidemiology of Human Arsenic Exposure," ***Biological and Environmental Effects of Arsenic***, Ed. B. Fowler, Elsevier, pp. 199-232, 1983.

Peterson, S., and Gee, G., "Interactions between Acidic Solutions and Clay Liners: Permeability and Neutralization:, ***Hydraulic Barriers in Soil and Rock***, ed. by A. Johnson,m R. Frobel, N. Cavalli and C. Pattersson, ASTM, Philadelphia, PA, pp 229-245, 1985.

Pickens, J., and Lennox, W., "Numerical Simulation of Waste Movement in Steady Groundwater Flow Systems," ***Water Resources Research***, Vol. 12, No. 2, pp. 171-180, April, 1976.

Pickens, J., Gillham, R., and Cameron, D., "Finite Element Analysis of the Transport of Water and Solutes in Tile-drained Soils", ***Journal of Hydrology***, vol. 40, pp 243-264, 1979.

Pickens, J., and Gillham, R., "Finite Element Analysis of Solute Transport under Hysteretic Unsaturated Flow Conditions", ***Water Resources Research***, vol. 16, No. 6, pp 1071-1078, 1980.

Pierce, M., and Moore, C. "Adsorption of Arsenite on Amorphous Iron Hydroxide from Dilute Aqueous Solution", ***Environmental Science and Technology***, vol. 14, No. 2, pp 214-216, 1980.

Pinder, G., "A Galerkin-Finite Element Simulation of Groundwater Contamination on Long Island, New York," ***Water Resources Research***, Vol. 9, No. 6, pp. 1657-1669, 1973.

Polubarinova-Kochina, P., ***Theory of Ground Water Movement***, Translated by J. De Wiest, Princeton University Press, Princeton NJ, 1962.

Posner, A., and Bowden, J., "Adsorption Isotherms: Should They be Split?", ***Journal of Soil Science***, Vol. 31, pp. 1-10, 1980.

Purcell, W., "Capillary Pressures- Their Measurement Using Mercury and The Calculation of Permeability Therefrom", ***American Institute of Mining and Metallurgical Engineers, Petroleum Transactions***, Vol. 186, pp. 39-46, February 1949.

Reddy, J. N., ***An Introduction to the Finite Element Method***, McGraw-Hill, Inc., 1984.

Saeed, M., and Fox, R., "Influence of Phosphate Fertilization on Zinc Adsorption by Topical Soils," ***Soil Science Society of America, Journal***, Vol. 43, pp. 683-686, 1979.

Scheidegger, A., ***The Physics of Flow through Porous Media***, University of Toronto Press, 3rd Edition, 1974.

Schnabel, R., and Potter, R., "Kinetics of Sulfate Retention on Soil as Affected by Solution pH and Concentration", ***Soil Science Society of America, Journal***, Vol. 55, pp 693-698, 1991.

Shackelford, C., "Laboratory Diffusion Testing for Waste Disposal - A Review", ***Journal of Contaminant Hydrology***, Vol. 7, No. 3, pp. 177-217, February, 1991.

Shackelford, C., and Daniel, D., "Diffusion in Saturated Soil. I: Background", ***Journal of Geotechnical Engineering***, ASCE, Vol. 117, No. 3, pp. 467-484, March, 1991a.

Shackelford, C., and Daniel, D., "Diffusion in Saturated Soil. II: Results for Compacted Clay", ***Journal of Geotechnical Engineering***, ASCE, Vol. 117, No. 3, pp. 485-506, March, 1991b.

Shackelford, C., "Contaminant Transport", in ***Geotechnical Practice for Waste Disposal***, David Daniel (Ed.), Chapman and Hall, 1993.

Shani, U., Dudley, L., and Hanks, R., "Model of Boron Movement in Soils," ***Soil Science Society of America, Proceedings***, Vol. 56, No. 5, pp. 1365-1370, 1992.

Sheng, J., ***Multiphase Immiscible Flow through Porous Media***, Dissertation, VPI&SU, 1986.

Shukla, V., and Mittal, S., "Characterization of Zinc Adsorption in Some Soils of India," ***Soil Science Society of America, Journal***, Vol. 43, pp. 905-908, 1979.

Stephens, D., and Rehfeldt, K., "Evaluation of Closed-Form analytical Models to Calculate Conductivity in a Fine Sand", ***Soil Science Society of America Journal***, Vol. 49, No. 1, 1985, pp. 12-19.

Streeter, V., and Wylie, E., ***Fluid Mechanics***, 7th Edition, McGraw-Hill, Inc., New York, 1979.

Swanson, R., and Dutt, G., "Chemical and Physical Processes that Affect Atrazine and Distribution in Soil Systems," ***Soil Science Society of America, Proceedings***, Vol. 37, No. 6, pp. 872-876.

Sykes, J., and Farquhar, G., "Modelling of Landfill Leachate Migration", ***Proceedings, Third International Conference on Finite Elements in Water Resources***, pp. 2.249-2.259, 1980.

Travis, C., and Etnier, E., "A Survey of Sorption Relationships for Reactive Solutes in Soil," ***Journal of Environmental Quality***, Vol. 10, No. 1, pp. 8-17, 1981.

Uppot, J., and Stephenson, R., "Permeability of Clays under Organic Permeants", ***Journal of Geotechnical Engineering***, vol. 115, No. 1, pp 115-131, 1989.

Valocchi, A., "Validity of the Local Equilibrium Assumption for Modeling Sorbing Solute Transport Through Homogeneous Soils," ***Water Resources Research***, Vol, 21, No. 6, pp. 808-820, 1985.

van Genuchten, M., Davidson, J., and Wierenga, Pl, "An Evaluation of Kinetic and Equilibrium Equations for the Prediction of Pesticide Movement Through Porous Media," ***Soil Science Society of America Proceedings***, Vol. 38, pp. 29-35, 1974.

van Genuchten, M., "A Closed - Form Equation for Predicting the Hydraulic Conductivity of Unsaturated Soils", ***Soil Science Society of America Journal***, Vol. 44, No. 5, pp. 892- 898, 1980.

Verruijt, A., ***Theory of Groundwater Flow,*** The Macmillan Press, Ltd., London, 1982.

Wallach, R., da Silva, F., and Chen, Y., "Unsaturated Hydraulic Characteristics of Composted Agricultural Wastes, Tuff, and Their Mixtures, ***Soil Science***, Vol. 153, No. 6, pp 434-441, June, 1992a.

Wallach, R., da Silva, F., and Chen, Y., "Hydraulic Characteristics of Tuff (Scoria) Used as A Container Medium",_***Journal of the American Society for Horticultural Science***, Vol. 117, No. 3, pp. 415-421, 1992b.

Westerink, J., and Shea, D., "Consistent Higher Degree Petrov-Galerkin Methods for the Solution of the Transient Convection-Diffusion Equation," ***International Journal for Numerical Methods in Engineering***, Vol. 28, pp. 1077-1101, 1989.

White, N., Duke, H., Sunada, D., and Corey, T. "Physics of Desaturation in Porous Materials", ***Journal of the Irrigation and Drainage Division***, ASCE, Vol. 96, No. IR2, pp.165-191, June 1970.

Woolson, E., "Emissions, Cycling and Effects of Arsenic in Soil Ecosystems," in ***Biological and Environmental Effects of Arsenic***, Ed. B. Fowler, Elsevier, pp. 51-140, 1983.

Wösten, J. and van Genuchten, M., "Using Texture and Other Soil Properites to Predict the Unsaturated Soil Hydraulic Functions", ***Soil Science Society of America Journal***, Vol. 52, No. 6, 1988, pp. 1762-1770.

Wyllie, M., and Spangler, M., "Application of Electrical Resistivity Measurements to Problem of Fluid Flow in Porous Media", ***Bulletin of the American Association of Petroleum Geologists***, Vol. 36, No. 2, pp. 359-403, February 1952.

Wyllie, M., and Gardner, G., "The Generalized Kozeny-Carman Equation: Part 1 - Review of Existing Theories", ***World Oil***, Vol. 146, No. 4, pp. 121-128, March, 1958a.

Wyllie, M., and Gardner, G., "The Generalized Kozeny-Carman Equation: Part 2 - A Novel Approach to Problems of Fluid Flow", ***World Oil***, Vol. 146, No. 5, pp. 210-228, April 1958b.

Yeh, G., "A Zoomable and Adoptable Hidden Fine-Mesh Aprroach to Solving Advection-Dispersion Equations," ***Computational Methods in Water Resources: Volume 2 - Numerical Methods for Transport and Hydrologic Processes***, Eds. Celia, Ferrand, Brebbir, Gray and Pinder, Elsevier, U.K., pp 69-74, 1988.

Yu, C., and Heinrich, J., "Petrov-Galerkin Methods for the Time-Dependent Convective Transport Equation," ***International Journal for Numerical Methods in Engineering***, Vol. 23, pp. 883-901, 1986.

Yu, C., and Heinrich, J., "Petrov-Galerkin Methods for the Multi-dimensional, Time-Dependent Convective Transport Equation," ***International Journal for Numerical Methods in Engineering***, Vol. 24, pp. 2201-2215, 1987.

Yule, D., and Gardner, W., "Longitudinal and Transverse Dispersion Coefficients in Unsaturated Plainfield Sand", ***Water Resources Research***, Vol. 14, No. 4, pp. 582-588, August, 1978.

Zimmie, T., "Geotechnical Testing Considerations in the Determination of Laboratory Permeability for Hazardous Waste Disposal Siting", in ***Hazardous Solid Waste Testing: First Conference***, ed. by R. Conway and B. Malloy, ASTM, Philadelphia, PA 1981.

VITA

The author was born in Winchester, Virginia in May 1961. The author obtained his BSCE and MSCE from West Virginia University in 1984 and 1986, respectively. He then worked as an Assistant Project Geotechnical Engineer for Schnabel Engineering Associates, in Richmond, Virginia from 1986 to 1990. The author began his doctoral program at Virginia Polytechnic Institute and State University in the Fall of 1990. He has been employed as an Assistant Professor in the Civil Engineering Department at Tri-State University, in Angola, Indiana since November 1993. The author is a registered Professional Engineer in the Commonwealth of Virginia. He is happily married and has 2 wonderful daughters, Christie and Chelsea.